Spring 2013

Black Carbon Measurements of Snow and Ice Using the Single Particle Soot Photometer: Method Development and an AD 1852-1999 Record of Atmospheric Black Carbon from a Mount Logan Ice Core

James Andrew Menking
Central Washington University

BLACK CARBON MEASUREMENTS OF SNOW AND ICE USING THE SINGLE PARTICLE SOOT PHOTOMETER: METHOD DEVELOPMENT AND AN AD 1852-1999 RECORD OF ATMOSPHERIC BLACK CARBON FROM A MOUNT LOGAN ICE CORE

A Thesis

Presented to

The Graduate Faculty

Central Washington University

In Partial Fulfillment

of the Requirements for the Degree

Master of Science

Geological Sciences

---

by

James Andrew Menking

June 2013

CENTRAL WASHINGTON UNIVERSITY

Graduate Studies

We hereby approve the thesis of

James Andrew Menking

Candidate for the degree of Master of Science

APPROVED FOR THE GRADUATE FACULTY

______________ ______________________________

Dr. Susan Kaspari, Committee Chair

______________ ______________________________

Dr. Carey Gazis

______________ ______________________________

Dr. Dominic Klyve

______________ ______________________________

Dean of Graduate Studies

ABSTRACT

BLACK CARBON MEASUREMENTS OF SNOW AND ICE USING THE SINGLE PARTICLE SOOT PHOTOMETER: METHOD DEVELOPMENT AND AN AD 1852-1999 RECORD OF ATMOSPHERIC BLACK CARBON FROM A MOUNT LOGAN ICE CORE

by

James Andrew Menking

June 2013

Black carbon (BC), produced by the combustion of fossil and biofuels, warms the climate by absorbing solar radiation when in the atmosphere and by reducing the albedo of snow and ice when deposited. Measuring BC in snow and ice is important for estimating albedo reduction and developing historical records of BC concentration. Experiments were conducted to further develop a method for measuring BC in snow and ice using the Single Particle Soot Photometer (SP2). Results suggest the optimal procedures for sample storage, treatment, and nebulization, and analysis and calibration of BC concentrations measured using the SP2 coupled to a CETAC ultrasonic nebulizer. The methods were then used to develop an AD 1852-1999 record of BC using an ice core from Mt. Logan in the Yukon Territory, Canada. The BC recorded at Mt. Logan is predominantly from biomass burning in Alaska, the Yukon Territory, and Siberia. Climatic implications of the BC record are discussed.

ACKNOWLEDGEMENTS

I am very grateful to have worked with the outstanding faculty on this committee. I thank Dr. Susan Kaspari for teaching me how to be a scientist, a writer, and an academic, Dr. Carey Gazis for showing me how to teach K-12 students and for pointing out that method development work is difficult, and Dr. Dominic Klyve for myriad interesting conversations about mathematics, science, music, history, academia, and juggling. I thank other colleagues at Central Washington University, Dartmouth College, the Paul Scherrer Institut, the Lawrence Berkeley National Laboratory, and the National Oceanic and Atmospheric Administration for their help with this research. Lastly, I thank friends and family for their continuing support.

TABLE OF CONTENTS

LIST OF TABLES

LIST OF FIGURES

LIST OF FIGURES (Continued)

Figure | Page

LIST OF FIGURES (Continued)

CHAPTER I

INTRODUCTION

Black carbon (BC) is the strongest light-absorbing component of the particle commonly known as soot. The climate is affected by BC because it absorbs solar radiation strongly in the visible spectrum, affecting the global radiative budget. The radiative effects of BC are direct and indirect; BC absorbs solar radiation in the atmosphere and when deposited on the surface of snow and ice (direct effects) (Chung et al., 2012; Ghan et al., 2012; Ocko et al., 2012; Ramanathan and Carmichael, 2008), and it influences climate by affecting cloud-forming processes (indirect effect) (Bahadur et al., 2012; Chen et al., 2010; Feichter and Stier, 2012; Ghan et al., 2012). In 2007, BC was identified as a large source of uncertainty in our physical understanding of climate change (IPCC, 2007) primarily due to our lack of knowledge concerning its absorption of solar radiation (direct and indirect effects), the timing, magnitude, and source of its emission, and its spatial distribution and temporal variability. This study has two objectives that address the latter uncertainties regarding BC's distribution in space and time: (1) to optimize a method of measuring the mass concentration of BC in snow and ice samples using relatively new instrumentation, and (2) to develop a record of historical BC in the atmosphere using an ice core from Mount Logan in the Yukon Territory, Canada.

The incomplete combustion of fossil and biofuels results in the emission of BC particles. Coal power plants and diesel engines are common sources of fossil fuel-derived BC emissions, and forest fires and residential wood burning (for cooking or heating homes) are examples of BC emissions from biofuel burning. The amount of fuel combusted contributes to the amount of BC emitted, but the consumption practices, or the efficiency with which fuels are burned, may be equally important in determining BC emissions (Bond et al., 2013; Bond et al., 2004). Since BC has an atmospheric residency on the order of ~ 1 week (compared to years for greenhouse gases like CO_2), mitigation efforts could quickly remove the BC component of radiative forcing from the climate system, slowing global warming (Ramanathan and Carmichael, 2008).

BC entrained in the atmosphere has the capacity to alter the Earth's climate because it absorbs solar radiation. BC is a major component of atmospheric brown clouds, which are known to cool the surface (dimming), warm the atmosphere, and influence cloud formation (the aerosol indirect effect) (Ramanathan and Carmichael, 2008). Studies show that aerosol pollutants in the atmosphere, of which BC is a significant player, are reducing Asian crop yields (e.g., Chameides et al., 1999), causing earlier and more intense onset of the Indian summer monsoon (e.g., Lau et al., 2006), influencing radiative transfer in the Arctic (e.g., McCarty et al., 2012; Zhou et al., 2012), and resulting in other regional climate changes (e.g., Chakrabarty et al., 2012; Menon et al., 2002; Pere et al., 2012; Qian et al., 2003).

BC also affects the climate when deposited on snow and ice because it reduces the albedo, or reflectivity, causing increased absorption of incident solar radiation and leading to accelerated melt (Brandt et al., 2011; Hadley and Kirchstetter, 2012; Ming et al., 2009; Qian et al., 2009; Warren, 1984; Warren and Wiscombe, 1985). Snow and ice coverage is closely linked to Earth's climate system because of its high albedo, and changes in snow and ice extent account for over half of the observed changes in planetary albedo (Budyko, 1969; Qu and Hall, 2005). Reductions in snow and ice cover by BC reduce the planetary albedo, causing a positive feedback. Additional feedbacks are at play when BC is deposited on snow; BC can accelerate snow grain growth, increasing the radiative effects of BC on the snow, and snowmelt can concentrate BC at the surface, causing larger albedo reductions (Flanner et al., 2007). Modeling results suggest that surface cooling (dimming) by carbonaceous aerosols in the atmosphere is outweighed by the darkening effect of impurities in snow (Flanner et al., 2009). Carbonaceous aerosols (of which BC is a major player) exert a net warming effect on snow and ice, which amounts to a net warming effect on global climate (Bond et al., 2013). This is true even in light of a recent study that found BC particles in snow tend to be larger than atmospheric BC particles, implying lower absorption efficiency and overestimation of the radiative effect of BC in snow in various climate models (Schwartz et al., 2013). The effect of BC on snow and ice albedo may account for a significant fraction of observed global warming, including the trend toward earlier springs in the Northern Hemisphere and thinning Arctic sea ice (Hansen and Nazarenko, 2004).

Snowmelt by BC (and other impurities) is also significant on a regional scale because it may impact basins where the snowpack is an important source of freshwater. Studies of snow in the Sierra Nevada Mountains, CA found sufficient BC concentrations to perturb the snowpack (Hadley et al., 2010; Sterle et al., 2009; Sterle et al., 2012), and similar conclusions have been drawn from studies of BC in snow from other regions including the Himalayas (Ming et al., 2009; Xu et al., 2009b; Yasunari et al., 2010). A study of the snowpack in the San Juan Mountains, CO found that albedo reductions due to dust deposition shortened snow cover duration by 21-51 days (Skiles et al., 2012). The case of dust deposition in the San Juan Mountains is an extreme example of albedo reduction by light absorbing impurities, but it is estimated that BC deposition is also shortening snow cover duration in the western United States (Qian et al., 2009).

The best estimate of the net radiative forcing attributable to BC is 1.1 W m^{-2} with a 90% uncertainty range of 0.17 to 2.1 W m^{-2} (Bond et al., 2013). This estimate makes BC the second most important anthropogenic climate-forcing agent, second only to CO_2 with a radiative forcing of 1.56 W m^{-2}. The total radiative forcing by BC includes the direct forcing of atmospheric BC (0.71 W m^{-2}), the forcing from BC cloud effects (0.23 W m^{-2}), and the forcing of BC in snow and ice (0.13 W m^{-2}) (Bond et al., 2013).

Model calculations currently underestimate the absorptive effect of BC in the atmosphere by a factor of 2.9 because they under-represent (1) the effect of BC mixing with other materials and (2) the amount of BC in the atmosphere (Bond et al., 2013). This study empirically addresses uncertainties related to (2). Previous studies estimated global BC emissions based on assessment of the fuels consumed regionally or on a country-by-country basis (e.g., Bond et al., 2007; Bond et al., 2004; Novakov et al., 2003; Streets et al., 2003; Streets et al., 2001). Problems with these estimates include

(1) uncertainties related to the consumption (particularly residential) of biofuels, and (2) estimation of emissions factors that account for the combustion practices (efficiency) employed (Bond et al., 2013; Ramanathan and Carmichael, 2008). These uncertainties highlight the need for empirical measurements of BC in the atmosphere, snow, and ice in order to constrain BC's abundance and spatial variability. In addition, records of BC's temporal variability may further constrain its climatic effects by providing insight into changes in the amount of BC in the climate system through time.

Ice cores present a tool for reconstructing the historical composition of the atmosphere. Annual accumulation of snow on glaciers preserves records of the dry and wet deposition of BC and other aerosols. Many other chemical constituents (e.g., major ions, trace elements, stable isotopes, and trace gases) are preserved through deposition, precipitation, or by preservation in air bubbles that become trapped within the ice. Variations in these records with depth are considered proxies for changes in their atmospheric concentrations through time. A number of previous studies have developed ice core records of BC, including records from Mount Everest (e.g., Kaspari et al., 2011; Ming et al., 2008), Greenland (e.g., Chylek et al., 1995; Chylek et al., 1992a; McConnell et al., 2007), the European Alps (e.g., Lavanchy et al., 1999; Legrand et al., 2007), Siberia (e.g., Eichler et al., 2011), East Antarctica (e.g., Bisiaux et al., 2012a), West Antarctica (e.g., Chylek et al., 1992b), China (e.g., Liu et al., 2008; Xu et al., 2009a), and British Columbia (e.g., Neff et al., 2012).

This study presents a qualitative record of changes in atmospheric BC that spans AD 1852-1999 and that was developed from an ice core retrieved from Mount Logan in the St. Elias Mountains, Yukon Territory, Canada. The ice core was collected in the summers of 2001 and 2002 from the Prospector-Russell (PR) Col on the summit plateau of Mt. Logan (60°35'N, 140°30'W; 5300 m.a.s.l.) (Fisher et al., 2004). The core is 186 m long and spans the time period 8000 BP-AD 1998. The core is unique in that the summit plateau is situated within the free troposphere > 5000 m.a.s.l, and the summit has previously been shown to capture Asian emissions that undergo trans-Pacific transport (e.g., Osterberg et al., 2008).

As scientific interest in BC persists, new methods and instrumentation for characterizing BC and measuring its concentration in the atmosphere and in snow and ice have been developed. The Single Particle Soot Photometer (SP2) is one such instrument, and it employs laser-incandescence to measure the optical diameter of individual BC particles (Filippov et al., 1999; Schwarz et al., 2010; Slowik et al., 2007; Stephens et al., 2003). The SP2 is promising for work with snow and ice cores because it requires low sample volumes (thereby providing higher temporal resolution from ice cores since available sample volumes are low), and it is not affected by other absorbing impurities like dust. Despite these advantages, BC concentrations measured in liquid samples with the SP2 have been shown to underestimate actual BC concentrations due to BC losses during sample storage and nebulization (Kaspari et al., 2011). Other methodological uncertainties include the choice of a calibration material, sample treatment prior to analysis, and the repeatability of the instrument setup. In addition to the record of BC from Mt. Logan, this study presents the results of experiments that address the aforementioned methodological uncertainties.

The primary objectives of this study are to (1) present the results of laboratory experiments that address methodological uncertainties in the BC analysis of liquid samples using the SP2, and (2) present a record of atmospheric BC from Mount Logan spanning the time period AD 1852-1999. The method development is discussed in detail in Chapter II including the presentation of results and explicit recommendations for SP2 users wishing to measure BC in snow and ice. Chapter III presents the BC record from Mount Logan including a discussion of the sources of BC, the record's variation through time, and its significance to climate. Chapter IV summarizes the conclusions of this work.

CHAPTER II

BLACK CARBON ANALYSIS OF LIQUID SAMPLES USING THE SINGLE PARTICLE SOOT PHOTOMETER: METHOD DEVELOPMENT

Introduction

Since 2004, black carbon (BC) has been increasingly recognized by the scientific community for its absorptive effects, which have contributed and continue to contribute to climate warming (Hansen and Nazarenko, 2004; IPCC, 2007; Ramanathan and Carmichael, 2008). In order to understand BC aerosol's influence on climate, researchers have made measurements of BC concentrations, BC mixing state, and BC particle morphology in the atmosphere (e.g., Schwarz et al., 2006). Measurements of BC in snow and ice have also become desirable since BC affects the climate when deposited on glacier and snow surfaces (Flanner et al., 2007). Uncertainty in climate analyses due to lack of understanding of BC's spatial and temporal variability led researchers to develop ice core records of BC concentrations (e.g., Bisiaux et al., 2012b; Kaspari et al., 2011; McConnell et al., 2007), which also requires measuring BC concentrations in ice samples. All measurements of BC in snow and ice require melting the sample to liquid so that the BC can be aerosolized or filtered. Other measurements of BC in liquid samples include rainwater (e.g., Ohata et al., 2011), lake water, and runoff (e.g., Bisiaux et al., 2011). This chapter explores the measurement of BC concentrations in liquid samples using the Single Particle Soot Photometer (SP2, Droplet Measurement Technologies, Boulder, CO, USA), an instrument traditionally used to measure BC in the atmosphere but that has recently been applied to studies of BC in snow and ice.

The SP2 measures the refractory mass of BC particles (Laborde et al., 2012), but other methodologies differ in terms of the mass that they designate as “black carbon.” As such, the term black carbon is operationally defined depending on the measurement technique employed; the most common (and most relevant to this work) terms are black carbon (BC), denoting a measurement based on optical properties of the soot, and elemental carbon (EC), denoting a measurement based on its thermal properties (Andreae and Gelencser, 2006; Laborde et al., 2012). The SP2 measurement is of the former type, and the term BC as used in this manuscript refers to the mass of refractory BC that is optically detectable by SP2 laser-induced incandescence. The term BC is also used in this manuscript to describe soot more generally when not specifically in the context of a thermal- or optical-based measurement.

Both optical and thermal-optical methods are currently used to measure BC and EC concentrations, respectively, and each method has its advantages and disadvantages. The thermal-optical method (Sunset Laboratories, Portland, OR), which has traditionally been used for measurements of BC in snow and ice samples, directly measures EC mass by combusting carbon that is pre-loaded on a quartz fiber filter. The filter is heated at different temperatures in different atmospheres (helium and oxygen), and the amount of combusted carbon is monitored by a flame ionization detector (Boparai et al., 2008). One advantage of the thermal-optical method is that a measurement of both organic carbon (OC) and elemental carbon (EC) are obtained.

This is possible because the reflectance of the filter is monitored, allowing the user to correct for the amount of OC that is charred during the heating process. When the filter returns to its original reflectance after charring has occurred, it is assumed that the remaining combustion is from EC. This is typically called the OC/EC split (Boparai et al., 2008). Another advantage of the thermal-optical method is that filters can be prepared in the field, allowing for the collection of samples from remote locations. The thermal-optical measurement has the drawbacks of potentially overestimating EC mass due to charring when organic carbon is present (Andreae and Gelencser, 2006; Chow et al., 2004; Schmid et al., 2001) and being affected by high dust loadings that interfere with the optical correction for charring (Kaspari et al., 2011). Additionally, preparing the samples relies on mechanical trapping of BC on filters, which usually requires large sample volumes (~0.1-1 L of liquid) and may introduce errors associated with filtering efficiency. Another tool that relies on sample filtration, the Integrating Sphere/ Integrating Sandwich Spectrophotometer (ISSW), characterizes the optical absorption of particulates on a filter and allows determination of BC concentration by comparison of the absorption measurements to laboratory standards of known BC mass (Grenfell et al., 2011). The method has the advantages of providing information about non-BC absorbing impurities on the filter and allowing for sample collection from remote locations. Filtering may still be problematic with the ISSW, however the pore size of the filters are well defined compared to that of the quartz-fiber filters used for the Sunset thermal-optical analysis. The absorption measurement of BC has the added drawbacks of being sensitive to dust loadings, to the size distribution of BC in the sample, and to the mixing state of the BC particles (Schwarz et al., 2012). Relative to the aforementioned optical and thermal-optical techniques, the SP2 has the advantages of being unaffected by the presence of OC, being unaffected by BC mixing state (Moteki and Kondo, 2007), having the ability to characterize the BC size distribution in samples, and being minimally affected by the presence of dust. Schwarz et al., (2012) found that very concentrated dust samples (~ $5x10^4$ μg/L) increased the SP2 BC measurement by 15 μg/L, but dust loadings of this magnitude are not relevant to the ice core samples or the laboratory experiments in this study. Another key advantage of the SP2 relative to the thermal-optical and ISSW methods is that it does not require a filtration step, allowing measurements to be made with substantially less sample volume (~ 2-5 mL versus ~ 100 mL, depending on BC concentration). This makes the SP2 promising for ice core studies, in which high temporal resolution is desired. Drawbacks of using the SP2 for liquid measurements of BC primarily have to do with (1) requiring an aerosolization step to suspend the BC particles in air before introducing them into the SP2, and (2) lacking an agreed-upon BC standard for calibration of the SP2 and for correction of the measurement to account for BC losses in the aerosolization step.

The SP2 has been used previously to measure BC concentrations in ice core, snow, and lake samples (e.g., Bisiaux et al., 2011; Bisiaux et al., 2012a; Bisiaux et al., 2012b; Kaspari et al., 2011; McConnell et al., 2007; Sterle et al., 2009), but further methodological development is needed with regard to several areas of the analysis. For one, there are the aforementioned uncertainties related to the use of a standard to correct for BC losses that occur during sample nebulization. These include (1) the choice of BC material to use as a standard, (2) the response of the SP2 to different BC standard materials, and (3) the stability of standards over time. The best methods of sample treatment for BC analysis are also unknown. Lastly, repeat analyses of samples stored in the liquid phase indicate that BC concentrations are not stable over time, but the magnitude and rate of the BC losses are uncharacterized and the best storage techniques/sample treatments to preserve/recover BC concentrations in liquid samples have not been determined. Uncertainties related to sample storage are not relevant to studies that use a continuous flow system for ice core analysis (e.g., McConnell et al., 2007), but they are relevant for analyses of archived samples, samples that melt during extraction from the field, and samples that are discrete for any other reasons.

This chapter continues with a description of how the SP2 functions and the whole-system instrumental setup for liquid sample analysis including discussions of optimal nebulizer settings, the calculation of BC concentration, the methods for monitoring sample flow rates to determine BC concentration, and the efficiency of the CETAC U5000 AT+ ultrasonic nebulizer at Central Washington University (CWU). Data that characterize the CWU whole-system repeatability are also presented. This is followed by information about the internal and external calibration of the SP2 for liquid sample analysis including the choice of BC material to use as a standard and the stability of that standard over time. Then, results of experiments are presented that characterize (1) the best sample treatments for BC analysis, (2) the behavior of BC concentrations of liquid samples stored in a variety of conditions, and (3) the effectiveness of various treatments at recovering BC concentrations in samples that experienced losses. The various methodological experiments are summarized in table 1. The discussion of method development concludes with a summary of the best protocol for determining BC concentration in liquid samples using the SP2.

Table 1 – Summary of SP2 methodological experiments discussed in Chapter II.

Experiment	**Variables Tested**	**Associated Figure(s)**
Nebulizer Parameters	Heating temperature	Figure 2
	Cooling temperature	
	Inlet pump flow rate	
	Air flow rate	
Nebulizer Efficiency	Particle size	Figure 5
Data Processing	Method for handling input and aerosol drain flow rates	Figures 3, 4
Instrument Repeatability	N/A	Figure 6
External Calibration (correction for nebulizer losses)	Calibration material	Figures 7, 8, 9
	Repeatability of standards	
Sample Storage	Concentration	Figure 10
	Vial type	
	Storage temperature	
	BC material	
Sample Treatment	Agitation	Figures 11, 12, 13, 14, 15
	Refreezing	
	Acidification	
	Surfactant	

Instrumental Background

The SP2 measures the diameter and mass of individual BC particles by laser incandescence (Filippov et al., 1999; Schwarz et al., 2006; Slowik et al., 2007; Stephens et al., 2003). BC particles are passed through a laser chamber (figure 1B) in which they heat to their boiling point and emit incandescent light. The peak intensity of light that a particle emits is linearly proportional to its size and mass (Schwarz et al., 2006; Slowik et al., 2007). The light is imaged by two photo-detectors (figure 1) that are configured to sense light in broadband (~350-800 nm) and narrowband (~630-800 nm) wavelength spectrums. The instrument also has a detector that senses light scattering from particles (useful for studying coatings on BC particles or purely scattering particles in atmospheric studies), but this detector is not used to measure particles in liquid samples. The ratio of the broadband to narrowband incandescent signals is related to the boiling point of an incandescent particle, which provides a constraint on the particle's composition (Schwarz et al., 2006; Schwarz et al., 2010). The signals of the broadband and narrowband detectors in the SP2 are electronically amplified through high and low gain channels in order to expand the detection size range of BC particles. In order to measure the widest range of BC particle sizes, we monitor the peak intensity of emitted incandescent light as sensed by the combined broadband-high gain and narrowband-low gain channels. The resulting detection limits of the SP2 are BC particles of size ~ 70-800 nm volume-equivalent-diameter (VED) (corresponding to particles of mass ~ 0.32-483 fg assuming spherical shape and BC density 1800 kg/m^3 (Moteki and Kondo, 2010; Slowik et al., 2007)). The total BC mass contribution by particles < 70 nm is estimated by fitting a lognormal function to the BC mass-size distribution.

Regarding the SP2 at CWU specifically, the instrument is calibrated up to 650 nm using a differential mobility analyzer and scanning mobility particle sizer at Washington State University (discussed below). For reasons related to the use of a nebulizer to extract dry BC particles from liquid samples and carry them to the SP2 (discussed below), the instrumental setup at CWU does not measure particles > ~ 500 nm VED (> ~ 118 fg) efficiently. Some particles at the upper end of the calibration are measured, but at much lower efficiency than particles < ~ 500 nm VED.

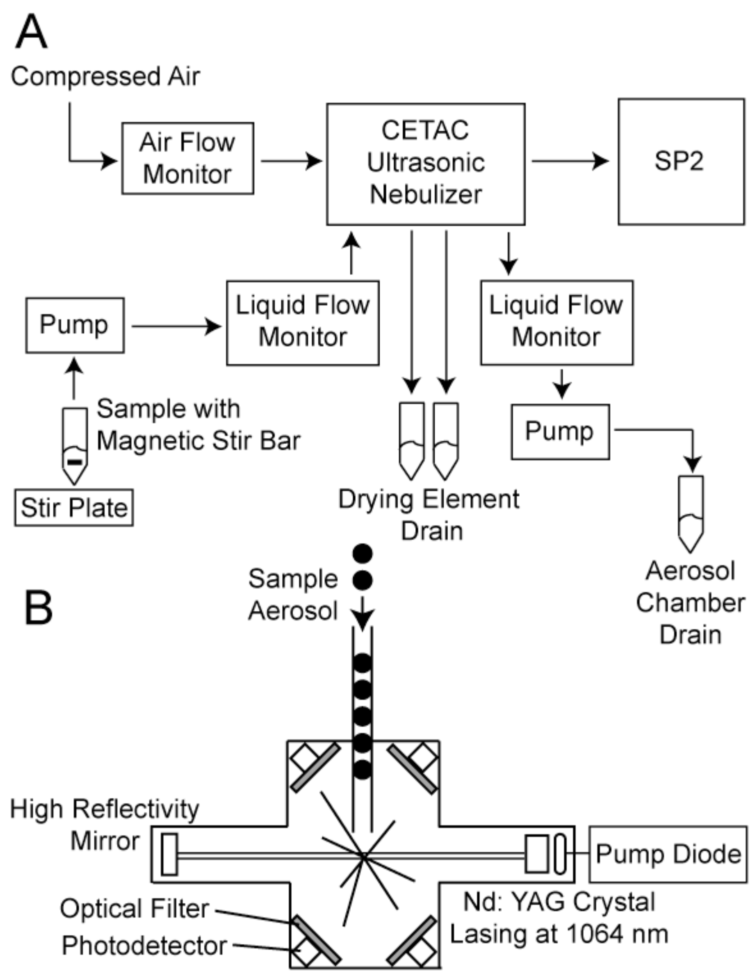

Figure 1 - Instrument schematic of Central Washington University (CWU) setup showing (A) the whole system including pumps (Ismatec peristaltic pumps), liquid flow monitors (Gas Expansion TruFlow), air flow monitor (Alicat Flow Logger), and CETAC U5000 AT+ ultrasonic nebulizer, and (B) the laser cavity of the SP2 where the peak intensity of incandescent light is measured as individual particles pass through a laser beam. Panel B is modified from Schwarz et al. (2006). Although four photodetectors are shown in panel B, the SP2 at CWU uses only two when measuring BC mass concentration.

Due to differences in the SP2 configuration during certain experiments, some of the measured BC concentrations reported in this chapter were determined by the combined broadband-high gain/ narrowband-high gain channels and excluded particles > ~ 400 nm. Additionally, data capture was triggered by the narrowband-high gain channel and particles < ~ 100 nm VED were excluded. The distinction between channel combinations is noted where necessary below, but the difference between the BC mass concentrations as determined by the combined broadband-high gain/ narrowband low gain versus the broadband-high gain/ narrowband-high gain combination is negligible for the purposes of this chapter in which reported BC concentrations are used exclusively for relative comparison between experimental laboratory samples.

CETAC U5000 AT+ Ultrasonic Nebulizer

The primary difference in the SP2 instrumental setup for liquid sample analysis versus atmospheric analysis is the use of a nebulizer to carry BC particles from the liquid sample to the SP2 as dry aerosol (figure 1). At CWU, we use the CETAC ultrasonic nebulizer (U5000 AT+, CETAC Technologies, Omaha, NE), which has been used in several previous studies for SP2 analysis of BC in liquid samples (e.g., Bisiaux et al., 2011; Bisiaux et al., 2012a; Bisiaux et al., 2012b; Kaspari et al., 2011; McConnell et al., 2007; Ohata et al., 2011; Schwarz et al., 2012; Sterle et al., 2009). In the CETAC system, the liquid sample is pumped (Ismatec peristaltic pump, polyfluoralkoxy-polymer (PFA) tubing) to a glass aerosol chamber where contact with an ultrasonic transducer causes the liquid containing the solid BC particles to become suspended as aerosol. A carrier gas (compressed air, laboratory grade) transports the aerosol through a heating and a cooling element, removing the liquid and leaving only dry aerosol to be introduced into the SP2.

Results of experiments suggest that the optimal settings on the CETAC system are 0.75 L/min purge airflow, 0.5 mL/min liquid sample inflow, 140°C heating temperature, and 3°C cooling temperature (figure 2). The operating temperatures are based on recommendations from the manufacturer and are restricted because of the need

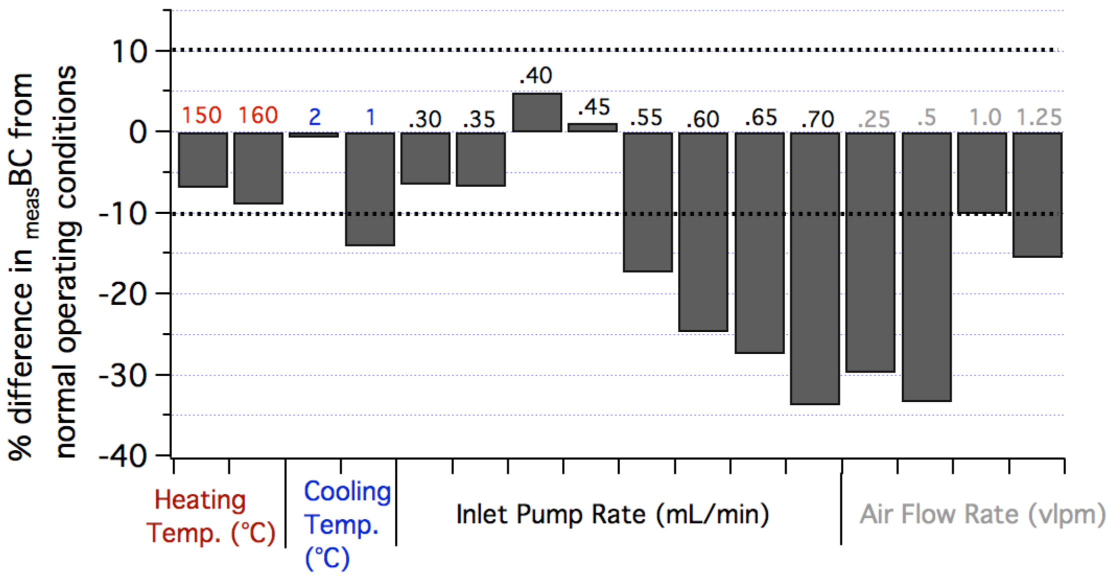

Figure 2 – Changes in $_{meas}$BC (BC mass concentration measured by the SP2, not calibrated for nebulizer losses, discussed below) that resulted from altering various nebulizer parameters (shown on horizontal axis). The values of particular settings (e.g., heating temperature, inlet pump rate, etc.) are indicated by the number above each bar. Dotted lines mark ±10% deviation from BC concentrations determined under normal operating conditions (heating element 140°C, cooling element 3°C, inlet pump 0.5 mL/min, purge air flow 0.75 vlpm). These measurements were performed using a ~ 5 µg/L sample of Aquadag (a BC standard material, product information in table 2).

to fully dry the aerosol before introducing it into the SP2. Minor temperature adjustments (140-160°C heating element, 2-3°C cooling element) did not result in significant changes in the signal of the SP2 (figure 2). Altering the airflow to higher and lower values resulted in lower SP2 signals (10-33% reduction in BC concentration from normal flow, figure 2). Similarly, liquid sample inlet flows of 0.55 mL/min and higher caused steadily greater reductions in BC concentration of up to 34% (figure 2). Altering these parameters may lead to inefficient nebulization of BC particles or inefficient transport of aerosolized BC particles to the SP2. The liquid flow rate described here is higher than that reported by Ohata et al., (2011) (0.18-0.42 mL/min).

The primary benefit of using the CETAC nebulizer as opposed to other nebulizer systems (e.g., APEX Q jet nebulizer, Collison-type nebulizer) is that the user is able to quantify the fraction of the sample that is nebulized. The CETAC (and APEX Q) also requires considerably less sample volume than the Collison-type. The efficiency of all nebulizers is dependent on particle size, but a drawback of the CETAC nebulizer is that the efficiency is more size-dependent relative to other nebulizers, and particles > ~ 500 nm VED are nebulized at much lower efficiency relative to smaller sizes (Schwarz et al., 2012). The CETAC nebulizer efficiency is discussed in more detail below.

Determination of BC Concentration

The SP2 allows users to calculate the BC mass concentration in liquid samples. This is obtained by summing the masses of the individual BC particles detected in a sample and dividing by the volume of liquid that was analyzed. For the particular combination of flow monitors and pumps at CWU, the BC mass concentration in a liquid sample is calculated by the equation:

$$\frac{C\ (\mu\text{g})}{time\ (\text{min}) \times water\ flow\ \left(\frac{\text{L}}{\text{min}}\right) \times \%\ H_2O \times \frac{SP2\ flow\ \left(\frac{\text{cc}}{\text{min}}\right)}{nebulizer\ flow\ \left(\frac{\text{cc}}{\text{min}}\right)}} \quad (1)$$

where *C* is the total mass of carbon (BC) measured by the SP2, *time* is the amount of time over which data were recorded, *water flow* is the flow rate of the inlet pump, *%* H_2O is the fraction of nebulized (analyzed) liquid sample (determined by the methods described below), *SP2 flow* is the air flow rate of dry aerosol into the SP2 inlet, and *nebulizer flow* is the flow rate of compressed air into the CETAC ultrasonic nebulizer. The SP2 at CWU is typically operated with *water flow* = 5 x 10^{-4} L/min, *SP2 flow* = 120 cc/min, and *nebulizer flow* = 750 cc/min.

The CETAC does not nebulize BC particles with perfect efficiency, and measured BC concentrations are often on the order of ~ 56% lower than known BC concentrations at least in part due to the loss of BC particles in the nebulizer. Some of these losses are size-dependent, and larger particles are known to be nebulized less efficiently (Schwarz et al., 2012). In addition to the preferential loss of larger particles, it is possible that small particles (< 200 nm VED) are also not nebulized as efficiently as particles 200-500 nm VED (Ohata et al., 2012; I. Wendl, Ph.D. Candidate at the Paul Scherrer Institut, Villigen, Switzerland, 2011, personal commun.). The CETAC efficiency is discussed in greater detail below. For now, it is noted that measured BC concentrations that are uncorrected for losses in the nebulizer are referred to as ${}_{meas}BC$ while measured BC concentrations that are corrected for nebulizer losses using calibration standards are referred to as ${}_{cal}BC$. The former designation is typical of data presented in this chapter, whereas the latter is used in the following chapter when BC concentrations in ice core samples are reported. When referring to known BC concentrations of liquid samples that were determined by mass, the designation ${}_{mass}BC$ is used.

Determination of the Fraction of Sample Nebulized

The CETAC nebulizer allows the user to quantify the fraction of liquid analyzed (*% H_2O* in equation (1)) and correct for it in the calculation of ${}_{meas}BC$ and ${}_{cal}BC$. This is necessary because the performance of the ultrasonic transducer may vary during use. Although having to account for drift in the fraction of sample nebulized is specific to ultrasonic nebulizers that rely on transducers to aerosolize the liquid, the ability to quantify the fraction of sample nebulized may represent an advantage over other nebulizers where the efficiency is assumed to be constant. The fraction of nebulized sample may be quantified in two ways: (1) by monitoring (using Gas Expansion TruFlow monitors) the flow of sample into the nebulizer and by monitoring the flow of sample that drains from the aerosol chamber (not nebulized) (figure 1), or (2) by collecting and measuring the mass of nebulized sample that drains from the drying element (figure 1) and the aerosol chamber in vials and determining the ratio between the two. Method (2) also involves characterizing the inlet pump rate before and after analysis, and assuming steady linear drift of the inlet pump flow through the duration of the analysis (pump flow drift is primarily due to stretching of the PFA tubing). The liquid that drains from the aerosol chamber includes sample that is not aerosolized by the ultrasonic transducer as well as sample that condenses on the glass walls of the aerosol chamber before reaching the heating and cooling elements. In order to properly characterize the flow rate from the aerosol chamber using the electronic flow monitor, the user must closely observe the rate at which sample drains and adjust the peristaltic pump as often as needed to account for changes in the flow of sample out of the chamber. The liquid that drains from the drying element is assumed to represent nebulized (analyzed) sample, although the system is not entirely closed and some small portion of the nebulized sample may be lost (J. Schwarz, Research Scientist III at NOAA Earth System Research Laboratory, 2012, personal commun.). The fraction of sample nebulized as determined by methods (1) and (2) is fairly consistent, so the losses in the drying element are likely minimal. One disadvantage of method (2) is that the system must run for a sufficiently long time to collect a measurable volume of liquid to determine the fraction of sample nebulized. Additionally, method (2) provides a coarse measure because it assumes linear drift in the inlet pump rate and constant efficiency of the ultrasonic transducer.

When using method (1), the user may process the flow rate data from the TruFlow monitors in one of three ways: (a) by determining the average flow rates during the exact time interval that the sample data was recorded using the time stamps from the SP2 raw data, (b) by assuming one-directional, linear drift in the nebulizer's efficiency over time and calculating the flow rates between end member instances, or (c) by fitting more than one linear segment to capture multi-directional drift in nebulizer efficiency and calculating the flow rates accordingly. Figure 3 shows typical inlet pump flow data and graphical representations of the methods for processing them. Method (1-a) provides the most accurate characterization of flow rates, however it is very time consuming to match SP2 time stamps to output data from the TruFlow monitors. Method (1-b) is much less time-intensive, but changes in nebulizer efficiency may not be accounted for if the changes are not simply linear or steady over the duration of the analysis. Method (1-c) is something of a compromise between (1-a) and (1-b) in which the user can capture positive and negative changes in nebulizer efficiency, but some detail may still be missed. A comparison was performed in order to estimate how much error could be introduced by characterizing flow rates using the different methods. Flow rates were calculated by methods (1 a-c) and data were processed using the Paul Sherrer Institut SP2 Toolkit for Igor Pro. Figure 4 shows that ${}_{meas}$BC in environmental snow, Aquadag (Aqueous Deflocculated Acheson Graphite, Acheson Industries Inc., Port Huron, MI, a graphite suspension more commonly used as an industrial lubricant that incandesces similarly to BC, more information in table 2), and Mt. Logan ice core samples do not (in most cases) vary significantly due to the method used to calculate flow rates. All BC concentrations determined using method (1-c) differed by $< 10\%$ (the estimated whole system repeatability, discussed below) from ${}_{meas}$BC determined using method (1-a), except for one Aquadag sample ${}_{mass}$BC ≈ 16 μg/L and one Aquadag sample ${}_{mass}$BC ≈ 4 μg/L (figure 4A). All ${}_{meas}$BC in Mt. Logan ice core samples

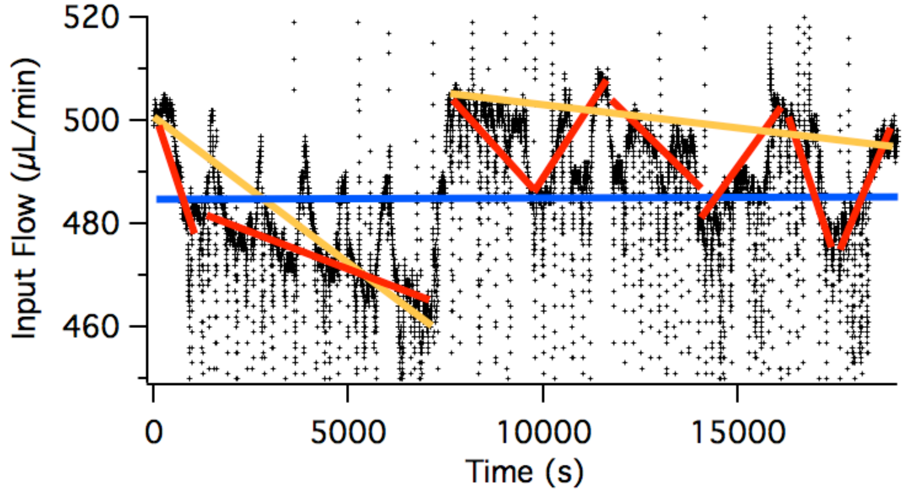

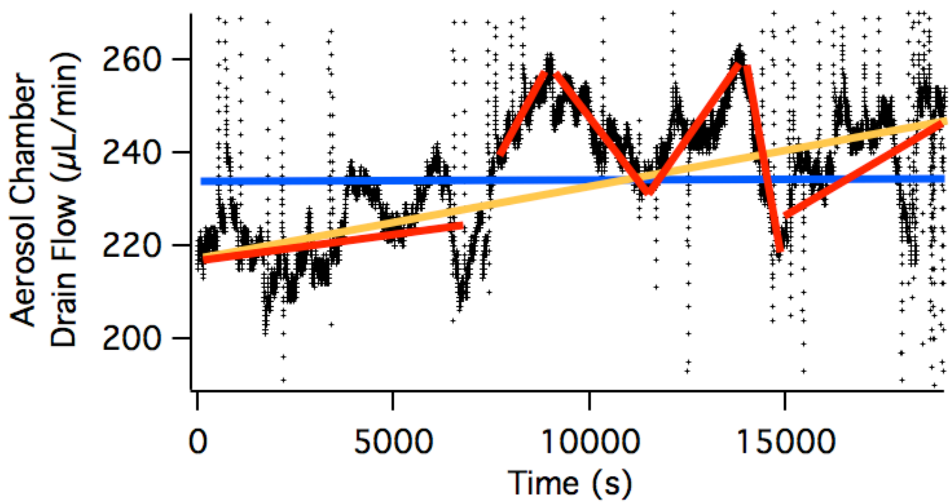

Figure 3 – (Top) Typical inlet pump and (bottom) typical aerosol drain flow rate data with graphics to illustrate how the user might interpret the data to determine *water flow* and *% H_2O* for calculating BC concentration using equation (1). The graphics illustrate how detail may be missed depending on the method chosen. Blue illustrates an average flow rate, orange illustrates the assumption of steady drift between end member data points (method 1-b), and red illustrates fitting multiple segments to capture more detail about the fraction of the sample that is nebulized (method 1-c). Averaging the input and drain flow for the duration of time that each individual sample was measured (method 1-a) is not illustrated in this figure. The very high and low flow rates are due to air bubbles passing through the flow rate monitors (more common in the inlet pump when samples are changed). The inlet pump was recalibrated at ~ 7500 s.

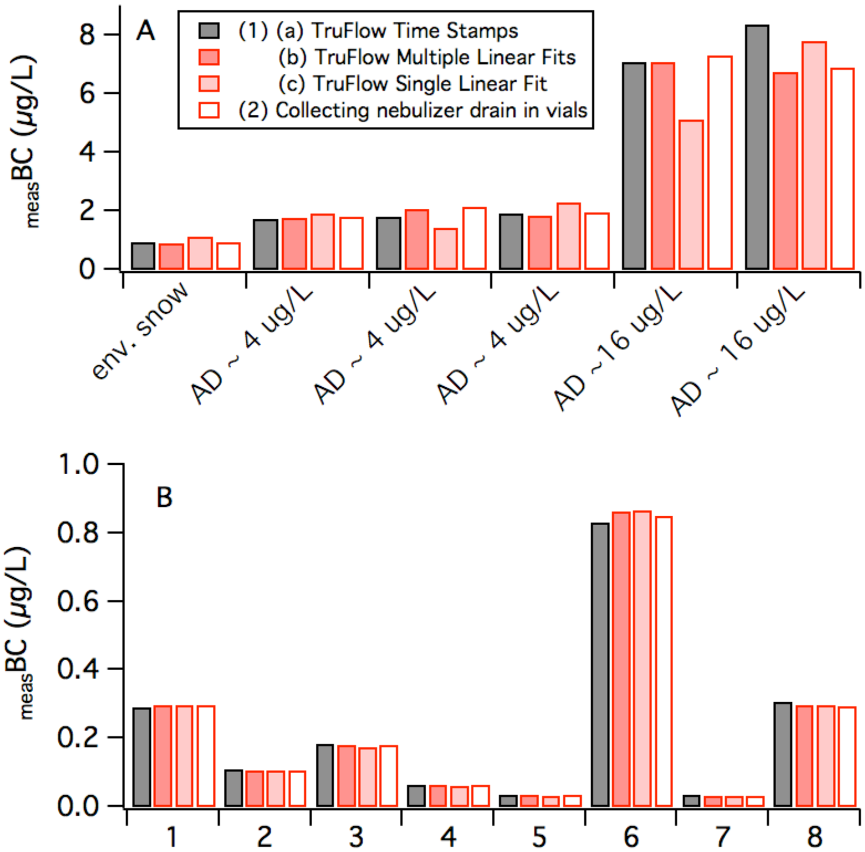

Figure 4 – ${}_{meas}$BC as determined by the various methods of characterizing nebulizer flow rates discussed in the text. Measurements were for (A) environmental snow samples (collected at Blewett Pass, WA) and Aquadag (AD) samples, and (B) Mt. Logan ice core samples (labeled with arbitrary numbers).

calculated using method (1-c) differed by < 5% from BC concentrations of the same samples calculated using method (1-a) (figure 4B). Because it saves time relative to method (1-a) and reasonably characterizes the nebulizer's efficiency, method (1-c) is the preferred procedure for handling flow rate data from the TruFlow monitors. The user should take care to monitor the nebulizer efficiency frequently during each analysis and inspect the flow rate datareturned from the TruFlow monitors. If drastic changes in nebulizer efficiency are evident by visual inspection of the aerosol chamber or the

TruFlow data, or the user desires the most accurate characterization of flow rates, he or she may use method (1-a) to ensure that the nebulizer efficiency is determined accurately. If flow rates appear steady throughout the duration of the analysis, it is possible to average the flow data and use a constant value when calculating the BC concentration of each sample (figure 3).

CETAC Ultrasonic Nebulizer Efficiency

The CETAC U500AT+ ultrasonic nebulizer does not nebulize particles of different sizes with uniform efficiency. A previous study used gravimetric standards of the material Aquablack 162 (Tokai Carbon Co. Ltd., Tokyo, Japan, table 2) to determine that the CETAC nebulized particles with 11.4% efficiency, though this number is highly dependent on the air flow, liquid flow, and the individual nebulizer used (Ohata et al., 2011). More recently, a study demonstrated that the efficiency of the CETAC nebulizer is size-dependent, and that particles > ~ 500 nm VED were not nebulized efficiently (Schwarz et al., 2012). Since the size-dependence of the efficiency of CETAC ultrasonic nebulizers is not necessarily the same for each device, this was tested for the CETAC at CWU using methods described by Schwarz et al., (2012). Standards of polystyrene latex spheres (PSLs) of sizes 220 nm, 356 nm, 505 nm, 771 nm, and 1025 nm (provided by J. Schwarz, 2012) were diluted to number concentrations ~1-4 x 10^5 particles per milliliter (determined gravimetrically). The standards were analyzed immediately after dilution using the CETAC-SP2 system. In order to detect the PSL spheres, the SP2 was configured to record data using the scattering detector (with high and low gains to amplify the signal), and the laser power was reduced when measuring PSLs of sizes > 505 nm to avoid saturating the optics. Number concentrations were determined from the SP2 measurement using the following equation:

$$\frac{n}{time\ (\min) \times water\ flow\ \left(\frac{\text{mL}}{\min}\right) \times \%\ H_2O \times \frac{SP2\ flow\ \left(\frac{\text{cc}}{\min}\right)}{nebulizer\ flow\ \left(\frac{\text{cc}}{\min}\right)}} \tag{2}$$

where *n* is the number of PSL particles detected, and the variables *time, water flow, %* H_2O*, SP2 flow,* and *nebulizer flow* are the same as equation (1). The number of PSL particles detected, *n*, was determined by first fitting a Gaussian function to the distribution of scattering peak heights to determine a reasonable range for the signal from a given size PSL, then by counting the number of particles whose scattering peak heights fell within that range. Efficiency was determined by dividing the resulting measured number concentration by the known number concentration of the standard. PSL particles of sizes 220 nm, 356 nm, and 505 nm nebulized with ~ 18% efficiency. PSL particles > 505 nm nebulized with substantially lower efficiency (figure 5), similar to the results of Schwarz et al., (2012). Other studies indicated a drop in the efficiency of the CETAC for particles < ~ 350 nm (e.g., Ohata et al., 2012), but equal nebulizing efficiency for 220 nm, 356 nm, and 505 nm PSLs was observed in this study. Smaller PSLs were not available for testing, so it is currently unknown if the efficiency of the CETAC at CWU drops for particles < 220 nm.

Previous studies have assumed that PSL spheres nebulize similarly to BC particles (e.g., Schwarz et al., 2012), and that the size-dependent efficiency shown in figure 5 applies to measurements of BC in snow and ice. If this is true, then the $_{meas}$BC of samples with particles > ~ 505 nm (and perhaps < 220 nm) is likely to be inaccurate when using the CETAC ultrasonic nebulizer. Schwarz et al. (2013) determined that ~28% of the BC mass in snow was from particles > 600 nm based on BC size distributions measured in snow samples from Denver, CO. It is noted, however, that the effect of the nebulizer efficiency on $_{meas}$BC will depend highly on the size distribution of the BC particles in the sample, which is a function of (1) the distance from and type of BC emissions, (2) the number of freeze-thaw cycles in the snowpack that lead to

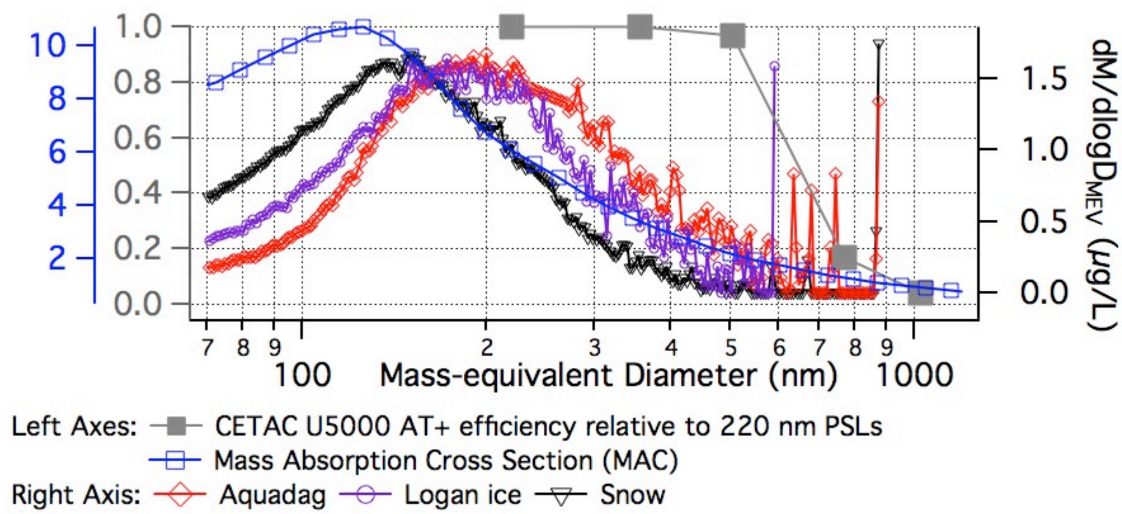

Figure 5 – The efficiency (relative to 220 nm PSLs) of the CETAC ultrasonic nebulizer for various size PSL spheres. Average mass-size distributions of BC in Aquadag, Mt. Logan ice core samples, and snow from Blewett Pass, WA are shown on the right axis. The size distributions were determined using the CETAC ultrasonic nebulizer and were therefore subject to its size-dependent efficiency. The size dependency of BC particle MAC is shown on the blue axis. Data may be found in Appendix A.

agglomeration of BC particles, and (3) the processes of deposition to the snowpack (Schwarz et al., 2013). It is also noted that the mass absorption cross section (MAC), a metric used to estimate BC's absorptive effects, is dependent on the size of the BC particle (figure 5). The largest MAC is associated with ~ 125 nm BC particles based on Mie theory (Schwarz et al., 2013). The MAC of 500 nm BC particles (above which the CETAC efficiency drops rapidly) is ~ 30% of the MAC of 220 nm BC particles (where CETAC efficiency is maximum), and the MAC continues to decline with increasing BC particle size (Schwarz et al., 2013). Thus, underestimates of $_{meas}$BC that occur due to inefficient nebulization of large particles will likely be due to exclusion of BC mass that falls in a less optically relevant size range.

Whole-system Repeatability

In order to further characterize the behavior of the SP2 at CWU, a whole-system repeatability experiment was performed to determine the natural variability that might be expected when repeatedly analyzing the same sample. Figure 6 shows the averages of repeat measurements of two Aquadag samples that took place on three different occasions. The samples were sonicated prior to analysis and analyzed while a stir bar agitated the liquid to prevent settling of BC particles or biased uptake of BC particles by the inlet pump tubing. Although the instrument was largely stable throughout the duration of this analysis, some measurements drifted toward higher values in the earlier part of 04-21-2012 (figure 6). The reason for this drift is unknown, but sources of variability in the system may include (1) unsteady BC particle losses in the nebulizer, (2) unsteady BC losses to pump tubing, (3) variation in SP2 response due to changes in laser power, optics, or electronics, and (4) variability in the sample. Excluding measurements prior to 12:00 on 04-21-2012 the standard deviation of all measured BC concentrations was < 10% of the mean ${}_{meas}$BC for both samples, which suggests that ~ 68% of measurements will fall within 10% of the mean. The value 10% is taken as an estimate of the natural variability of the SP2-CETAC system. The use of a laboratory standard for repeat measurements is advised in order to track ${}_{meas}$BC and identify rare instances of drift in the instrument similar to that on 04-21-2012. A snow sample has been used for this purpose at CWU.

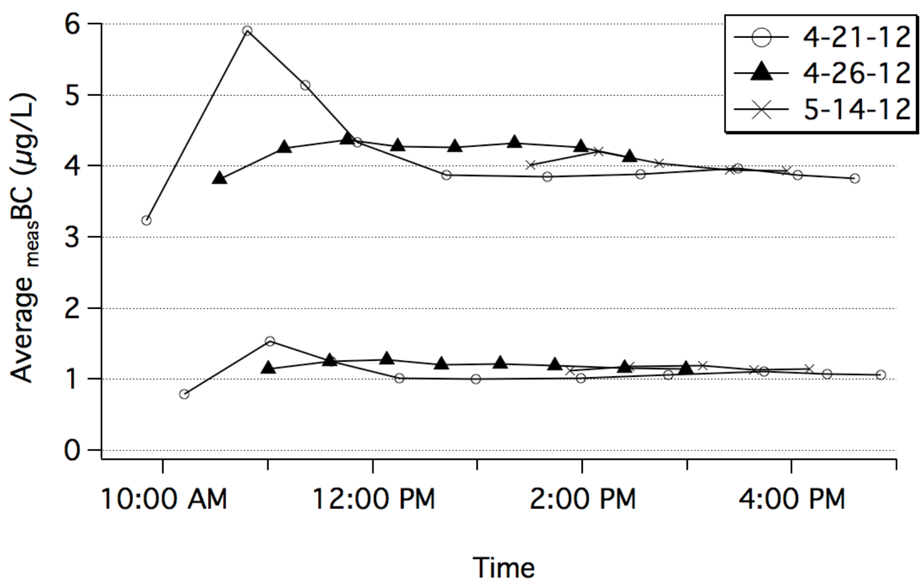

Figure 6 – Mean ${}_{meas}$BC for repeat measurements (~ 50 measurements every ~ 25 minutes) of two Aquadag samples (higher and lower concentration). Approximately 1000 individual measurements were made for each sample.

SP2 Internal Calibration

The SP2 requires empirical calibration with BC particles of known size. The SP2-CETAC system also requires calibration with BC standards of known concentration to correct for losses in the nebulizer. The former is referred to as the internal calibration, and the latter is referred to as the external calibration. The internal calibration is discussed first.

Once a relationship is built between SP2 response and BC particle size, the mass of particles may be calculated by assuming that the BC particles are spherical and that BC density does not vary (Gysel et al., 2011; Schwarz et al., 2006). To perform the internal calibration, a differential mobility analyzer (DMA) is used to size-select particles from a high concentration mixture of polydisperse BC particles and milli-Q water (MQ). The polydisperse BC standard is made from Aquadag (table 2), which we use because its polydisperse size distribution includes the range of BC particle sizes across which we wish to calibrate (70-650 nm, figure 7), and the SP2 response to Aquadag BC particles is similar to the response to BC in environmental snow samples (M. Gysel, Scientist at the Paul Scherrer Institut, Villigen, Switzerland, 2012, personal commun.). Recently, the SP2 community has adopted Fullerene Soot (table 2) as an internal calibration material for measurements of atmospheric BC, where historically Aquadag had been used (Baumgardner et al., 2012). Currently there is not consensus among SP2 users about the best calibration material for measurements of BC in liquid samples. During the internal calibration, the DMA is used to introduce particles into the SP2 of specific sizes (the sizes are 70 nm, 80 nm, 90 nm, 100 nm, 110 nm, 120 nm, 130 nm, 140 nm, 150 nm, 170 nm, 190 nm, 210 nm, 240 nm, 270 nm, 300 nm, 330 nm, 360 nm, 390 nm, 420 nm, 450 nm, 480 nm, 500 nm, 550 nm, 600 nm, and 650 nm). It is preferable to not size-select in continuously increasing or decreasing increments so as to offset any drift that may occur in the DMA system. The SP2 response to particles of each size is monitored, and quadratic splines that relate the average incandescent peak height to particle size are fit to generate the calibration curves. This procedure is used to calibrate the incandescence channels of the SP2 (broadband high gain, broadband low gain, narrowband high gain, and narrowband low gain). During the calibration, a

Table 2 – Various BC materials mentioned in this manuscript.

Material and Lot # (if available)	**Manufacturer and Source**	**BC Material**	**BC (EC) Portion of Solid Mass**	**Source of BC Content Information**	**Confidence in BC Portion**
Aquadag # N/A	Acheson Industries Inc., Port Huron, MI	graphite	0.70	Sunset thermal-optical analyses (Gysel, 2012, personal commun.; Subramanian, 2011, personal commun.; Wendl, 2011, personal commun.)	High due to multiple results from different laboratories
Aquablack 162 # N/A	Tokai Carbon Co. Ltd., Tokyo, Japan	carbon black	0.74	Sunset thermal-optical analysis, CWU	Low due to large spread in data (σ = 0.1)
Cabojet 200 # 1312497	Cabot Corp., Boston, USA	carbon black	0.88	Sunset thermal-optical analysis, CWU	High due to small spread in data (σ = 0.01)
Fullerene Soot #F12S011 (filtered)	Sigma-Aldrich Corp., St. Louis, MO, USA	carbon black and fullerenes	1.0	(Gysel, 2013, personal commun.; Gysel et al., 2011; Ohata, 2013, personal commun.)	Not analyzed by thermal-optical
Flame Soot	Lawrence-Berkeley National Laboratory	flame-generated soot	1.0	(Kirchstetter, 2012, personal commun.) (Kirchstetter and Novakov, 2007)	Not analyzed by thermal-optical

Collison-type nebulizer is used to aerosolize the BC particles, and a condensation particle counter is run in parallel to assess the counting efficiency of the SP2. The Paul Scherrer Institut Toolkit for Igor Pro is used to process the calibration data.

Thermal-optical analysis of Aquadag indicates that ~ 70% of the solid material is EC (M. Gysel, Scientist at the Paul Scherrer Institut, Villigen, Switzerland, 2012, personal commun.; R. Subramanian, Research Scientist at the Carnegie Mellon University, Pittsburgh, PA, USA, 2011, personal commun.), which introduces an

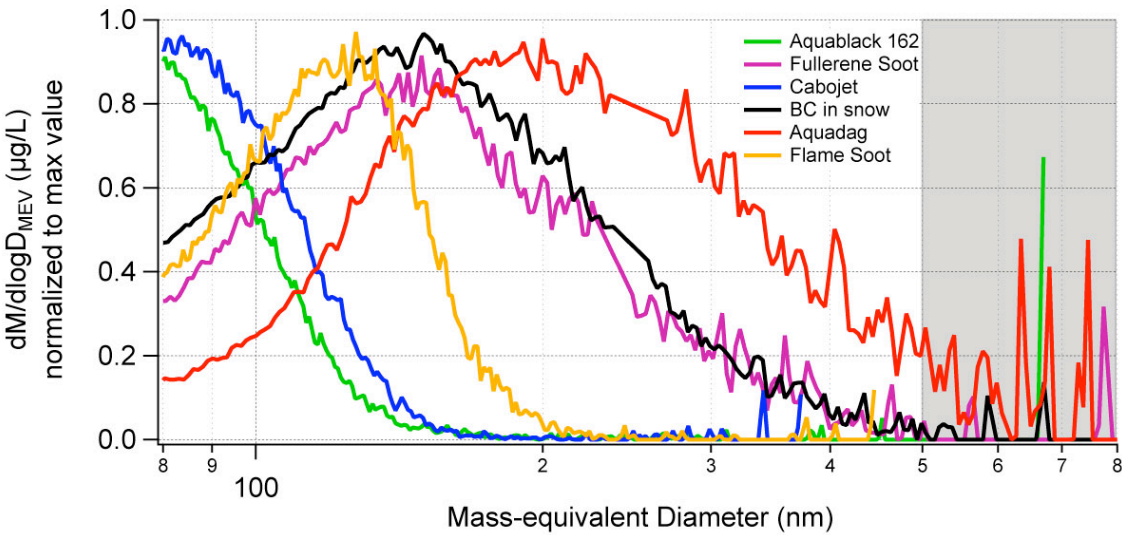

Figure 7 – Average mass-size distributions of various BC materials - Aquadag, Cabojet 200, Aquablack 162, Flame Soot, Fullerene Soot (BC materials information in table 2), and environmental BC in snow. The shaded region indicates the mass fraction of the size distributions > 500 nm where the nebulizer efficiency decreases. Large particles were allowed to settle out of the Fullerene Soot prior to measurement according to Schwarz et al. (2012) for the purposes of testing the external calibration (discussed in text). The environmental snow trace was obtained by analyzing snow samples from Blewett Pass, WA. The lower limit of the horizontal axis is set at 80 nm because this is the lower limit of the internal calibration of the SP2. Note that the internal calibration is extrapolated > 650 nm. Data may be found in Appendix B.

overestimate of ~ 30% to measurements made with the SP2 when internally calibrated using Aquadag. This occurs because the non-EC mass is integrated into the Aquadag particles (M. Gysel, Scientist at the Paul Scherrer Institut, Villigen, Switzerland, 2013, personal commun.). During internal calibration, a 400 nm Aquadag particle, for example, is size-selected by the DMA, and the incandescence of the particle is measured by the SP2. The calibration curve assigns that incandescent peak height response to BC particles of size 400 nm, but the original 400 nm Aquadag particles used for the internal calibration were only 70% BC. An environmental particle of smaller size that is 100% BC could incandesce similarly to Aquadag particles of 400 nm, and its mass would be overestimated by the Aquadag calibration. Users may elect to account for this when processing SP2 data, but it is unnecessary if performing an external calibration to correct for BC losses in the nebulizer (discussed below) because the correction factor simply cancels out of the calculation.

Whole-System External Calibration

In addition to the internal calibration, the SP2 measurement requires external calibration with standards of known concentration in order to correct for BC losses that occur in the CETAC nebulizer. Previous BC in snow and ice studies used BC standards to correct for losses in the CETAC nebulizer, but the BC material used for this purpose has varied between studies. BC materials used previously for external calibration were glassy carbon suspensions called Cabojet 200 (e.g., McConnell et al., 2007) or Aquablack 162 (e.g., Bisiaux et al., 2011; Ohata et al., 2011) (table 2). However, significant portions of the mass of Aquablack 162 and Cabojet 200 fall below the detection limits of the SP2, which may affect the external calibration (figure 7). Furthermore, the incandescence monitored by the SP2 is known to vary for different BC materials (Laborde et al., 2012), but the relative effect that different materials have on the calibration of liquid sample measurements is unknown. Experiments were performed to determine how various BC materials affect the external calibration of SP2 measurements of liquid samples. Standards of the BC materials Aquadag, Aquablack 162, Cabojet 200, Flame Soot, and Fullerene Soot were created gravimetrically and analyzed using the SP2. The BC content of each material was accounted for using the information in table 2. Fullerene Soot was previously allowed to settle before making the gravimetric standards, essentially removing large particles that do not nebulize efficiently in the CETAC system (Schwarz et al., 2012).

Figure 8 shows that, on average, Aquadag standards give the highest $_{meas}$BC for a given standard $_{mass}$BC. Changes in the CETAC nebulizer efficiency between analyses forbid the direct comparison of Fullerene Soot to the other calibration materials in figure 8, however the Fullerene Soot results are still reported below (figure 9). Differences in $_{meas}$BC for the same $_{mass}$BC of Aquadag versus Cabojet 200 or Aquablack 162 (evident in figure 8, also noted in other studies (e.g., Brandt et al., 2011) may be due to the fact that contributions to the mass of Cabojet 200 and Aquablack 162 are from particles that are too small to be seen by the SP2 (figure 7). A previous study noted that 17% of the mass of Aquablack 162 fell below the SP2 detection limits (Ohata et al., 2011). However, differences in particle size distributions cannot explain all of the differences in ${}_{meas}BC$. For example, Cabojet 200 standards return higher ${}_{meas}BC$ than Flame Soot standards, even though the particle size distribution of Flame Soot falls almost entirely within the SP2 detection range (figure 7). Differences in the sensitivity of the SP2 to the different BC materials, which has to do with the physical, chemical, and optical properties of the particles, are likely also responsible for the observed discrepancies in ${}_{meas}BC$ (Baumgardner et al., 2012; M. Gysel, Scientist at the Paul Scherrer Institut, Villigen, Switzerland, 2012, personal commun.; Laborde et al., 2012). Because the SP2 response to Aquadag is most like the response to BC in environmental

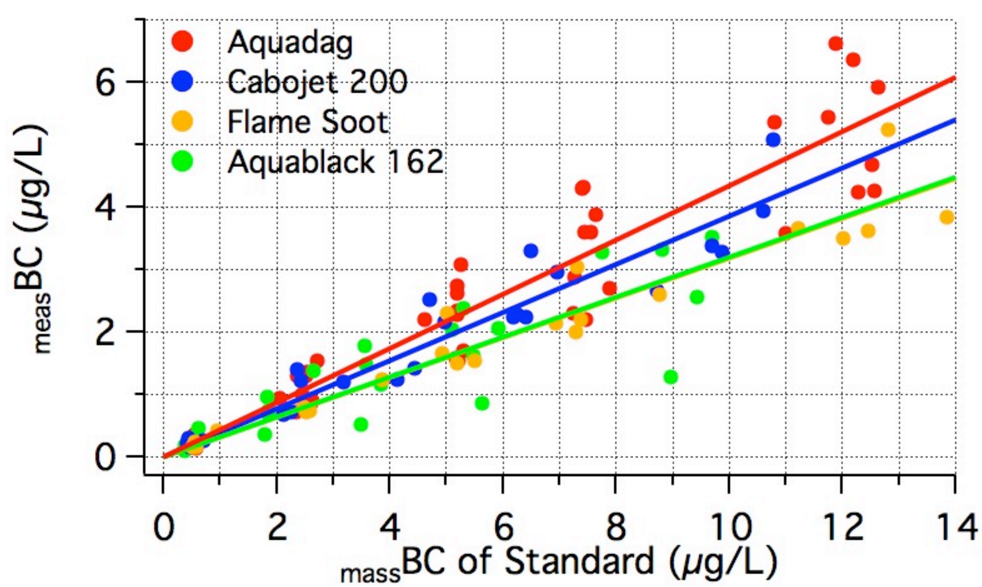

Figure 8 - Calibration curves created by linear regression of data from measurements of Aquadag, Cabojet 200, Aquablack 162, and Flame Soot. The Flame Soot calibration curve is not visible because it has approximately the same slope as the Aquablack 162 calibration curve. The measurements of each material were made on dilution series (standards of ${}_{mass}BC \approx 0.5$, 2.5, 4-6, 6-8, and 9-14 µg/L) that were created on different days from a stock mixture. The calibration curves shown here are the best-fit lines to all of the data from a given calibration material.

snow and ice samples (M. Gysel, Scientist at the Paul Scherrer Institut, Villigen, Switzerland, 2012, personal commun.) and the size distribution of Aquadag falls withinthe detectable range of the SP2, Aquadag is chosen as the preferred BC material for external calibration of SP2 snow and ice measurements. Figure 8 demonstrates that using other calibration materials will result in a higher $_{cal}$BC relative to using Aquadag (12.6% higher for Cabojet 200, 35.9% higher for Aquablack 162, and 37.1% higher for Flame Soot). It is important to note that the spread of the BC concentrations externally calibrated by each material (σ = 16% of the mean) is greater than the estimated variability of the system (10%). The spread in the data for each calibration material and reasons for the variability between each standard series are addressed below.

Reproducibility of Standards

In order to determine the reproducibility and stability of BC standards for use in the laboratory, an experiment was conducted in which standards of known concentration were created from single stock mixtures ($_{mass}$BC ≈ 1500 μg/L) on multiple occasions over the course of two months. Standards were created by mass in 1 L glass jars with $_{mass}$BC approximately 0.5, 2.5, 5.0, 7.5, and 12.0 μg/L. The BC content of each material (table 2) was accounted for when creating the original stock concentration and subsequent dilutions. The stock mixtures from which standards were created were stored in a refrigerator to reduce BC degradation over time (storage procedures and experiments discussed in more detail below), and standards were analyzed immediately after creation.

Importantly, the response of the SP2 scales linearly with the $_{mass}$BC of the standards (figure 9). The fact that measurements of dilution series did not drift in one direction over time indicates that the stock mixtures were stable over at least two months (figure 9). Repeat trials of standard creation and analysis indicate that the slopes of the calibration curves (best-fit lines, not shown) varied for each calibration material from day to day (figure 9). This variability is likely due to errors associated with standard creation, drift in nebulizer BC losses, or natural variability in the SP2 response due to changes in laser power, optics, or electronics. Snow samples were measured as independent standards each day that dilution series were created and analyzed. The snow samples were kept in glass containers in the refrigerator to minimize sample degradation over time (sample storage procedures discussed in more detail below). The fact that the measurements of snow were largely stable from day to day (figure 9) indicates that the variability in the calibration curves is likely due more to errors in standard creation than changes in the instrumentation. Although stock mixtures were agitated for 20 minutes in a sonicator, it is possible that the BC particles in the stock mixtures or the intermediate dilutions were not homogenously mixed, or that BC particles were not transferred uniformly when aliquoting.

Fullerene Soot was not originally tested in this experiment, but measurements of standards created from filtered Fullerene Soot were appended in an effort to create a calibration curve using a BC material that has minimal mass contribution from particles > 500 nm since the efficiency of the CETAC declines for large particle sizes (figure 5). Fresh Aquadag standards were also created and analyzed at the same time. Analysis of the Aquadag standards in April and May 2013 resulted in calibration curves with lower slopes than the Aquadag calibration curves from the original experiment conducted June-August 2012 (figures 9E and 9A). It is possible that changes in the CETAC efficiency occurred during the time between analyses, perhaps due to aging of the transducer, resulting in lower calibration curves than before. Of course this makes the direct comparison between Fullerene Soot calibration curves and calibration curves from the other BC materials problematic since differences may be due largely to differences in nebulizer efficiency rather than the physical properties of the materials. As such, the Fullerene Soot results are not shown in figure 8. Changes in nebulizer efficiency are not likely problematic for comparison of calibration curves from the BC materials originally tested in this experiment (Aquadag, Flame Soot, Cabojet 200, and Aquablack 162) because one-directional drift in the slopes of the curves was not observed (i.e. consecutive calibration curves did not have only smaller or larger slopes), and the analyses were conducted within a relatively small time frame (< 2 months).

Although the direct comparison of Fullerene Soot calibration curves from 2013 to other BC material calibration curves from 2012 is problematic, some useful information may be gleaned about using Fullerene Soot for external calibration of the SP2 measurement of liquid samples. It is known that the SP2 is less sensitive to Fullerene Soot than to Aquadag by 23-29% (Baumgardner et al., 2012) due to physical and chemical properties of the material that affect how it incandesces. However, the Fullerene Soot calibration curves were not significantly offset from the Aquadag curves created at the same time (figure 9E). Large particles were allowed to settle out of the

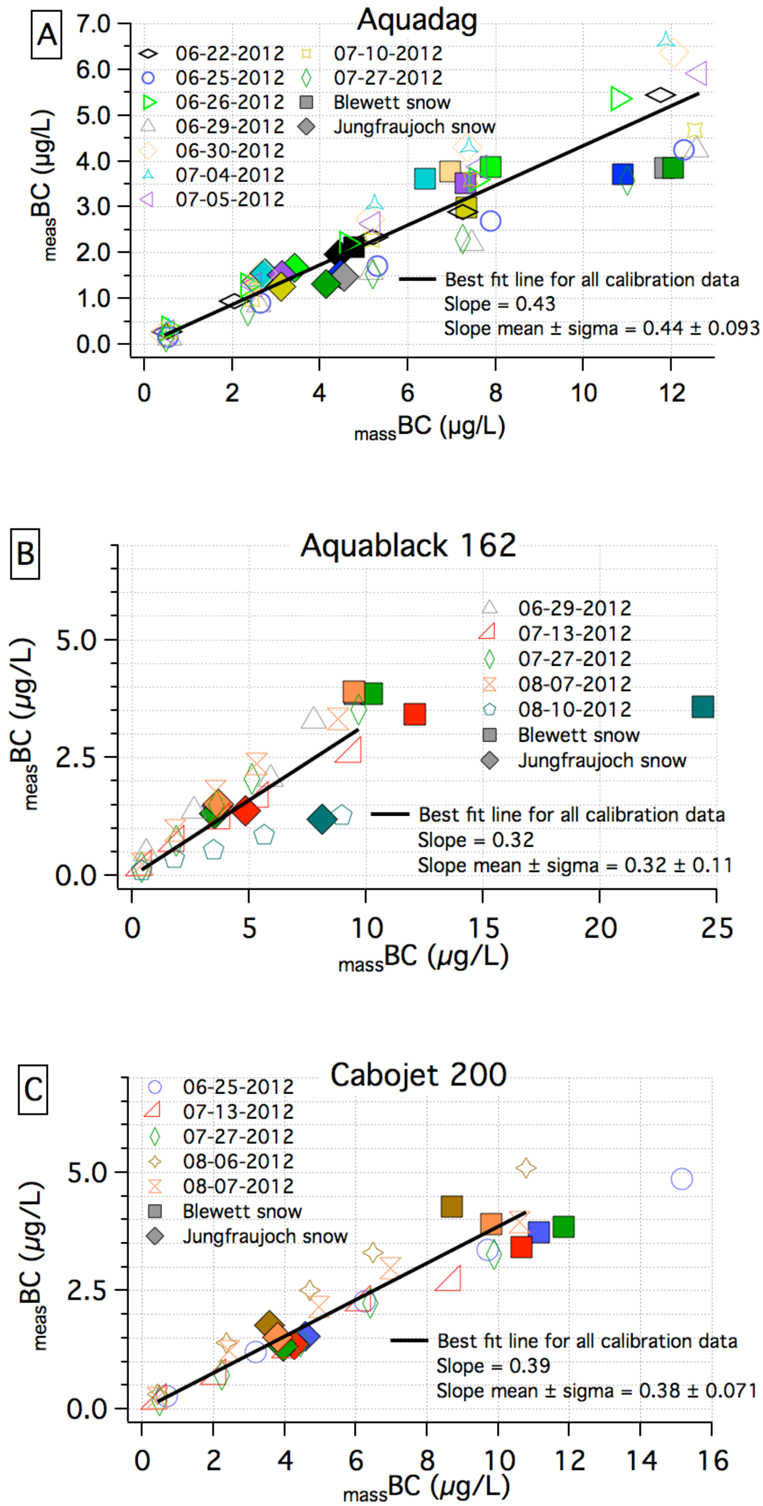
A
Aquadag
06-22-2012
06-25-2012
06-26-2012
06-29-2012
06-30-2012
07-04-2012
07-05-2012
07-10-2012
07-27-2012
Blewett snow
Jungfraujoch snow
Best fit line for all calibration data
Slope = 0.43
Slope mean ± sigma = 0.44 ± 0.093
measBC (µg/L)
massBC (µg/L)
B
Aquablack 162
06-29-2012
07-13-2012
07-27-2012
08-07-2012
08-10-2012
Blewett snow
Jungfraujoch snow
Best fit line for all calibration data
Slope = 0.32
Slope mean ± sigma = 0.32 ± 0.11
measBC (µg/L)
massBC (µg/L)
C
Cabojet 200
06-25-2012
07-13-2012
07-27-2012
08-06-2012
08-07-2012
Blewett snow
Jungfraujoch snow
Best fit line for all calibration data
Slope = 0.39
Slope mean ± sigma = 0.38 ± 0.071
measBC (µg/L)
massBC (µg/L)

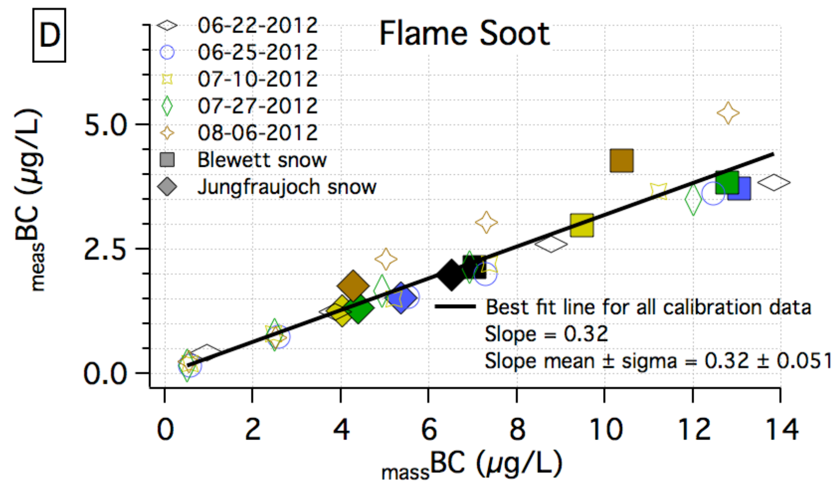

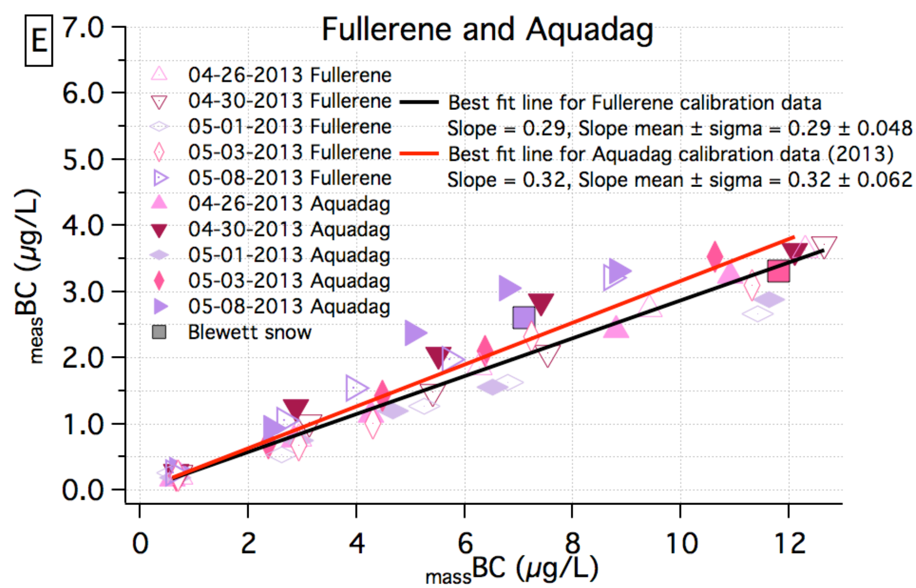

Figure 9 – $_{meas}$BC of standards of (A) Aquadag, (B) Aquablack 162, (C) Cabojet 200, and (D) Flame Soot. Each color indicates a different day that a standard dilution series was created and analyzed, and the color scheme is consistent for all panels A-D. The measurements of the dilution series are indicated by open symbols. All SP2 analyses occurred the same day the standards were created so that measurements reflected BC concentrations of fresh standards without degradation. The black line indicates the best-fit line to all calibration data for a given BC material, and the slope mean reported in each panel is the mean of the slopes of linear regressions of each individual dilution series (lines not shown). Sigma is one standard deviation of those slopes. Bold colored diamonds and squares in panels A-D indicate measurements of snow from Jungfraujoch, Switzerland and Blewett Pass, WA, respectively. The bold color of the diamond or square symbol corresponds to the color of the standard series symbol and indicates the day that the snow was analyzed. The snow measurements are plotted on

the calibration curve that was generated on the same day from analysis of the standards (individual calibration curves not shown), indicating the calibrated BC concentration of the snow (read off the horizontal axis). Panel (E) shows $_{meas}$BC for Fullerene Soot standards and Aquadag standards that were analyzed at the same time. The color/symbol scheme is similar to panels A-D except that bold colors indicate measurements of Aquadag dilution series. Measurements of snow from Blewett Pass, WA are indicated by square symbols, and these are plot on the calibration curve that was generated on the same day using the Fullerene standards (individual calibration curves not shown). Data may be found in Appendix C.

Fullerene Soot prior to standard creation and analysis (Schwarz et al., 2012), but this treatment was not used for Aquadag. It is possible that the removal of large particles that would otherwise be inefficiently nebulized affects the calibration curve enough to offset the sensitivity differences between Aquadag and Fullerene Soot. That is, perhaps a significant portion of the mass of Aquadag is not seen by the SP2 due to poor nebulizer efficiency for particles > ~ 500 nm, which depresses the calibration curves to appear more similar to those of Fullerene Soot.

This experiment does not provide sufficient evidence to persuade the use of Fullerene Soot versus Aquadag, but it does demonstrate that (1) the choice of calibration material significantly affects the correction of $_{meas}$BC, (2) certain materials may be preferable to others given their size distributions, the detection limits of the SP2, and the size dependence of the nebulizer efficiency, (3) standards should be used often to monitor changes in the nebulizer efficiency, and (4) stock mixtures are stable over the course of 1-2 months if stored in glass containers in a refrigerator, and they may be used for repeat creation of standard series.

Sample Storage

Repeat measurements of previously melted snow samples indicate that the $_{meas}$BC of samples stored in the liquid phase may not be stable over time (Jenkins, 2011). In some cases it might be desirable to measure the BC concentration of liquid samples that have been previously melted (e.g. archived samples that weren't analyzed for BC). It is logistically challenging to keep samples frozen when they are retrieved from remote locations, and investigators may want to measure the BC concentration of samples that melted during retrieval. Furthermore, if BC standards remain stable it would be possible to store them in the liquid phase for repeat use. Experiments were designed to assess the stability of samples stored in the liquid phase, and to determine the most stable conditions for their storage prior to SP2 analysis.

Liquid dispersions of the BC materials Aquadag, Aquablack 162, Cabojet 200, and Flame Soot, as well as environmental snow samples from Blewett Pass, WA were stored in polypropylene and glass vials at 25°C and 2°C. Teflon vials were not used in the experiment because samples stored in Teflon vials did not nebulize properly after sonication (M. Gysel, Scientist at the Paul Scherrer Institut, Villigen, Switzerland, 2012, personal commun.). The BC concentration of the samples was measured immediately after standard creation or melting for the various BC-like materials and the snow, respectively. The samples were re-measured for BC concentrations over a time span of 18 days to assess sample stability under the various conditions and over different time periods. All samples (including samples in other experiments discussed elsewhere in this text) were sonicated ~20 minutes and analyzed while a magnetic stir bar agitated the sample to keep BC particles homogenously mixed in suspension. These experiments were performed using the CETAC-SP2 system, so measurements were subject to the nebulizer efficiency issues discussed previously.

Sample stability for Aquadag and environmental snow samples over an 18-day period suggests that storing samples at 25°C in polypropylene vials results in substantial BC losses compared to storage in glass vials or storage at cold temperature (figure 10). Samples stored in glass vials at cold temperatures remained nearly stable for 18 days (figure 10). Samples stored in glass vials at 25°C and polypropylene vials at 2°C experienced variable BC losses (figure 10). These results were consistent for Aquadag and environmental snow samples.

In addition, these experiments indicate that the magnitude of BC losses in storage may be related to sample concentration. After 18 days, Aquadag samples stored in polypropylene vials at 25°C showed 80 %, 65 %, and 40 % losses for low concentration ($_{mass}BC \approx 3$ μg/L), medium concentration ($_{mass}BC \approx 10$ μg/L), and high concentration ($_{mass}BC \approx 15$ μg/L) samples, respectively (figure 10). This result would imply that the magnitude of losses is higher for low concentration samples compared to high concentration samples, but note that the total BC mass lost in the low concentration samples ($_{mass}BC \approx 1$ μg/L equivalent) is less than the mass of BC lost in the medium and high concentration samples ($_{mass}BC \approx 3$ μg/L equivalent). It seems that while BC losses may be proportionally higher for low concentration samples, total BC mass lost in storage is greater in samples that are more concentrated. This would imply that relative differences between samples might appear smaller than they actually are if the samples have undergone BC losses in storage.

It is assumed that BC losses in liquid samples are due to particles adhering to vial walls or agglomerating to larger sizes outside of the SP2 detection range. These results indicate that snow and ice samples are best kept frozen until just prior to BC analysis with the SP2 in order to avoid losses that occur while the samples are stored in the liquid phase.

Since researchers may want to analyze liquid samples for BC concentration that have been archived for months or years, it is necessary to see if BC losses in storage continue over longer periods of time. An experiment similar to the one described above was carried out in order to track BC concentrations in Aquadag, Aquablack 162, Cabojet 200, Flame Soot, and environmental snow samples for 210 days. Due to changes in the SP2 configuration during the experiment, ${}_{meas}$BC could not be tracked for all samples without running into issues comparing ${}_{meas}$BC values that represented different size ranges of BC. For this reason, general conclusions that may be drawn from the experiment are stated, but data are not shown. Contrary to results shown in figure 10, tracking samples for a longer period of time indicated that BC losses might occur in samples stored in polypropylene vials at 2°C and in glass vials at 25°C, although these losses were neither as rapid nor as great as the losses in samples that were stored in polypropylene vials at 25°C. BC losses up to 95% in polypropylene vials stored at 25°C appeared to level off after 55 days in storage. These losses were apparent in Aquablack 162, Cabojet 200, and Flame Soot samples in addition to Aquadag and

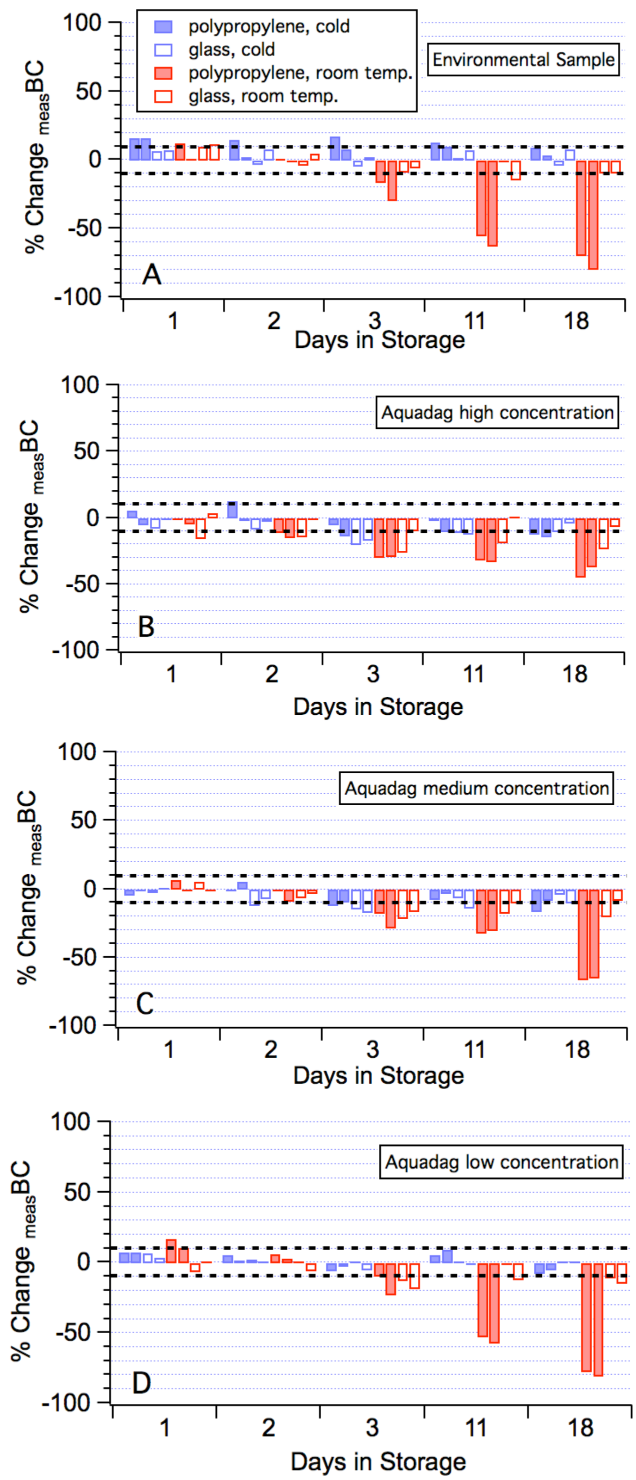

Figure 10 – Percent change in $_{meas}$BC in (A) environmental snow, (B) Aquadag $_{mass}$BC ≈ 15 μg/L, (C) Aquadag $_{mass}$BC ≈ 10 μg/L, and (D) Aquadag $_{mass}$BC ≈ 3 μg/L samples tracked for 18 days in various storage conditions. The bars express the $_{meas}$BC on a

given day as a percentage of the $_{meas}$BC (before any losses due to storage, not shown). Each bar represents one sample. Black dotted lines indicate ±10% natural variability expected in the SP2-CETAC system. Data may be found in Appendix D.

environmental snow. As stated previously, it is advised that samples be melted just prior to BC analysis with the SP2. However, if storage of liquid samples is necessary before the analysis, it is recommended that the samples be stored in glass vials at ~ 2°C and analyzed as soon as possible to minimize potential BC losses.

Melted ice core samples are often refrozen in order to provide stable conditions for ions, trace elements, and other chemical species of interest for future analyses. Liquid samples of environmental snow were refrozen to see if this procedure affects BC stability during storage. Refreezing and thawing snow samples after the first melt resulted in BC losses up to 60% (figure 11). A second freeze-thaw cycle resulted in further losses of the same magnitude. Losses from refreezing may be due to the agglomeration of BC particles (to sizes larger than the SP2 detection range) when the

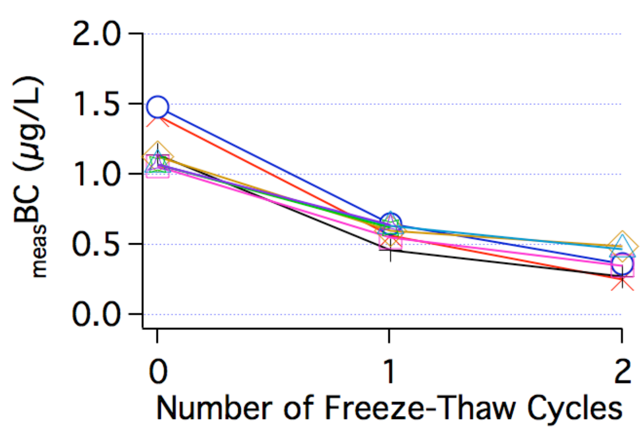

Figure 11 - $_{meas}$BC of environmental snow samples that underwent freeze-thaw cycles. Each colored line/ symbol represents a different snow sample. Snow was collected at Blewett Pass, WA.

particles are rejected by the matrix of ice crystals (Schwarz et al., 2013). However, like Schwarz et al. (2012), significant shifts in the mass size distribution of samples that underwent freeze-thaw cycles were not observed. It is possible that agglomeration occurs, but that the larger particles fall out of the detectable range of the SP2 or are too large to be nebulized by the CETAC ultrasonic nebulizer. It is also possible that refreezing somehow increases plating of BC particles to the vial walls. In either case, it is advised not to refreeze melted samples for future BC analysis.

An experiment was also designed to test whether acidification affected sample stability during storage. Environmental snow and Aquadag samples ($_{mass}$BC ≈ 10 µg/L) were acidified to 0.5 M using 68.5% Suprapur nitric acid immediately after melting (snow) or creating (Aquadag) the samples. The BC concentration of each sample was measured directly after acidification and was tracked over 13 days to monitor stability. It was found that acidification did not halt or slow BC losses when those samples were stored in the liquid phase (figure 12). Additionally, acidification caused immediate losses of up to ~35% in all of the Aquadag samples before any losses due to storage (figure 12).

It is strongly advised to keep snow and ice samples frozen until just prior to BC analysis with the SP2. If this can't be done, samples should be stored in glass vials at cold temperature (~2°C). It is also advised to avoid refreezing or acidifying samples since these procedures led to BC losses in the described experiments. Even if samples are stored under these conditions, it will be necessary to account for changes that do occur to the samples while stored in the liquid phase, which is challenging and/ or impossible to do quantitatively. In all scenarios, BC concentrations of snow or ice samples that were not melted just prior to analysis must be interpreted with the caveat that BC losses may have occurred.

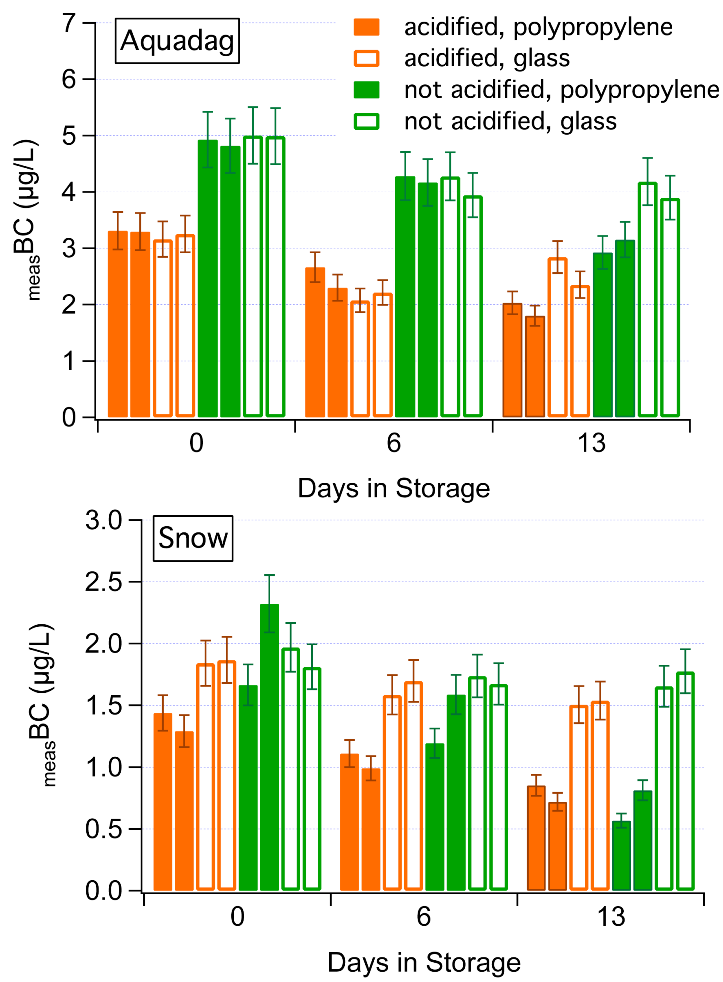

Figure 12 – Repeat measurements of BC concentrations in (A) Aquadag ($_{mass}$BC ≈ 10 µg/L) samples and (B) environmental snow samples for acidified, not acidified, glass, and polypropylene storage conditions. All samples were stored at ~25°C. Error bars represent ± 10% of the measurement.

Recovery of BC in Stored Samples and Other Sample Treatments

In addition to testing vial type and storage temperature, various agitation, acidification, and other treatments were performed on samples that had experienced BC losses during storage to find out if any particular treatment could recover the lost BC. If BC recovery was possible, archived samples could potentially be analyzed without the aforementioned uncertainties. The treatments that were tested included (1) acidification, (2) addition of a dispersing agent (sodium pyrophosphate decahydrate), (3) agitation in a sonicator, and (4) agitation with a magnetic stir bar. The results of these experiments are presented below.

Kaspari et al. (2011) suggested acidifying samples in order to recover BC lost during refreezing, but further testing in this study points against acidification. Sixteen samples were acidified to 0.5 M with 65% suprapur nitric acid, of which six responded with between 10-100% recovery of the lost BC, and ten samples showed no recovery or further losses of 10-40% (figure 13). Schwarz et al. (2012) noted a shift toward smaller particle sizes after acidification and surmised that acid helped to break up agglomerated particles. Significant shifts in the particle size distributions of samples after acidification are not observed. However, it was observed that all samples for which acidification caused some BC recovery were stored in polypropylene vials, whereas all samples stored in glass vials showed no recovery of lost BC or further losses. Since vial type seems to addition of HNO_3 helped to free BC from the walls of the polypropylene vials. No distinct difference in BC recovery after acidification was evident based on different sample composition (Aquadag and snow samples).

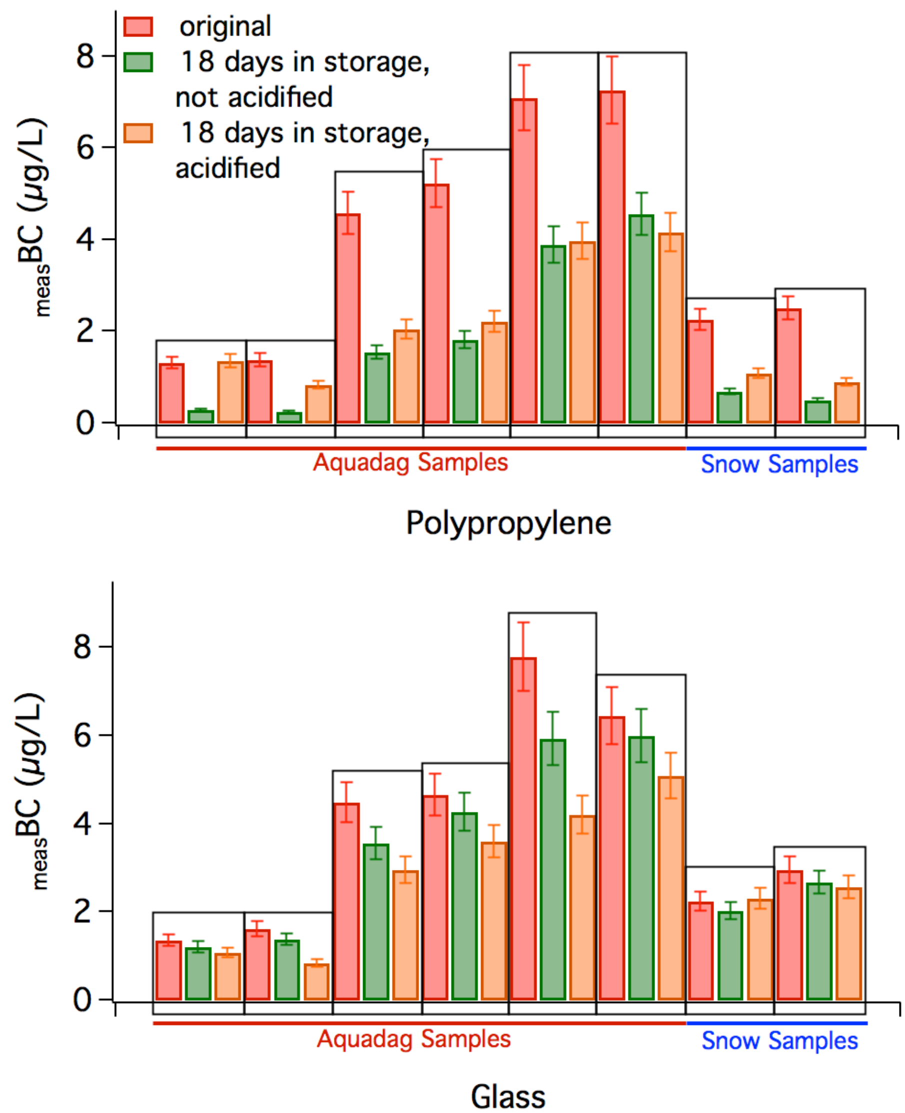

Figure 13 - Results of an experiment to test the recovery effect of HNO_3. BC concentrations were first measured for Aquadag of varying $_{mass}$BC and environmental snow samples (red bars), then measured after the samples had been stored for 18 days and experienced BC losses (green bars), and measured once again after acidification to 0.5M HNO_3 (orange bars). Each bar represents an individual measurement of a sample, and individual samples are grouped by thin black boxes. Error bars indicate ±10% of the measurement.

As for fresh samples, it is not recommended to acidify prior to BC analysis on the SP2 due to the varied effects of acidification on BC concentration seen in this study and the shift in particle size distribution observed by others (e.g., Schwarz et al., 2012). Similar to acid, treatment with the dispersing agent sodium pyrophosphate decahydrate yielded varying results with BC recovery in some samples and further BC losses in others. Thus, we do not recommend the use of a dispersing agent to treat fresh or stored samples either.

In addition to testing the ability to recover lost BC using acid and dispersant, experiments were conducted to determine the effect of agitating samples in a sonicator and with a magnetic stir bar. Results do not definitively indicate that sonication and stirring improve the BC measurement (figure 14 and 15), although previous work

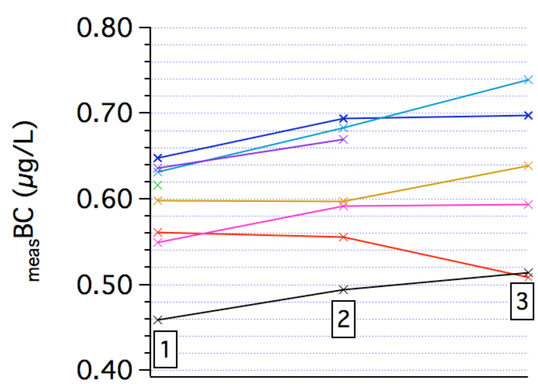

Figure 14 – ${}_{meas}$BC of snow samples (Blewett Pass, WA) that underwent agitation treatments before analysis. Samples were analyzed (1) without sonication or stirring (magnetic stir bar), (2) without sonication but with stirring, and (3) with sonication and stirring treatments. Each colored line indicates a separate snow sample.

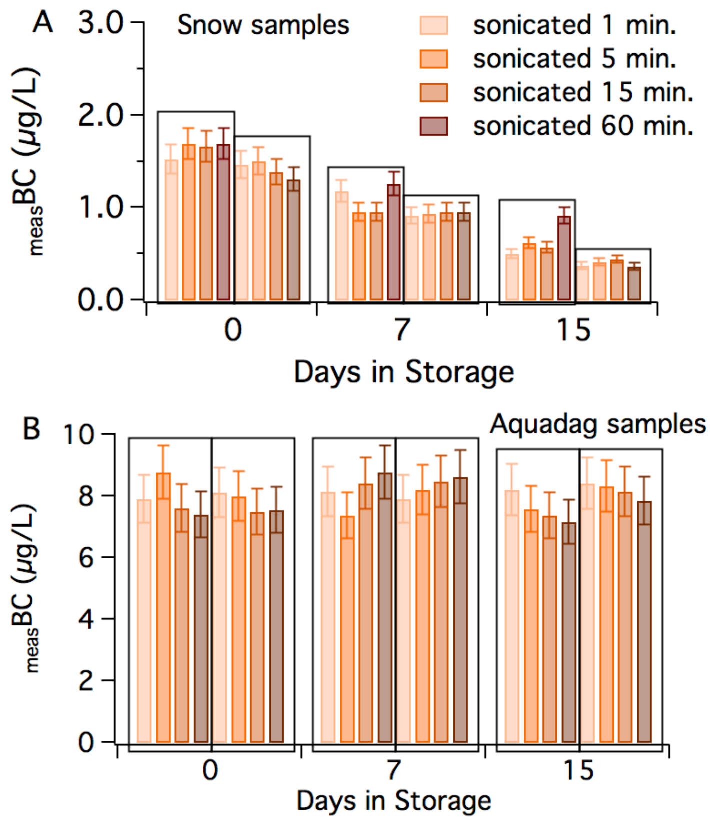

Figure 15 – $_{meas}$BC of snow samples (A) and Aquadag samples $_{mass}$BC ≈ 15 µg/L (B) after samples were sonicated for varying lengths of time (1-60 minutes). Individual samples are indicated with boxes. The experiment was performed three times to allow BC losses to occur in the samples, which were stored in polypropylene vials at room temperature. Error bars indicate ±10% of the measurement.

suggests that they do (Jenkins, 2011; Kaspari, Assistant Professor at Central Washington University, Ellensburg, WA, USA, 2011, personal commun.), particularly in samples with high dust loadings. Although much of the increase in $_{meas}$BC that occurred after agitation treatments is within the estimated 10% variability of the instrument, it is encouraging that $_{meas}$BC increased for most of the snow samples (figure 14). The results presented in figure 15 indicate that varying the amount of time in a sonicator (1-60 minutes) may increase $_{meas}$BC in some instances and decrease the measurement in others, but the differences are largely within the estimated variability of the instrument (± 10%). Though these results do not strongly suggest that agitation treatments make a significant difference in the BC measurement, the use of a magnetic stir bar and a sonicator are simple procedures that do not hurt the BC measurement. As such, sonication for ~ 20 minutes prior to analysis and the use of a magnetic stir bar during sample analysis are procedures adopted at the SP2 lab at CWU.

Summary of the Protocol for BC Analysis of Liquid Samples Using the SP2

This chapter concludes with a summary of the protocol for BC analysis of liquid samples using the SP2 at CWU. The steps are listed in an approximate order assuming that the user begins with a frozen ice or snow sample. The protocol is based on the experimental results and interpretations described above.

1. Create Aquadag standards of ${}_{mass}BC \approx 0.5, 2.5, 5.0, 7.5$, and 12.0 μg/L. If diluting from a stock mixture, sonicate the stock mixture for 20 minutes prior to aliquoting. Keep the stock mixture stored in glass at cold temperature (in a refrigerator). If making the standards from scratch, be sure to account for the moisture content of the BC material and the portion of non-BC solid mass.
2. Melt the snow or ice sample at room temperature, in an oven, or in a warm bath (sonicator).
3. Sonicate all liquid samples for 20 minutes to ensure homogenous mixing of BC particles and break-up of agglomerated BC particles. If standards are allowed to

sit for multiple hours after creation, it is advised to sonicate them for 20 minutes prior to analysis.

4. Establish consistent liquid flow rates into and out of the CETAC ultrasonic nebulizer. It is particularly important to establish a consistent flow rate for the liquid draining from the aerosol chamber since the user must closely monitor that the peristaltic pump is set to the same rate that liquid sample is draining from the aerosol chamber if accurate characterization of the aerosol drain flow rate is desired.
5. Establish consistent nebulization in the CETAC aerosol chamber. If the aerosol cloud looks thin or inconsistent, the CETAC may need maintenance.
6. Establish low enough background in the system (using MQ) appropriate for the analysis.
7. Use a magnetic stir bar to agitate the liquid sample while it is introduced into the CETAC at a flow rate of 0.5 mL/min.
8. Establish a steady signal on the SP2 before recording data.
9. Record at least 10,000 particles over a period of at least one minute to ensure a statistically robust measurement of the BC mass concentration.
10. Use the best-fit line to the Aquadag standard data to generate a calibration curve for correcting the BC concentration measurements. It is preferable to use an average calibration curve (the best fit line to data from at least 5 separate analyses of standard dilution series) if the user is certain that the nebulization efficiency has not changed drastically from the time the average calibration

curve was determined. Using an average of multiple calibration curves is preferable because errors in standard creation cause calibration curves to vary from day to day. Running at least one standard (an Aquadag sample or a snow sample) is useful for monitoring the nebulizer efficiency.

11. Characterize the background BC concentration in the system and subtract this from the measurements.
12. If samples are to be stored for later BC analysis, store them in glass containers at cold temperature (in a refrigerator). Do not refreeze or acidify samples. While these conditions may preserve BC concentrations for up to 18 days, it is important to stress that BC concentrations measured by the SP2 should only be trusted when samples are analyzed immediately after the first melt. If samples that have been stored in the liquid phase are to be analyzed, it is useful to compare them to fresh samples (if they are available) to assess the BC losses that may have occurred (e.g., ice core samples from the same core and the same depth that are kept frozen until just prior to analysis). If fresh samples are not available for such a comparison, the user may proceed with the analysis knowing that differences in BC concentrations between samples may only reflect qualitative differences if the samples have undergone BC losses.

CHAPTER III

AN AD 1852-1999 ICE CORE RECORD OF BLACK CARBON FROM MOUNT LOGAN, YUKON TERRITORY, CANADA

Introduction

Black carbon (BC), a byproduct of the combustion of fossil and biofuels, is considered the second most important climate-forcing agent next to CO_2 (Bond et al., 2013). Studies have shown that BC directly affects the climate system when it is suspended in the atmosphere (e.g., Ramanathan and Carmichael, 2008) and when it is deposited on glacier and snow surfaces (e.g., Flanner et al., 2007; Hadley and Kirchstetter, 2012; Hansen and Nazarenko, 2004). Because it reduces the surface albedo of snow and glacier surfaces, BC is leading to increased melt of snow and ice with important implications for water resources (Qian et al., 2009). Despite having a significant influence on climate and hydrology, there are large uncertainties associated with the amount of BC distributed in space and through time (IPCC, 2007), highlighting the need for empirical records to constrain historical fluxes of BC in the atmosphere and on glaciers and snow. Ice cores offer a means to reconstruct records of BC in the atmosphere (and on the glacier surface), which allows the study of the historical variability of BC, identification of trends in BC concentrations through time, attribution of the BC to specific sources, and estimation of the effect of BC on climate.

This chapter presents a record of BC concentrations that spans AD 1852-1999 and was developed using an ice core retrieved from Mount Logan in the Yukon

Territory, Canada. Mount Logan is the highest mountain in Canada and is located in the heavily glaciated St. Elias Mountains at the end of the main North Pacific storm track where moisture arrives to Northwest Canada (Moore et al., 2002a; Rupper et al., 2004). Mt. Logan is the coldest site in the region (Holdsworth et al., 1996), which minimizes snowmelt and allows the retrieval of long-term (> 8000 year) records with which to study the atmospheric circulation and the paleoclimate of the North Pacific (Osterberg et al., 2008). Records in Mt. Logan ice are climatologically interesting because they capture decadal trends in North Pacific climate variability and have significant teleconnection signatures of climate patterns like the El Niño Southern Oscillation (Moore et al., 2001; Rupper et al., 2004). Most previous work on ice cores from Mt. Logan has sought to understand the paleoclimatology of the North Pacific through the recent Holocene including changes in atmospheric circulation, and past variability of the El Niño Southern Oscillation, the Pacific Decadal Oscillation, and the Pacific North America pattern (Fisher et al., 2008; Fisher, 2011; Kang et al., 2005; Moore et al., 2002a, 2003; Moore et al., 2001, 2002b; Rupper et al., 2004). Other work has used Mt. Logan ice to study atmospheric pollution in the North Pacific (e.g., Holdsworth et al., 1984; Monaghan and Holdsworth, 1990; Yalcin and Wake, 2001), including the identification of Asia as an upwind source for pollution in the region (Osterberg et al., 2008). A record of BC from Mt. Logan is important because it potentially furthers understanding of atmospheric pollution (anthropogenic and naturally-sourced) in the North Pacific, and because BC may have climate implications for a region of established climatological interest.

Sources of BC emissions that could be recorded at Mt. Logan include (1) forest fire emissions, (2) industrial emissions (including emissions from manufacturing, power production, and the transportation sector), (3) emissions from the residential use of coal and biofuels (e.g., smoke from residential heating/ cooking), and (4) emissions from open biomass burning (e.g., land clearing). Because of the geographic location and prevailing atmospheric circulation patterns, Mt. Logan is situated to record locally sourced BC in addition to BC that is transported across the Pacific Ocean from Asian sources (Hadley et al., 2007; Jaffe et al., 1997; Osterberg et al., 2008). The relative attribution of the BC signal in the ice core to various sources is discussed more thoroughly in a following section of this chapter. Contextual information for the aforementioned sources of BC is provided below followed by a description of the ice core and the location of its retrieval.

Forest Fires

The scientific community has recognized that forest fires are of large consequence to the natural world because they shape the landscape, influence forest structure and composition, and affect the ecology of forested regions (Behling et al., 2004; Flannigan et al., 2000). Trends in forest fire frequency allow scientists to make inferences about changes in vegetation, forests, and biogeochemical cycles through time (Behling et al., 2004; Eichler et al., 2011; Higuera et al., 2009). Trends in forest fire frequency are also indicative of trends in human activity including land use changes (e.g., Marlon et al., 2008) and human occupation of specific regions (e.g., Behling et al., 2004). Broadly speaking, forest fires have increased in the latter half of the Holocene in association with increases in human populations and practices (Carcaillet et al., 2002).

The occurrence of forest fires is tightly linked to regional climate (Flannigan et al., 2000; Gillett et al., 2004; Han et al., 2012; Schoennagel et al., 2004; Stocks et al., 1998). Forest fire emissions affect regional meteorology (Youn et al., 2011), and studies have also identified parallels between longer-term global warming/ cooling trends and increases/ decreases in the frequency of forest fires (e.g., Gillett et al., 2004; Lynch et al., 2004; Marlon et al., 2008; Pierce et al., 2004). The area burned each year in North America has been linked to changes in the dynamics of teleconnections associated with climate patterns (e.g., the Pacific Decadal Oscillation, the El Niño Southern Oscillation, and the Arctic Oscillation) that cause prolonged drought and rapid drying of biofuels (Fauria and Johnson, 2006, 2008). Fires are also linked to climate because they are natural sources of aerosols and greenhouse gas emissions (Keywood et al., 2013; Youn et al., 2011), and they are an important player in the global carbon flux (Flannigan et al., 2000). The effect of forest fires on carbon cycling and climate is estimated to be the greatest in the carbon-rich boreal zone (Stocks et al., 2002), and the interaction between forest fires and climate is compounded by the fact that models predict increasing forest fire frequency, severity, and extent in a warming climate (Flannigan et al., 2000; McCoy and Burn, 2005; Stocks et al., 1998).

Because of geographical proximity and/or being located upwind of Mt. Logan (atmospheric circulation at Mt. Logan is discussed in more detail below), the likely source regions of fire emissions captured at Mt. Logan include the boreal forests in

Alaska, the Yukon Territory, and Siberia. Information about past forest fires in these regions comes primarily from charcoal in lake sediments (e.g., Lynch et al., 2004; Marlon et al., 2008), fire spatial statistics from land management bureaus (e.g., Kasischke et al., 2002), and glaciochemical records from ice cores (e.g., Eichler et al., 2011; Legrand et al., 1992; Whitlow et al., 1994; Yalcin et al., 2006). According to analyses of spatial statistics, Canadian annual burn area has increased over the past four decades (Gillett et al., 2004; Weber and Stocks, 1998) with the frequency and intensity of forest fires being linked to changes in climate (Fauria and Johnson, 2006; McCoy and Burn, 2005). In Alaskan lakes, charcoal accumulation over the past 1000 years has been highest since AD 1850, implying more frequent and larger Alaskan forest fires, although the past 1000 years have been characterized by low charcoal accumulation rates relative to the rest of the Holocene (Lynch et al., 2004). Analysis of the spatial statistics of Alaskan fires since AD 1950 indicates that most burn area occurs in a relatively small number of high fire years occurring every ~ 4 years, and that average burn area has changed little between the 1960s and 1990s (Kasischke et al., 2002). Unlike Alaskan fires, Siberian forest fires have increased in frequency over the past century (Kawamura et al., 2012), which is consistent with fire statistics and a recent trend toward more frequent extreme fire years (Soja et al., 2007). These trends are evident in ice core records of vanillic acid and dehydroabietic acid (biomass burning tracers) from the Ushkovsky ice cap in the Kamchatka Peninsula, but they are inconsistent with ice core records from the more central Siberian Altai that suggest no significant increase in forest fire frequency in the last 300 years (Eichler et al., 2011).

The differences between these records may be explained by the fact that different chemical species were being interpreted and that the ice cores were retrieved from different geographic locations.

Studies have also invoked forest fires as an explanation for trends in the variability of BC concentrations observed in ice core records (e.g., McConnell et al., 2007) and lake sediments (e.g., Han et al., 2012), and these records allow researchers to make inferences about the timing and magnitude of forest fire events and emissions. A BC record from Mt. Logan will potentially provide more information about the size and frequency of forest fires in Alaska, the Yukon Territory, and Siberia.

Industrial Emissions

The abundance of many atmospheric constituents has increased since pre-industrial times due to anthropogenic emissions associated with industrialization. Different chemical species have multiple and contrasting effects on climate (IPCC, 2007), but BC in particular is extremely absorptive of shortwave radiation and has a high potential to cause climate warming (Bond et al., 2013). The scientific consensus is that there is a very high probability BC has warmed the climate since pre-industrial times and continues to do so, and this consensus is based on the high absorption efficiency of black carbon and the change in the amount of BC in the atmosphere during the industrial era (AD 1750-2000) (Bond et al., 2013). The increase observed during this time is largely due to BC emissions from the industrial combustion of fossil fuels, including emissions related to manufacturing, coal power plants, and diesel engines.

The United States and Europe are estimated to have contributed substantially to global BC emissions at the turn and the early part of the 20th century, but developing regions such as East Asia are estimated to be the largest emitters of BC in the present day (Bond et al., 2007; Ramanathan and Carmichael, 2008) with Asian BC emissions having doubled since 1950 (figure 16) (Novakov et al., 2003; Wang et al., 2012). China alone is estimated to contribute one fourth of the global anthropogenic BC (Streets et al., 2001). Although records of black carbon in ice cores have been used previously to

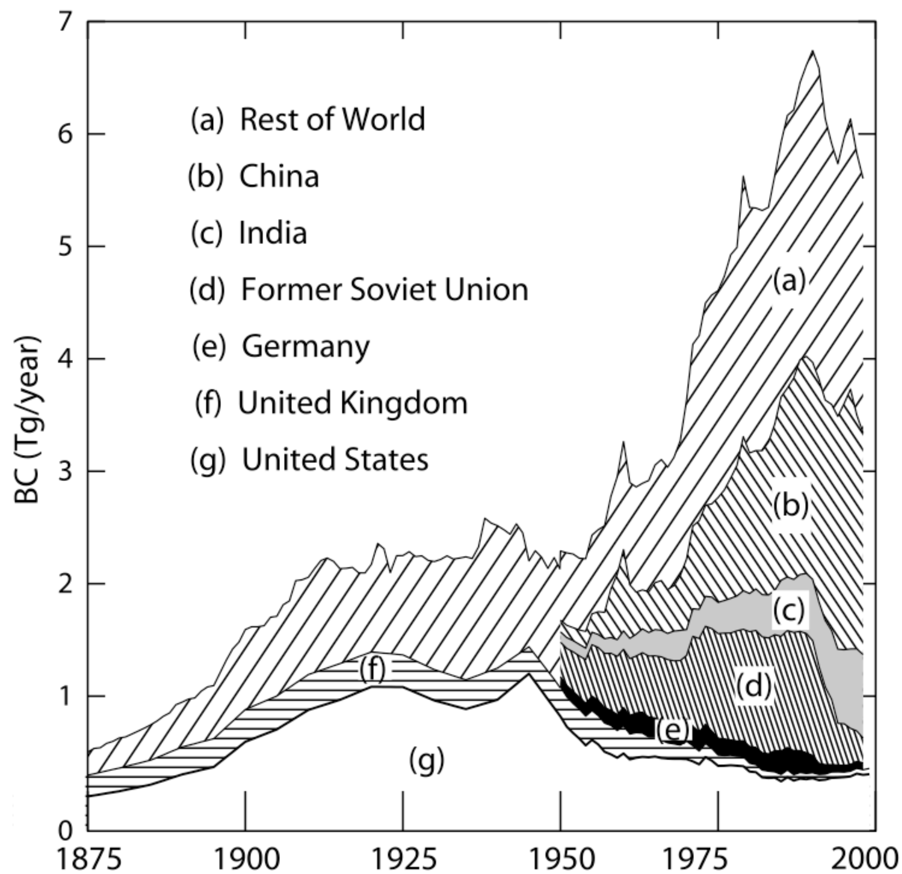

Figure 16 – Estimated historical BC emissions from burning of fossil fuels for various parts of the world. Figure from Novakov et al. (2003).

constrain the timing and magnitude of industrial emissions of BC (e.g., Kaspari et al., 2011; McConnell et al., 2007), most of our understanding of BC emissions related to industrial practices comes from estimates based on inventories of combustible fuels (Bond et al., 2007; Bond et al., 2004). Calculations that estimate BC emissions are based on fuel consumption data and BC emissions factors that vary regionally depending on fuel type, combustion type, and emission controls (Bond et al., 2004). Observational records are still needed to address uncertainties in the spatial extent and temporal variability of BC from industrial sources.

Other BC Emissions Sources

Other important sources of BC in the atmosphere besides forest fires and industrial emissions include the residential use of biofuels and coal for cooking and heating homes (Rehman et al., 2011), and the open burning of land for agricultural purposes (e.g., clearing of forests for pastureland or planned removal of debris from cropland) (McCarty et al., 2012). BC emissions from these sources are extensive and globally significant, perhaps comprising over 35% of total global BC emissions (U. S. Environmental Protection Agency, 2012). Residential BC emissions are estimated to be greater in developing parts of the world, and they are particularly prevalent in China where the residential burning of coal and biofuel were estimated to be the two largest sources of BC in 2007 (Wang et al., 2012). Open land burning (including forest fires) is estimated to be greatest in Africa, South America, and Asia (U.S. Environmental Protection Agency, 2012). Despite making up such a large contribution to the global

BC, these types of emissions are the most poorly quantified. Poor constraints on residential and agricultural BC emissions result primarily from the lack of accurate information to characterize the extent to which these practices occur and the extent to which they produce BC (Bond et al., 2007; Bond et al., 2004; Ramanathan and Carmichael, 2008).

The Prospector Russell Col Ice Core

In the summers of 2001 and 2002, the Canadian Geological Society collected a 186 m ice core from the Prospector Russell (PR) Col near the summit of Mount Logan in the St. Elias Mountains, Yukon Territory, Canada (60°35'N, 140°30'W, 5300 m.a.s.l., figure 17) (Fisher et al., 2004). Mt. Logan is located ~100 km from the Gulf of Alaska and is unique in that the summit plateau is situated within the free troposphere > 5000 m.a.s.l. The ice core spans the time period 8000 BP - AD 1999, so pre- and post-industrial periods are represented in the ice.

Atmospheric Circulation and Sources of Air Masses and Moisture at Mt. Logan

Previous work on Mt. Logan included the analysis of stable isotopes of oxygen and hydrogen (Fisher et al., 2008; Fisher et al., 2004; Fisher, 2011; Holdsworth et al., 1991; Holdsworth and Krouse, 2002) and concentrations of major ions and trace elements (Osterberg et al., 2008; Osterberg et al., 2006). Stable isotope records suggest that the PR Col has been influenced by different airflow regimes over the last 8000 years that shifted between more zonal and more mixed transport of moisture

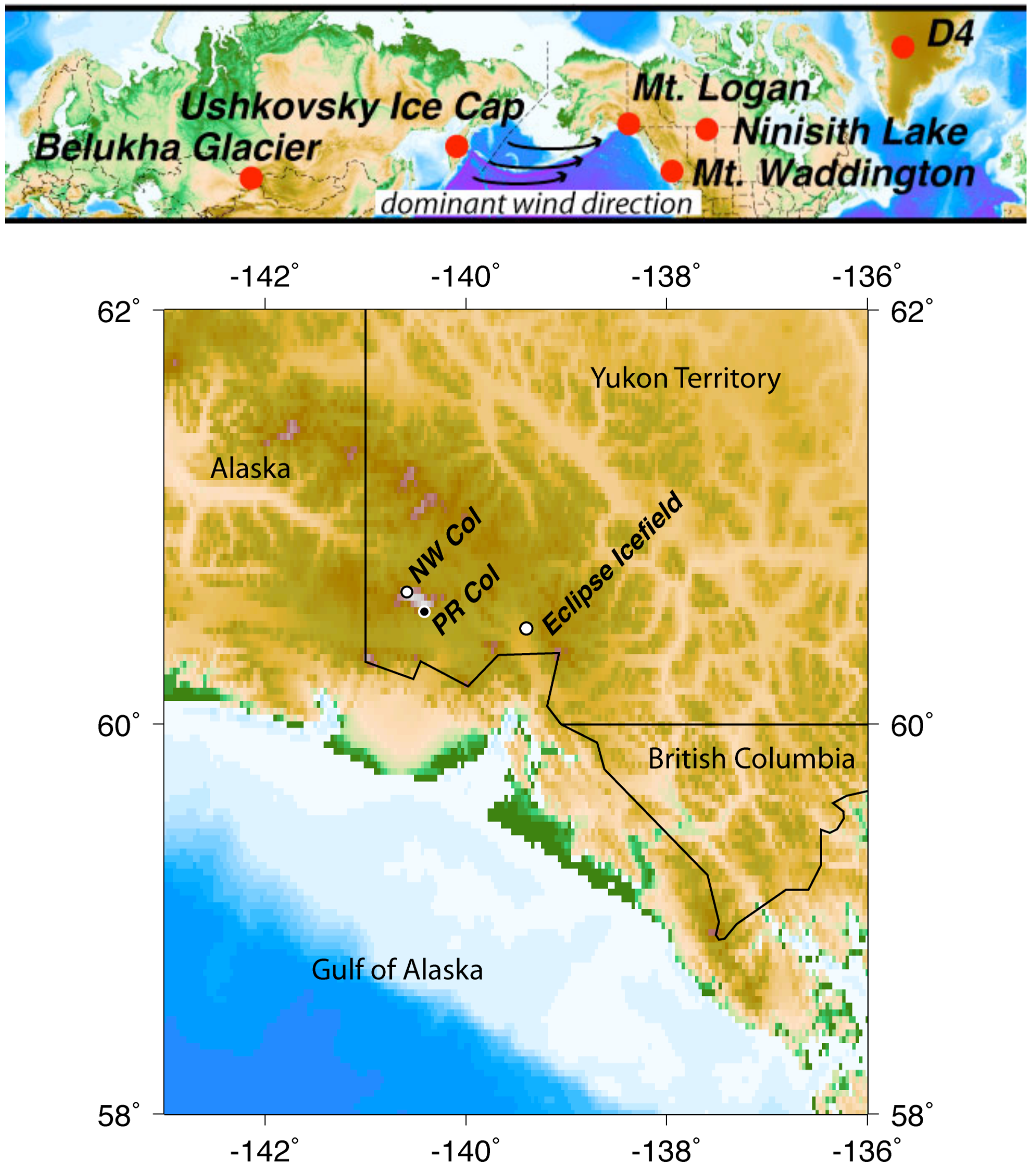

Figure 17 – Maps of ice core drill sites and the collection sites of other records mentioned in this manuscript including arrows to indicate the prevailing wind direction. The lower panel is an enlarged map of Mt. Logan and the surrounding area. The Prospector Russell (PR) Col and Northwest (NW) Col sites are located 5300 m.a.s.l. and 5430 m.a.s.l., respectively, near the summit of Mt. Logan. The Eclipse Icefield is ~ 45 km distant, and ice cores from that site were retrieved ~ 3000 m.a.s.l. (e.g., Kelsey et al., 2012; Yalcin and Wake, 2001). These maps were generated using the USGS Woods Hole Scientific Center map generator (http://woodshole.er.usgs.gov/mapit/).

(Fisher et al., 2008; Fisher et al., 2004). The shifts are likely related to large-scale changes in the El Niño Southern Oscillation, the most recent (AD 1840) initiating a regime characterized by mixed southerly and westerly sources of moisture delivery, and that shift predates the record of BC examined here (Fisher et al., 2004). A distinct characteristic of the Mt. Logan stable isotope records is that a discontinuous, stair-step pattern is evident in the variation of isotopes with altitude. The accepted interpretation is that the atmosphere is multi-layered with distinct air masses from different sources, and that Mt. Logan precipitation samples different layers depending on the elevation (Holdsworth et al., 1991). The layers are segregated into a lower region < ~ 3 km that is more locally influenced, an upper region > ~ 5.3 km elevation associated with more distal sources of moisture, and a mixed layer that extends 1-2 km in between, each with distinct glaciochemistry (Holdsworth and Krouse, 2002). The PR Col (5300 m.a.s.l.) samples the upper layer, so a distal source must be considered when interpreting records from Mt. Logan.

More recently, Asia was identified as a distal source for the air masses sampled at Mt. Logan because a time series of Pb recorded in the PR Col core was interpreted to reflect rising Asian Pb emissions associated with recent industrialization, the burning of leaded gasoline, and less strict regulations of toxic emissions relative to European and North American policies (Osterberg et al., 2008). Mt. Logan is situated to record Asian emissions that undergo trans-Pacific transport (figure 17), thus fossil and biofuel emissions from large population centers in Asia must be considered as possible sources when interpreting the BC records preserved at the PR Col. The influence from Asian industrial emissions makes the PR Col core interesting for BC analysis because East Asia is thought to be the largest contributor of global BC (e.g., Bond et al., 2007; Bond et al., 2004; Novakov et al., 2003; Ramanathan and Carmichael, 2008; Streets et al., 2003; Streets et al., 2001) with known climate effects, including influence on temperatures and the timing and magnitude of precipitation (Lau et al., 2006; Menon et al., 2002; Qian et al., 2003), which in turn alters flood regimes and negatively affects agriculture for over 20% of the world's population (Auffhammer et al., 2006; Chameides et al., 1999; Menon et al., 2002).

Potential Sources of Black Carbon Recorded at Mt. Logan

Given its high elevation and geographical position relative to the predominant atmospheric circulation patterns (figure 17), Mt. Logan is likely influenced by some combination of both distal and local sources of BC. Local sources are likely dominated by Alaskan and Yukon forest fires with minimal contribution from anthropogenic sources given the sparse populations in those regions; however, it is noted that local shipping traffic in the Gulf of Alaska is a potential BC source. Hadley et al. (2007) modeled long-range transport of BC aerosols in the year 2004 and suggested that BC from Asia totaled 77% of the estimated BC emissions for North America. The majority of the BC was transported at high elevation (> 2 km) in the mid-troposphere (Hadley et al., 2007), where the PR Col is known to sample atmospheric pollutants (Holdsworth et al., 1991; Osterberg et al., 2008). Distal BC is likely dominated by Asian emissions from all of the emissions sources discussed previously in this chapter, but Asia is expected to deliver more anthropogenically-sourced BC compared to Alaska and the Yukon Territory given its large population centers and high level of industrial activity. This includes BC from the industrial sector (including manufacturing, power production, and transportation), residential emissions including coal and wood burning, and BC from agricultural land burning. Asian forest fires are also an important potential source of BC recorded at Mt. Logan.

Interpretations of other chemical records in ice from Mt. Logan and nearby sites indicate that forest fires are an important source of the delivery of chemical species to the region. NH_4^+ peaks in the Northwest (NW) Col ice core record (AD 1750-1979, location shown in figure 17) were interpreted to represent individual biomass burning events that likely occurred in Siberia (Whitlow et al., 1994). Records from nearby locations have also been interpreted to record Local forest fires; for example, CO_2 and limited soot measurements (measured by thermal-optical method described in Chapter II, (Chylek et al., 1992a)) in the NW Col record revealed a late 19th century increase in biomass burning associated with the Pioneer Agriculture Revolution, a period of episodic biomass burning (AD 1860-1890) associated with land clearing and agricultural practices in North America (Holdsworth et al., 1996). Yalcin et al. (2006) identified similar increases in Alaskan and Yukon biomass burning at the turn of the 19th century in ice core records from the Eclipse Icefield (location shown in figure 17).

Studying BC in the ice core from the PR Col on Mt. Logan is scientifically interesting because it furthers our understanding of forest fire frequency and intensity in Alaska, the Yukon Territory, and Siberia, and it provides insight into the effects that fire-born light-absorbing impurities have on climate. BC at Mt. Logan may also reflect East Asian BC from industrial and biofuel emissions that undergo trans-Pacific transport (Berntsen et al., 1999; Hadley et al., 2007; Heald et al., 2006; Jaffe et al., 1997; Jaffe et al., 2003; Osterberg et al., 2008; Primbs et al., 2007). Lastly, the BC record in the PR Col ice core allows us to estimate the albedo reduction by BC particles in the St. Elias Mountains.

This chapter continues with a brief discussion of sampling and analytical methods followed by the presentation of the AD 1852-1999 BC record from the PR Col ice core. The best judgment of source attribution for the BC is presented along with evidence to support the interpretation. Comparisons between the BC record from the PR Col and other relevant records are made including discussion of the factors controlling BC preservation at Mt. Logan that could cause differences between the records. The chapter concludes with an assessment of the climate impacts due to albedo reduction that could have occurred at the PR Col given the observed BC concentrations in the ice.

Sampling Methods

The 186 m ice core from the PR Col was sampled using a continuous melter at the Climate Change Institute at the University of Maine (Osterberg et al., 2006). The sampling resulted in 6900 total samples at 1-5 cm/sample depth resolution, and 5-30 samples/year for the ~ 8,000 continuous years represented in the core (Osterberg et al., 2008). The core was dated prior to this work by annual layer counting of the oscillations in $\delta^{18}O$, [Na^+], and [U], and by identification of historic volcanic eruptions in the crustal element records (Osterberg et al., 2008). The samples used for BC analysis in this study were previously analyzed for major ions (ion chromatography (IC)), trace elements (inductively coupled plasma mass spectrometry (ICPMS)), and stable isotopes (mass spectrometry (MS)) at the Climate Change Institute, University of Maine (Osterberg et al., 2008; Osterberg et al., 2006), and many of these (and other) chemical records are used in this study for assessment of the BC record (table 3).

Two thousand sixty nine samples were analyzed for BC concentration to create a high-resolution record of BC that spans AD 1852-1999. Every available sample was analyzed for BC for the period AD 1939-1999 resulting in 20-40 samples/ year for the period AD 1939-1989 and 5-15 samples per year for the period AD 1990-1999. Every other sample was analyzed prior to AD 1939 due to the large number of samples and the amount of time demanded by the analysis, which resulted in 10-20 samples/ year. BC concentrations in the PR Col were measured at CWU using the Single Particle Soot Photometer (SP2) coupled to a CETAC U5000 AT+ ultrasonic nebulizer. The protocol for liquid sample analysis of BC concentrations outlined in Chapter II was followed for all samples. Each sample was sonicated for 20 minutes prior to analysis and agitated with a magnetic stir bar while introduced into the CETAC nebulizer. Data for ten thousand BC particles were recorded over multiple minutes of integration time when possible, but this was not always allowed by sample volume limitations (typical sample volumes 1-3 mL). Measured BC concentrations ($_{meas}$BC) were calibrated using Aquadag standards following the methods described in Chapter II. The calibrated BC concentrations are hereafter reported as $_{cal}BC$. It is important to note that $_{cal}BC$ does not reflect a true BC concentration since the measurement includes BC losses that occurred

Table 3 – Chemical records from ice cores and lake sediments presented in this chapter or discussed for comparison to the BC record in the PR Col ice core. Previously unpublished data are indicated with an asterisk. Published data was obtained from the NOAA National Climatic Data Center (http://www.ncdc.noaa.gov/paleo). BC analysis was performed at Central Washington University, Ellensburg, WA, USA. The analyses of major ions and trace elements in the PR Col and Eclipse ice cores were performed at the University of Maine, Orono, ME, USA. The analyses of major ions and trace elements in the Bulkha Glacier core were performed at the Paul Scherrer Institut, Villigen, Switzerland. The location of the analysis of charcoal in sediments from Ninisith Lake, Alberta, Canada is unknown. The analyses of BC and Vanillic Acid in the Greenland D4 ice core and BC in the Mt. Waddington ice core were performed at the Desert Research Institute, Reno, NV, USA.

Record	Analysis	Core, Region, or Site	Reference
$_{cal}BC^{*}$	SP2	PR Col	This Work
$[K^{+}]^{*}$	IC	PR Col	(Osterberg et al., unpublished data)
$[NO_3^{-}]^{*}$	IC	PR Col	(Osterberg et al., unpublished data)
[Pb]	ICPMS	PR Col	(Osterberg et al., 2008)
$[SO_4^{2-}]$	IC	PR Col	(Osterberg et al., 2008)
$[Fe]^{*}$	ICPMS	PR Col	(Osterberg et al., unpublished data)
[Al]	ICPMS	PR Col	(Osterberg et al., 2008)
$[Na^{+}]^{*}$	IC	PR Col	(Osterberg et al., unpublished data)
$[U]^{*}$	ICPMS	PR Col	(Osterberg et al., unpublished data)
$\delta^{18}O$	MS	PR Col	(Fisher et al., 2004)
$[NH_4^{+}]$	IC	Eclipse	(Yalcin et al., 2006)
$[K^{+}]$	IC	Eclipse	(Yalcin et al., 2006)
$[NO_3^{-}]$	IC	Eclipse	(Yalcin et al., 2006)
$[K^{+}]$	IC	Belukha	(Eichler et al., 2011)
$[NO_3^{-}]$	IC	Belukha	(Eichler et al., 2011)
BC	SP2	D4	(McConnell et al., 2007)
Vanillic Acid	MS	D4	(McConnell et al., 2007)
BC	SP2	Waddington	(Neff et al., 2012)
Burn Area	-	Alaska	(Kasischke et al., 2002)
Burn Area	-	Yukon	(Yukon Wildland Fire Management)
Charcoal	counting	Ninisith Lake	(Larsen et al., 2000)

in the samples due to treatments and storage procedures that are standard for the previous IC and ICPMS analyses (described below). The designation $_{cal}$BC simply refers to a measurement that has been corrected for losses in the CETAC nebulizer using Aquadag standards according to the procedure described in Chapter II.

Because of the other analyses performed on the PR Col samples, the samples had been acidified, refrozen, melted, and stored in the liquid phase in polypropylene vials at room temperature for multiple years prior to BC analysis at Central Washington University (CWU) (E. Osterberg, Research Assistant Professor, Dartmouth College, 2011, personal commun.). The results of experiments conducted at CWU indicated that each of the aforementioned treatments could cause BC losses (agglomeration or losses to vial walls), resulting in underestimated BC concentrations in measured samples (see Chapter II for thorough discussion of methodological experiments). Because of these treatments, the BC concentrations in the PR Col samples represent minimum estimates of actual BC concentrations, but a qualitative record of BC changes in the atmosphere is still preserved. Such a record is useful for assessing the timing and relative magnitude of changes in the amount of BC in the atmosphere. The evidence that a qualitative record of BC is preserved in the archived core comes from the BC analysis of samples that were cut from segments of fresh ice that had been stored frozen since the retrieval of the core in 2002 and 2003. Samples were cut at ~ 5 cm/sample resolution in December 2012 from multiple sections of the core that totaled ~ 8 m in length. The samples were analyzed using the SP2 at CWU following the protocol outlined in Chapter II. Importantly, samples were kept frozen until just prior to analysis. Almost every ${}_{cal}$BC peak in the archived record is reflected by a ${}_{cal}$BC peak in the record developed from the fresh ice (figure 18). The ${}_{cal}$BC measurements from fresh ice samples were consistently higher than ${}_{cal}$BC in the archived samples, but the magnitude of the difference in ${}_{cal}$BC is not consistent enough to allow correction of the entire archived record (figure 18). Linear regression of the data indicate that 39% of the variation in the fresh ice ${}_{cal}$BC may be explained by variation in the ${}_{cal}$BC measured in archived samples ($n = 148$, $R^2 = 0.39$, $p < 0.001$) (figure 19). The records were resampled to the same depth resolution in order to perform the regression. A direct 1:1 correlation is not expected for the two records because of small-scale variability in the ice, potential depth offsets that could occur naturally between the two slabs, or depth offsets that resulted from using different sampling procedures for the archived and fresh

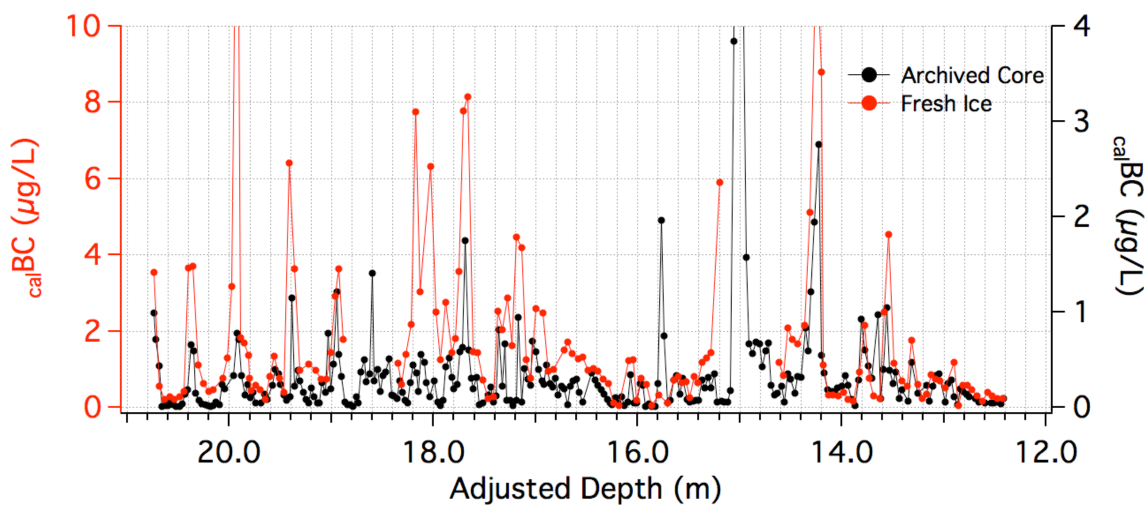

Figure 18 – ${}_{cal}$BC measured in the archived PR Col samples compared to ${}_{cal}$BC measured in fresh PR Col samples that were kept frozen until just prior to analysis.

samples. Importantly, every peak in ${}_{cal}$BC in both the archived and fresh ice records is comprised of multiple samples (figure 18), suggesting that the archived PR Col core preserves a real (albeit qualitative) record of BC concentrations through time, and that the observed changes in ${}_{cal}$BC in the archived record (and the fresh ice record) are indicative of real fluctuations in the deposition of BC to the PR Col drill site. Fluctuations in the deposition of BC are considered a proxy for BC concentrations in the atmosphere, although quantitative determination of true atmospheric BC concentration is not possible from the ice core record regardless of the BC losses in the archived samples because BC deposition is influenced by other factors besides the amount of BC in the atmosphere (e.g. atmospheric circulation, precipitation, scavenging efficiency, and post-depositional processes), and a reliable model to back out

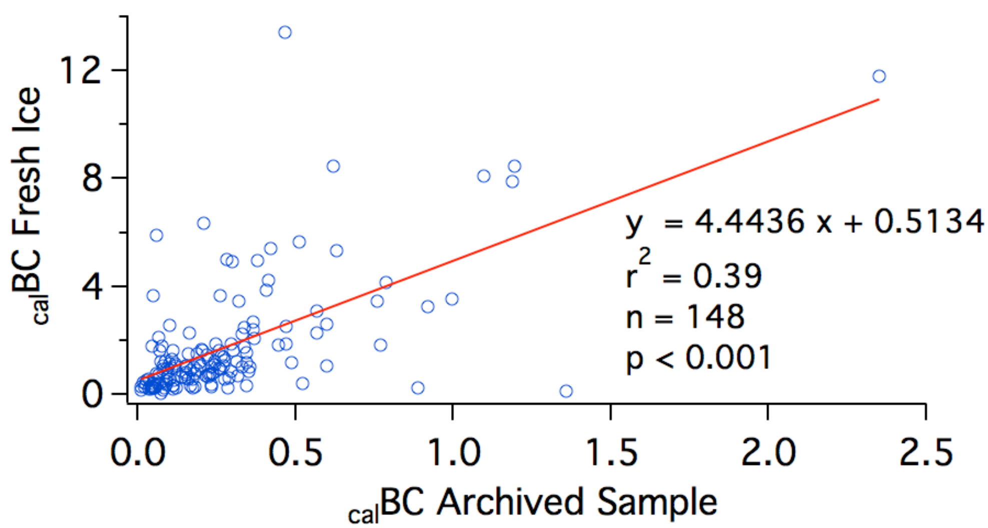

Figure 19 – Linear regression of 148 ${}_{cal}$BC measured in fresh ice (no BC losses) and archived samples (experienced BC losses). The ${}_{cal}$BC depth series were resampled to 5 cm resolution.

atmospheric BC concentrations from ice core records does not exist. The timing and magnitude of changes in $_{cal}BC$ and the source of the BC observed in the record are explored below.

Results and Discussion

The BC Record from the Prospector-Russell Col, Mt. Logan

Parts of the BC record appear to preserve a seasonal signal, which is also reflected in the [K^+] record, however seasonality in the BC signal is not evident in the majority of the time series (figure 20). The BC seasonality is most obvious during the period AD 1970-1980 (figure 20C), although the seasonality during that period is less apparent in the [U] and [Na^+] records that were used to date the ice core by annual layer counting (Osterberg et al., 2008). Annual layer counting of seasonal oscillations in chemical records is often sufficient for delineating the depth-age relationship at yearly timescales, but it can be insufficient for defining the sub-annual temporal scale if the seasonality is not well preserved in the chemical records. Since the seasonality in the [U] and [Na^+] records does not appear similar to the seasonality preserved in the $_{cal}BC$ record for the best section of BC seasonality (figure 20C) and because much of the core was analyzed for BC at lower resolution than the major ions and trace elements with which the core was dated, the interpretation of sub-annual trends in the BC record is avoided.

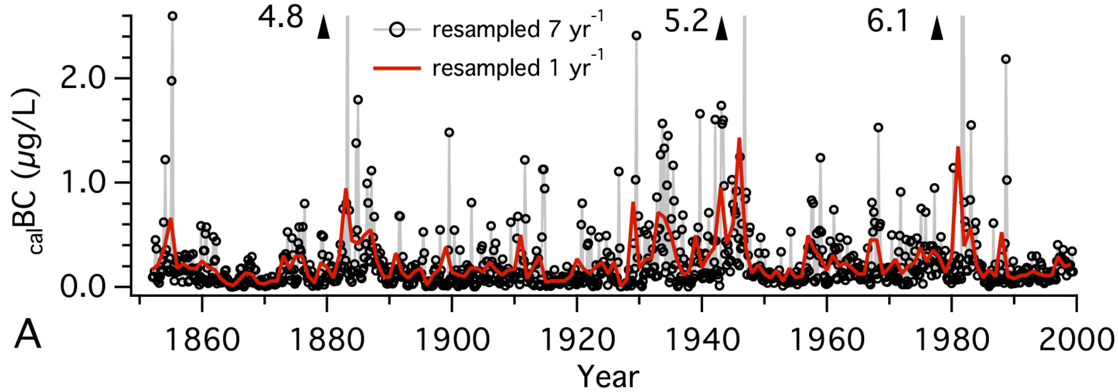

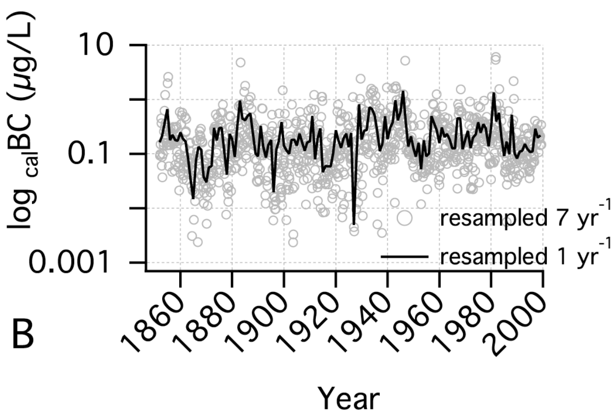

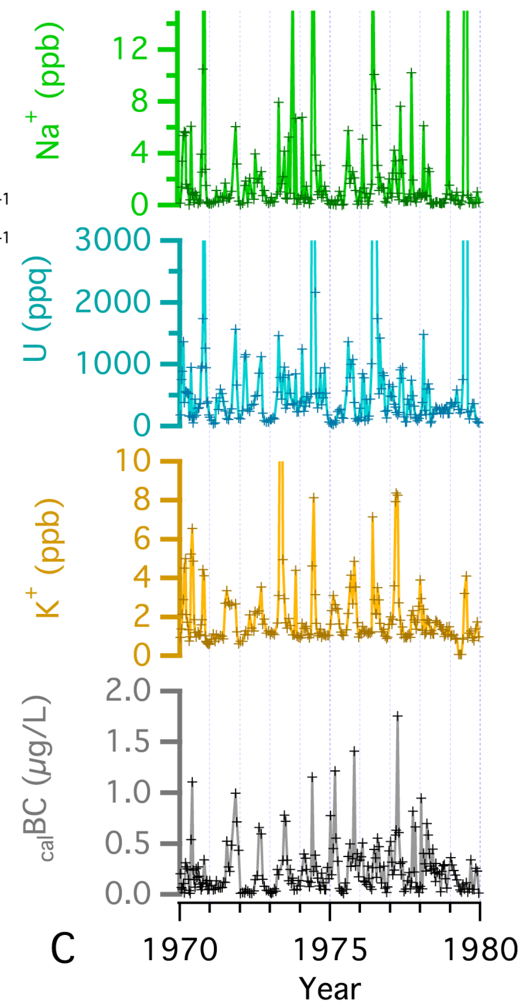

Figure 20 - (A) Detailed records of $_{cal}$BC from the PR Col ice core, and (B) log $_{cal}$BC. The time series in (A) and (B) were resampled to the same resolution (7 samples/yr) because of layer thinning that occurs with depth in the core. (C) AD 1970-1980 section of the BC record at high resolution compared to [K^+], [U], and [Na^+] records also from the PR Col core. The records in (C) are high-resolution data that were not resampled to 7 samples/yr.

The Logan PR Col $_{cal}$BC record is characterized by low BC concentrations (mean $_{cal}$BC = 0.25 μg/L, max $_{cal}$BC = 6.1 μg/L) punctuated by peaks in $_{cal}$BC from 0.47-6.1μg/L (Fig 20A). The detailed $_{cal}$BC record was resampled to the same resolution (7 samples/yr) because of thinning of layers that occurs at depth in the core due to glacier flow. The record indicates 5-10 year periods of elevated $_{cal}$BC (figure 20A). These periods of time are most apparent in the 1850s, 1880s, 1930s, 1940s, and 1980s (figure 20A). A rise in the background $_{cal}$BC is also evident during these time periods (figure 20B).

BC Source Attribution

In order to separate and weigh the relative importance of different sources of the BC observed in the PR Col ice core, various technique are employed to partition the BC broadly into biomass burning and industrial sources. These techniques include a statistical method called empirical orthogonal function (EOF) analysis that associates various chemical time series depending on their co-variance (Meeker and Mayewski, 2002), the examination of other relevant chemical records from Mt. Logan and neighboring locations (listed in table 3), analysis of individual peaks in the BC record and peaks in other chemical records that coincide at depth in the PR Col core, and examination of satellite imagery to identify smoke plumes over Mt. Logan.

Co-Variance of BC and other Chemical Records

EOF analysis (Meeker and Mayewski, 2002) was performed to analyze the co-variance of multiple chemical records from the PR Col (listed in table 3) through time and determine whether and to what extent the records vary together. The results of the EOF analysis indicate that variation in ${}_{cal}BC$ is primarily associated with two function groups (EOF 2 and EOF 5) that explain 15% and 7.4% of the total variance in the dataset of all records, respectively (table 4). EOF analysis is useful because associations

Table 4 –EOF analysis on the suite of available chemical records from the PR Col ice core listed in table 3. Only the five function groups that explain the most variation in the dataset are shown. The EOF analysis was run on the high-resolution datasets prior to resampling. High co-variance is highlighted in each function group.

	EOF	1	2	3	4	5
	Total Variance Explained	38.8	15	10.6	7.7	7.4
Variance in Chemical Signal Explained by EOF	[Pb]	27.4	14.7	10.7	9.2	16.7
	[Al]	56.2	-14.1	1.1	-13.8	1.4
	[Fe]	71.1	-13.4	0.9	-6.1	0.7
	[K^+]	19.4	27.8	-14.8	0	-14.1
	[NO_3^-]	38.2	11.9	-1.7	-6.9	-7.1
	[Na^+]	51.5	-1.6	-0.1	13.9	-7.4
	$\delta^{18}O$	0	8.6	75.1	-0.3	-12.2
	[U]	73.9	-6	0.2	0.1	-0.2
	[SO_4^{2-}]	40.9	0.2	-0.9	19.4	1.2
	${}_{cal}BC$	9.1	51.3	-0.4	-7.5	13.3
	General Interpretation	Mixed Seasonal	Biomass Burning	Precipitation	Marine	Fossil Fuel

between chemical species become apparent when high portions of their variance are loaded in the same function group. BC is associated in such a way with [K^+] in EOF 2 and [Pb] in EOF 5 (table 4). The function groups relevant to BC are discussed in more detail below with justifications for their interpretation, but for now it is noted that the general interpretations of EOF 2 and 5 are biomass burning and fossil fuel emissions, respectively. A third function group (EOF 1) that explains 38.8% of the variation in the whole dataset is likely a mixed seasonal signal particularly influenced by dust because of the high loadings of the crustal elements Al, Fe, and U (table 4). EOF 3 and 4 are generally interpreted as precipitation and marine signals because of the high loadings of $\delta^{18}O$ and Na^+, respectively (table 4).

Biomass Burning Source

Previous studies have noted the usefulness of ice core records of [K^+], [NO_3^-], and [NH_4^+] as tracers of biomass burning events (e.g., Eichler et al., 2011; Whitlow et al., 1994; Yalcin et al., 2006). Nitrogen oxides are emitted during forest fires, which are quickly converted to HNO_3 and NO_3^- aerosols (Eichler et al., 2011). Elevated [K^+] has also been identified in aerosol plumes associated with biomass burning events (e.g., Owega et al., 2004; Song et al., 2005). The relationship between the [K^+] and [NO_3^-] records and the $_{cal}$BC record from the PR Col is explored below. [NH_4^+] was not measured in the PR Col ice core.

EOF 2, in which there are high loadings of $_{cal}$BC and [K^+] (table 4), is suggestive of a biomass burning source and is interpreted as evidence that the BC signal in the PR Col ice core is in part due to BC emitted from biomass burning events. [NO_3^-] plays a relatively minor role in EOF 2 and is loaded less heavily than [Pb], but it is noted that

Pb is also known to be emitted during biomass burning events (Hegg et al., 2009), and the amount of variance in [NO_3^-] (and [Pb]) is not insignificant in EOF 2 (table 4). Periods of elevated [K^+] and [NO_3^-] coincide with periods of elevated $_{cal}$BC in the 1880s, 1930s, 1940s, and 1980s (figure 21). Visual inspection of the detailed records indicates that individual peaks in $_{cal}$BC are coincident with peaks in [K^+] and [NO_3^-] (figure 21), which may be indicative of co-emission with BC during biomass burning events. An analysis of individual peaks in $_{cal}$BC was performed in order to examine how many peaks in the [K^+] and [NO_3^-] records were preserved at the same depth as peaks in $_{cal}$BC and to assess whether those $_{cal}$BC peaks were indicative of emissions from biomass burning events by their association with [K^+] and [NO_3^-]. Peaks in the $_{cal}$BC, [K^+], and [NO_3^-] time series were defined as concentration elevated above the mean plus one standard deviation ($_{cal}$BC > 0.68 μg/L, [K^+] > 5.2 ppb, [NO_3^-] > 80.3 ppb). Samples with $_{cal}$BC > 0.68 μg/L that were adjacent at depth in the core were not counted as individual peaks since they likely resulted from the same event during which BC deposition was elevated. Forty-four peaks were identified in the $_{cal}$BC record, 60% of which occurred coincidentally with peaks in [NO_3^-] or [K^+] and likely indicate increased fire emissions. These events are marked in figure 21, and the statistics of the peak analysis are summarized in table 5. If peaks were defined more loosely (concentration elevated above the mean plus one half the standard deviation), the number of $_{cal}$BC peaks that occur coincidentally with peaks in [NO_3^-] or [K^+] is 72% of the total peaks in $_{cal}$BC (table 5). The fact that the majority of peaks in the $_{cal}$BC record

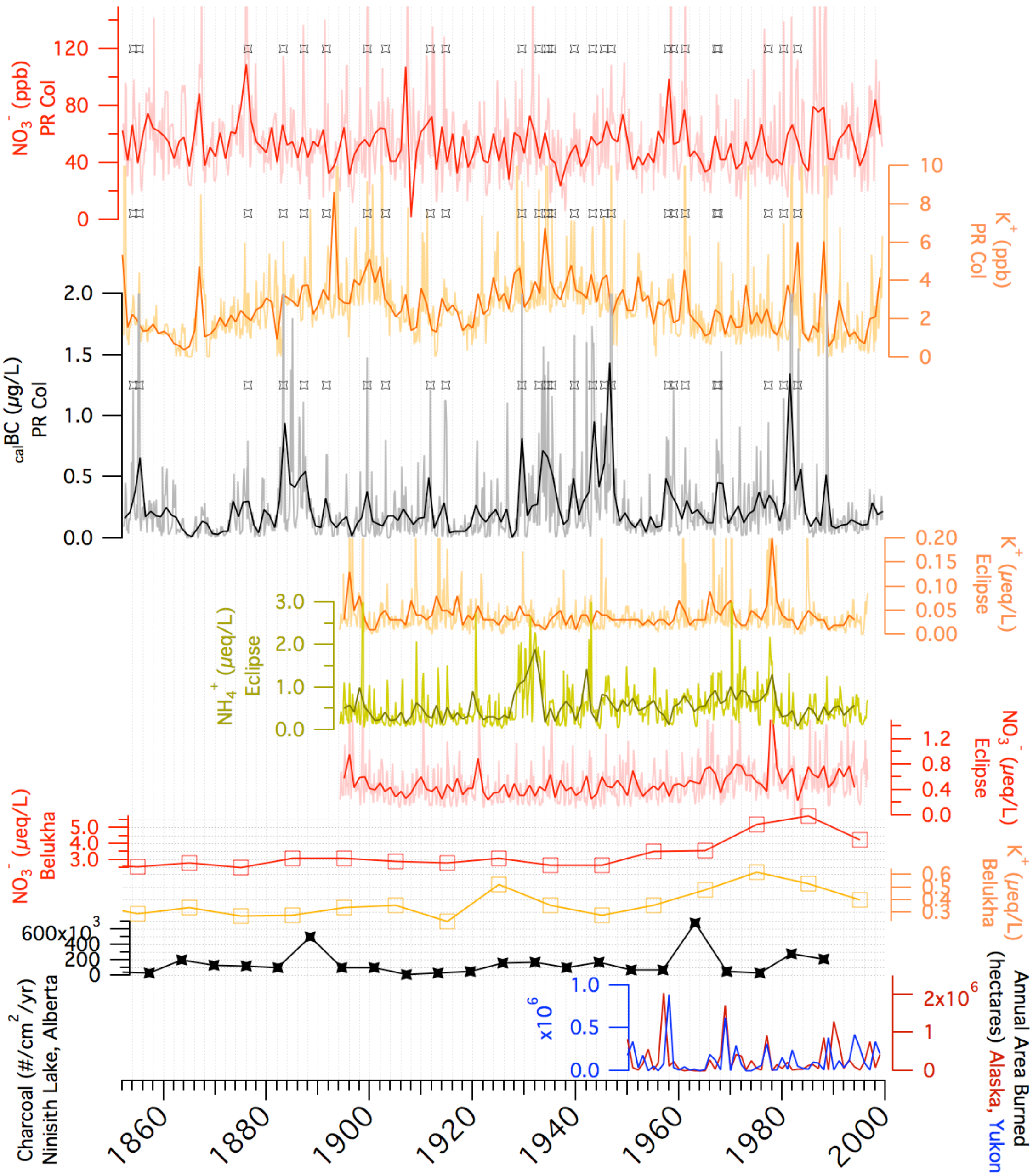

Figure 21 – The record of $_{cal}$BC from the PR Col compared to other glaciochemical records relevant to biomass burning including records from the PR Col, the Eclipse Icefield, and Belukha Glacier in the Siberian Altai (described in table 3). A charcoal record from Ninisith Lake, Alberta, Canada, and annual fire spatial statistics from the Yukon Territory and Alaska are also included (also described in table 3). Individual fire events identified by analysis of peaks in the $_{cal}$BC, [NO_3^-], and [K^+] records from the PR Col are marked with black boxes. Detailed glaciochemical records (resampled to 7 samples/year) are shown in light colors, and annual records are shown in bold colors.

Resolution of the records from the Belukha Glacier and Ninisith Lake are 1 sample/10 years and 1 sample/6 years, respectively.

Table 5 – Summary of analysis of peaks in the $_{cal}$BC, [K^+], and [NO_3^-] records. Peaks were either defined as concentration > mean plus one standard deviation ($_{cal}$BC > 0.68 μg/L, [K^+] > 5.2 ppb, [NO_3^-] > 80.3 ppb) or concentration > mean + one half standard deviation ($_{cal}$BC > 0.47 μg/L, [K^+] > 3.9 ppb, [NO_3^-] > 38.8 ppb). The number of peaks in $_{cal}$BC is reported along with the number of those peaks that are coincident with peaks in [K^+] and [$NO_3^=$] and the number of $_{cal}$BC peaks coincident with either [K^+] or [NO_3^-]. $_{cal}$BC peaks coincident with peaks in [Pb] were not counted, even if there were coincident peaks in [K^+] or [NO_3^-]. The portion of $_{cal}$BC peaks denotes the fraction of the total peaks identified in $_{cal}$BC.

Chemical Species	*# peaks*	*portion of $_{cal}$BC peaks*
	peak = concentration > mean + σ	
$_{cal}$BC	44	
$_{cal}$BC with [K^+] and [NO_3^-]	13	0.3
$_{cal}$BC with [K^+] or [NO_3^-]	26	0.6
	peak = concentration > mean + ½ σ	
$_{cal}$BC	71	
$_{cal}$BC with [K^+] and [NO_3^-]	28	0.4
$_{cal}$BC with [K^+] or [NO_3^-]	51	0.72

are coincident with peaks in [K^+] or [NO_3^-] is interpreted as evidence that some portion of the BC signal in the PR Col is related to biomass burning.

More evidence for a biomass burning source for the BC observed in the PR Col core comes from observations of forest fire smoke plumes over Mt. Logan. Holdsworth et al. (1988) noted that from the Eclipse Icefield (location shown in figure 17) "Mount Logan was almost obscured by blue haze on 4 July [1986]" (Holdsworth et al., 1988) and that snowfall occurring at the same time exhibited elevated concentrations of NO_3^-. Although the ceiling of the smoke was estimated at < 4000 m elevation, below the PR Col drill site, other plumes have been observed at Mt. Logan with ~ 5000 m ceilings

(Holdsworth et al., 1996), and the observers concluded that the impact of forest fire smoke on Mt. Logan snow chemistry must be considered when interpreting chemical records from Mt. Logan ice cores (Holdsworth et al., 1988). Satellite imagery of smoke from forest fires occurring in Alaska and Western Canada in 2004 also suggests a biomass burning source for the BC observed in the PR Col ice core (figure 22). Interestingly, the haze observable in figure 22B extends into Siberia. Although the fire smoke captured in that image was sourced by forest fires in Alaska and the Yukon Territory, the extent of the smoke suggests that Siberian forest fires may also be a source for BC at the PR Col. Future examination of satellite imagery from periods of time that overlap with the BC record from the PR Col might be valuable for matching peaks in ${}_{cal}$BC to individual forest fire events.

If BC recorded at Mt. Logan indeed originates from biomass burning, it is likely that forest fires in Alaska, the Yukon Territory, and Siberia are the predominant source regions. Other records interpreted as forest fire records must be examined in order to identify the similarities and differences between those records and the record of ${}_{cal}$BC and to determine how the source regions interpreted for those records relates to the record of ${}_{cal}$BC. Records will not appear identical to the records from the PR Col ice core because of differences in atmospheric circulation that transport emissions to the various sites, but similarities between records might be interpreted as large-scale fire activity and/or atmospheric circulation patterns that transported BC (and other chemical species) over wide areas. Whitlow et al. (1994) identified peaks in the [NH_4^+] record from the NW Col ice core, which is located on Mt. Logan 5430 m.a.s.l. near the PR Col

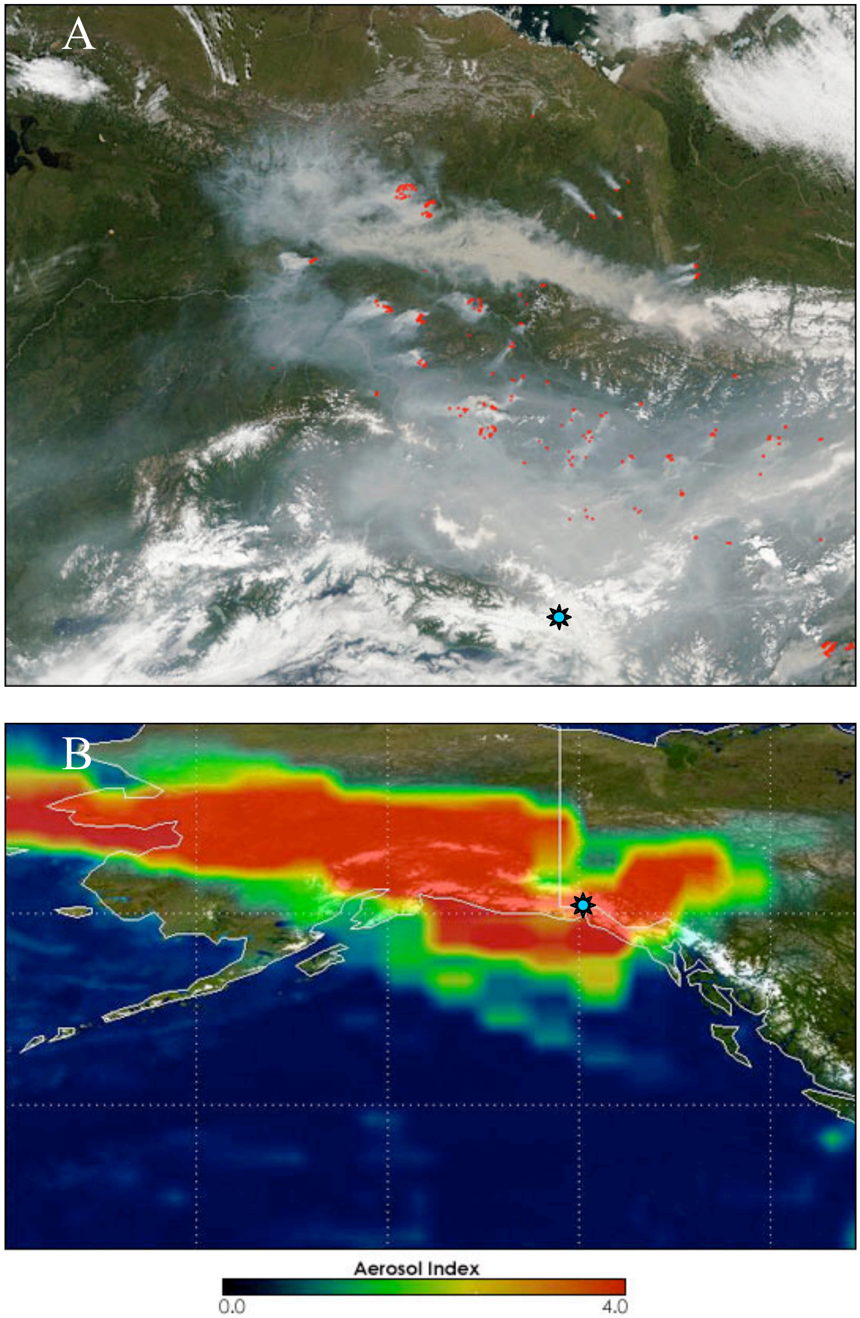

Figure 22 – Satellite imagery of smoke over Mt. Logan. Image (A) was captured by the NASA Moderate Resolution Imaging Spectroradiometer (MODIS) on June 27, 2004. The boundaries of individual fires are delineated in red. Image (B) is aerosol optical depth interpreted by the NASA Total Ozone Mapping Spectrometer (TOMS) on June 30, 2004. Areas with the greatest amount of particles in the atmosphere are colored red.

Mt. Logan is marked with a blue star in both images. Images were downloaded from the NASA Earth Observatory (http://earthobservatory.nasa.gov).

(location shown in figure 17). Peaks in [NH_4^+] were associated with peaks in [K^+] and [NO_3^-] (data not shown) and were attributed to individual biomass burning events (Whitlow et al., 1994). [NH_4^+] peak frequency was high for the periods AD 1850-1870 and AD 1930-1980, which are periods of time that coincide with elevated $_{cal}$BC observed in the PR Col ice core (figure 21). Whitlow et al. (1994) noted that there is not a one-to-one correspondence between [NH_4^+] peaks and documented large fires. This is also the case for peaks in the $_{cal}$BC record from PR Col, although it is noted that there is some coincidence between years of documented high burn area in Alaska and the Yukon Territory and high $_{cal}$BC in the PR Col record (figure 21). Differences between the NW Col [NH_4^+] record and records of [NH_4^+] in Greenland ice cores led to the interpretation that the source region for biomass burning emissions was different for the two sites and that the NW Col was more influenced by Siberian forest fires (Whitlow et al., 1994). The PR Col likely also records emissions from Siberian fires, but it is probable that the factors controlling the transport and deposition of BC to the PR Col cause the source region to change depending on the conditions (e.g. sometimes more local, sometimes more distal). Factors controlling BC deposition to Mt. Logan are described in more detail below.

Similar to Whitlow et al. (1994), peaks in the [NH_4^+] and [K^+] records from the Eclipse Icefield (location shown in figure 17) were interpreted to represent periods of high fire activity in the 1860s, 1880s, 1890s, 1920s-1940s, and 1980s (Yalcin et al., 2006). The Eclipse Icefield is located at lower elevation (3000 m.a.s.l.) than the PR Col (5300 m.a.s.l.) and may sample different air masses with different source regions. Detailed records of [NH_4^+], [K^+], and [NO_3^-] were only available from the Eclipse Icefield for the period AD 1894-1997, but time periods when these records are elevated show some coincidence with time periods when $_{cal}$BC is elevated in the PR Col ice core, particularly for the periods AD 1930-1950 and AD 1960-1990 (figure 21). The records from the Eclipse Icefield resembled ice core records from Greenland more closely than the records from the nearby NW Col ice core, and the investigators concluded that the Eclipse Icefield was likely more influenced by local Alaskan and Yukon fires while Mt. Logan was more influenced by Siberian fires (Yalcin et al., 2006).

Ice core records of [NO_3^-] and [K^+] from the Belukha Glacier were used to reconstruct a history of Siberian forest fires (Eichler et al., 2011). The authors concluded that there was no significant rise in forest fire activity in Siberia over the past 300 years, however the records from Belukha Glacier do indicate elevated [NO_3^-] and [K^+] for the period AD 1960-1980, which is coincident with elevated $_{cal}$BC in the PR Col core (figure 21). Ice core records of vanillic acid and dehydroabietic acid (biomass burning tracers) from the Ushkovsky ice cap in Northern Siberia (figure 17) suggest that forest fires have increased in frequency over the past century (Kawamura et al., 2012). This is consistent with fire statistics that indicate a recent trend toward more frequent extreme fire years (Soja et al., 2007) but inconsistent with the aforementioned records from the Siberian Altai. The Belukha Glacier in the Siberian Altai is geographically located in central Asia and likely does not record all fires in Northern Siberia that are important for BC delivery to Mt. Logan (figure 17), whereas the Ushkovsky ice cap is downwind of boreal forests in Northern Siberia and is more likely to record similar events as Mt. Logan. Although the BC record from the PR Col core does not suggest rising forest fires frequency over the last century, some large fire events recorded in the Ushkovsky records are reflected in the Logan BC record, particularly large fires identified in AD 1883, 1915, and 1949 (Kawamura et al., 2012). Additionally, comparison to a charcoal record from Ninisith Lake, Alberta, Canada (Larsen et al., 2000) also reveals some coincidence between elevated $_{cal}$BC and high charcoal counts in the lake sediments in the 1880s (figure 21).

The similarities and differences between other records and $_{cal}$BC presented in this study suggest that BC, K^+, and NO_3^- delivery to the PR Col and the other sites discussed here is complex with a number of factors likely controlling the transport of biomass burning emissions to Mt. Logan. It is also unlikely that biomass burning is the sole source for the BC observed in the PR Col core (other sources are discussed below). Several general conclusions may still be drawn at this point. For one, biomass burning is a source of the BC deposited at the PR Col, and the BC measured in the PR Col ice core that is attributed to biomass burning is likely sourced by a combination of forest fires from Alaska, the Yukon Territory, and Siberia. Prevailing wind conditions, the amount of convective energy available to lift BC particles to > 5000 m.a.s.l., and the occurrence of precipitation events to scavenge the BC from the atmosphere and preserve it in snow at the PR Col are all processes that could affect the preservation of BC in the PR Col ice core and lead to differences between the $_{cal}$BC record and other records that have been interpreted as forest fire records. Other sources of BC (e.g. industrial emissions) could also influence the $_{cal}$BC record from the PR Col, and different sources could have been more influential at different times in the past. The possibility of an industrial source for the BC measured in the PR Col ice core is evaluated below.

Industrial Source

Possible industrial sources of BC deposited at the PR Col include activities like manufacturing, power production, and shipping and transportation. These emissions could be sourced from Asia or more locally (e.g. Alaska and the Yukon Territory), but Asia is the more likely source region because of the higher number of large population centers and greater amount of industrial activity. Similar to the assessment of a biomass source in the previous section, a variety of techniques are employed to determine the likelihood of an industrial source for the BC observed in the PR Col ice core. These include EOF analysis, an analysis of individual peaks in the $_{cal}$BC record to identify coincident peaks in chemical species associated with industrial emissions (e.g. [Pb]), and comparison to other time series that have been interpreted as industrial emissions records. This section continues with the presentation of results that suggest an industrial source for the BC in the PR Col ice core and discussion of the source regions for industrial BC.

Statistical EOF analysis indicates that there is a linkage between $_{cal}$BC in the PR Col core and industrial emissions because EOF 5 is characterized by relatively high loadings of ${}_{cal}$BC and [Pb] (table 4). Although it has been associated with forest fire emissions (e.g., Hegg et al., 2009), Pb is predominantly an industrial pollutant that is emitted from metal smelting, fossil fuel burning, and the use of leaded gasoline (Osterberg et al., 2008; Pacyna and Pacyna, 2001). It is also noted that [NO_3^-] and [K^+] are negatively loaded in EOF5, indicating that when [Pb] and ${}_{cal}$BC increased, [NO_3^-] and [K^+] decreased. The inverse association between [NO_3^-], [K^+], and [Pb] in EOF 5 is evidence that EOF 5 is representative of an industrial source, and the positive association between [Pb] and ${}_{cal}$BC and in EOF 5 is evidence that BC recorded at the PR Col is to some extent sourced by industrial emissions.

Individual peaks in the ${}_{cal}$BC record were analyzed to see if peaks in [Pb] were coincident at depth. Peaks in ${}_{cal}$BC coincident with [Pb] could indicate times when conditions were right for the trans-Pacific transport of industrial emissions from Asia or periods of higher industrial activity in Asia or locally. Significantly fewer peaks in ${}_{cal}$BC are coincident with peaks in [Pb] relative to the number of peaks in ${}_{cal}$BC that are coincident with peaks in [K^+] or [NO_3^-] (tables 5 and 6). It is noted that all of the coincidental peaks in the [Pb] and ${}_{cal}$BC records are also concurrent with peaks in [K^+] and/or [NO_3^-], which are known to be associated with forest fire smoke plumes (see previous section and Eichler et al., 2011). The peaks with simultaneously elevated [Pb], ${}_{cal}$BC, [K^+] (and/or) [NO_3^-] were not counted in the previous analysis when interpreting elevated biomass burning emissions (results in table 5) because of the conclusion of previous investigators that [Pb] observed in the PR Col ice core is largely attributed to Asian industrial emissions (Osterberg et al., 2008). However, it is noted that Pb is also known to be associated with forest fire smoke plumes, particularly in Russian forest fires (Hegg et al., 2009), which means that the possibility of simultaneous peaks in $_{cal}$BC and [Pb] reflecting increased biomass burning rather than industrial emissions cannot be ruled out. In either case, the number of such peaks is small compared to the number of peaks in $_{cal}$BC and [K^+] or [NO_3^-] in which there is no elevated [Pb] (tables 5 and 6). The small number of peaks in $_{cal}$BC coincident with elevated [Pb] could simply

Table 6 - Summary of analysis of peaks in the $_{cal}$BC and [Pb] records. Peaks were either defined as concentration > mean plus one standard deviation ($_{cal}$BC > 0.68 μg/L, [Pb] > 59.7 ppb) or concentration > mean + one half standard deviation ($_{cal}$BC > 0.47 μg/L, [Pb] > 38.8 ppb). The number of peaks in $_{cal}$BC is reported along with the number of those peaks that are coincident with peaks in [Pb]. The portion of $_{cal}$BC peaks denotes the fraction of the total peaks identified in $_{cal}$BC.

Chemical Species	*# peaks*	*portion of $_{cal}$BC peaks*
	peak = concentration > mean + σ	
$_{cal}$BC	44	
$_{cal}$BC with [Pb]	2	0.05
	peak = concentration > mean + ½ σ	
$_{cal}$BC	71	
$_{cal}$BC with [Pb]	11	0.15

be a function of the nature of industrial emissions, which do not necessarily fluctuate in distinct events and are typically reflected in ice core records by changes in signal background rather than sharp peaks (e.g., McConnell et al., 2007; Osterberg et al., 2008). Such a change in background $_{cal}$BC is evident for certain periods of time, but not in such a way that reflects gradual and large-scale changes in regional industrialization (figure 20B). The association of $_{cal}$BC and [Pb] in EOF 5 (table 4) is still strong evidence that some of the BC signal is associated with industrial emissions regardless of having few coincident peaks in the signals. The sources of industrial BC recorded at Mt. Logan are examined below.

Likely industrial sources for the BC recorded in Mt. Logan ice include (1) local industrial emissions such as exhaust from shipping traffic in the Gulf of Alaska, and (2) industrial emissions from Asian factories, coal power plants, and the transportation sector that are transported across the Pacific Ocean. Previously, elevated [Pb] in the PR Col ice core during the period AD 1980-1999 (figure 23) was interpreted to reflect increases in Asian industrial activity and the increased use of leaded gasoline (Osterberg et al., 2008). The Pb observed in the PR Col was linked to Asian sources by three lines of evidence: (1) The trends in [Pb] are distinct from other ice cores that were interpreted to record European and North American sources of industrial emissions, (2) the migration of dust plumes from Asia to the Yukon Territory has been observed in satellite imagery, and (3) Asia was the only region to increase its Pb emissions during the period AD 1980-1999 (Osterberg et al., 2008). The $_{cal}$BC record from the PR Col does not reflect the trend of rising [Pb] during the last 20 years of the record, although some years do show elevated$_{cal}$BC (figure 23). $_{cal}$BC also does not reflect estimated BC emissions from East Asia or the Former USSR (figure 23), but some times of elevated $_{cal}$BC parallel times when BC emissions from the Former USSR were estimated to be relatively high (AD 1930-1950 and AD 1980-1990, figure 23).

Other ice core records have shown long-term trends associated with the timing of industrialization of different regions. For example, elevated BC concentrations from ~ AD 1890-1950 in a record from a Greenland ice core (figure 23) were attributed to

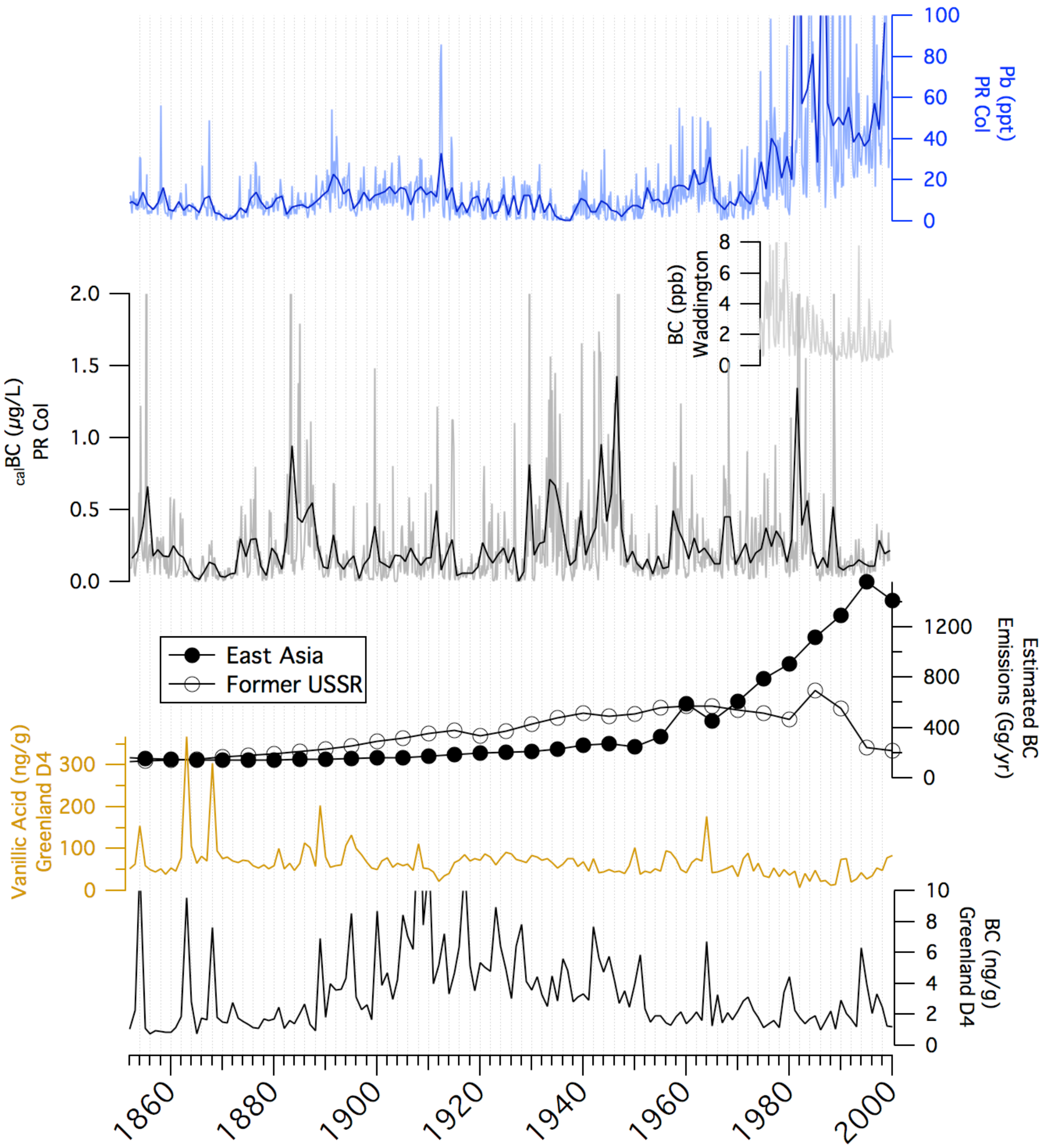

Figure 23 - The record of $_{cal}$BC from the PR Col compared to other glaciochemical records relevant to industrial emissions including records from the PR Col, the D4 site in Greenland, and Mt. Waddington, British Columbia, Canada (locations shown in figure 17). The resolution of the detailed records (light colors) from the PR Col and Mt. Waddington is 7 samples/year. The resolution of the records from Greenland is 1 sample/year. Estimated BC emissions based on documented fuel consumption are

shown for relevant source regions (Bond et al., 2007). More information about the records including references provided in table 3.

rising (and then falling) BC emissions in North America (McConnell et al., 2007). The BC was interpreted to be largely industrially sourced because BC concentrations that were in concert with vanillic acid concentrations (a tracer for forest fires) prior to the turn of the century distinctly rose out of phase with the vanillic acid beginning in the late 19thcentury (figure 23) (McConnell et al., 2007). The same trend is not reflected in the record from the PR Col, but this is expected since different source regions influence Mt. Logan andGreenland. Greenland is more ideally situated to record emissions from North America than Mt. Logan, which is upwind of most North American population centers (figure 17).

It is more surprising that BC observed in the PR Col ice core does not resemble the [Pb] record since (1) Pb and BC are known industrial pollutants, (2) Asia has been identified as an important source region upwind of Mt. Logan (e.g., Osterberg et al., 2008; Whitlow et al., 1994; Yalcin et al., 2006), and (3) East Asia is estimated to have emitted more BC in recent decades than other regions in the world (figure 16) (Bond et al., 2007; Bond et al., 2004; Novakov et al., 2003; Ramanathan and Carmichael, 2008; Streets et al., 2001). It is also surprising that the $_{cal}$BC time series does not more closely resemble the BC emissions estimates for the Former USSR since this region is also upwind of Mt. Logan and has had high BC emissions in the past (figure 23).

Although the $_{cal}$BC record from the PR Col is distinct from these records and estimates, the EOF analysis of other chemical records from the PR Col ice core indicates that there is some linkage between BC and industrial emissions at Mt. Logan. This raises the question, why is an industrial signal not stronger in the BC record from Mt. Logan? Feasible explanations include (1) that BC is not transported across the Pacific Ocean or deposited at Mt. Logan as efficiently as Pb, (2) that the industrial signal in $_{cal}$BC is weak enough to be overwhelmed by inputs from other sources such as biomass burning, or (3) that an industrial BC signal is complicated by the emission of BC from the residential use of coal and biofuels and/or open land burning in Asia. This study has thus far not touched on these two critical sources of BC. Both of these sources are likely more influential from Asia than more regional sources given the lack of large populations or extensive agriculture in Alaska or the Yukon Territory. The residential use of biofuel and coal is particularly important in Asia since the residential sector is estimated to contribute a considerable portion of the total Asian BC emissions (Bond et al., 2007; Bond et al., 2004; Ramanathan and Carmichael, 2008). It is possible that preservation of BC from the Asian residential sector was occurring prior to industrialization and that changes in the relative amount of BC from the residential and industrial sectors over time mask an otherwise apparent industrial signature in the record. The best assessment of the relative contribution of various sources to the BC record is briefly summarized in the following section.

Relative Contribution of Sources to BC at Mt. Logan

The contribution of biomass burning and industrial sources to the BC observed at Mt. Logan cannot be quantitatively determined from the analyses presented here, but the results of the EOF analysis and the comparison to other records shed light on the relative contribution of these broad types of emissions to the $_{cal}$BC record. The EOF analysis suggests that a biomass burning source is more influential than an industrial source. More of the variation in $_{cal}$BC is associated with the biomass function group (EOF 2, also associated with variation in [K^+]) than with the industrial function group (EOF 5, also associated with variation in [Pb]) (table 4). The biomass function group also explains more of the total variation in all of the data that were analyzed by the EOF method (table 4). Furthermore, peaks that were coincident in the $_{cal}$BC, [K^+], and [NO_3^-] records were suggestive of increased biomass emissions. These peaks occurred more frequently than $_{cal}$BC peaks coincident with elevated [Pb] that might suggest increased industrial emissions. In addition, more similarities can be drawn between the $_{cal}$BC record and other biomass burning records compared to the similarities that can be drawn between $_{cal}$BC and industrial emissions records. Thus, the conclusion is drawn that the $_{cal}$BC record is more influenced by emissions from biomass burning than industrial emissions, although it is noted that BC emissions from industry (as well as the residential use of coal and biofuels and open land burning) likely contribute to the BC signal.

BC from biomass burning that is recorded in Mt. Logan ice is likely sourced from local forest fires in Alaska and the Yukon Territory and distal forest fires in Siberia. Delivery of BC from these source regions is geographically logical (figure 17) and consistent with previous interpretations of other records preserved in the ice (e.g., Osterberg et al., 2008; Whitlow et al., 1994; Yalcin et al., 2006). More information and further study are required to determine the relative importance of each source region. Though less influential than forest fires, industrial emissions still contribute to the BC signal observed in the PR Col core. Asia is likely the dominant source of industrial emissions, but the possibility that more local sources of industrial emissions (e.g. shipping in the nearby Gulf of Alaska) influence the BC record cannot be eliminated.

BC Transport to Mt. Logan

This study has focused on identifying the possible regions and emissions sources for the BC recorded in the PR Col ice core, however the BC record is likely also influenced by changes in atmospheric circulation that enhance or inhibit the transport of BC to Mt. Logan. Changes in atmospheric circulation that have implications for BC transport are investigated in this section with particular emphasis on climate variability related to the Pacific Decadal Oscillation (PDO).

The PDO has been identified as a pattern of large-scale variability in Pacific oceanic and atmospheric conditions that varies on inter-decadal timescales with its largest climatic signature in the North Pacific Ocean (Hare et al., 1999; Latif and Barnett, 1996; Mantua et al., 1997). The "warm" or positive phases of the PDO are characterized by anomalously cool sea surface temperatures in the central North Pacific and warmer sea surface temperatures along the west coast of the Americas (Mantua and Hare, 2002). During these warm phases, lower sea level pressure over the North Pacific causes enhanced westerly and counter-clockwise winds that could enhance the trans-Pacific transport of BC and other chemical species to Mt. Logan (figure 24) (Mantua et al., 1997). "Cold" or negative phases of the PDO are characterized by the opposite of the conditions described above. Large-scale shifts in the PDO were identified in 1925, 1947, and 1977 (figure 25) (Hare et al., 1999; Mantua and Hare, 2002; Mantua et al., 1997).

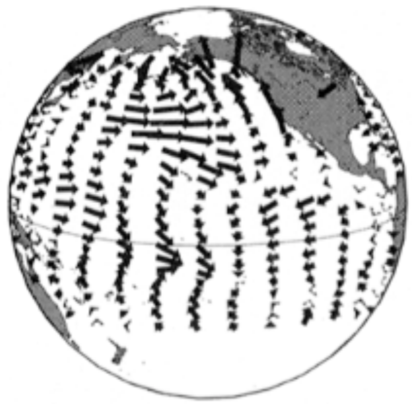

Figure 24 – Wind stress anomalies associated with the positive phase of the PDO. The largest vectors represent a wind stress of 10 m^2/s^2. Figure from (Mantua and Hare, 2002).

Comparing the historical PDO index to the BC record reveals that elevated BC concentrations are coincident with positive phases in the PDO, particularly in the 1930s, 1940s, and 1980s (figure 25). Negative PDO occurred in the 1950s and 1960s when relatively low BC concentrations are observed in the ice core (figure 25). It is possible that changes in the PDO altered the efficiency with which BC was transported across the Pacific Ocean, causing the variation in BC concentrations observed in the ice core record. It is also possible that changes in the scavenging efficiency of BC at Mt. Logan explain some of the variation in the BC record since positive PDO is correlated with increased precipitation along the coast of the Gulf of Alaska (Mantua and Hare, 2002).

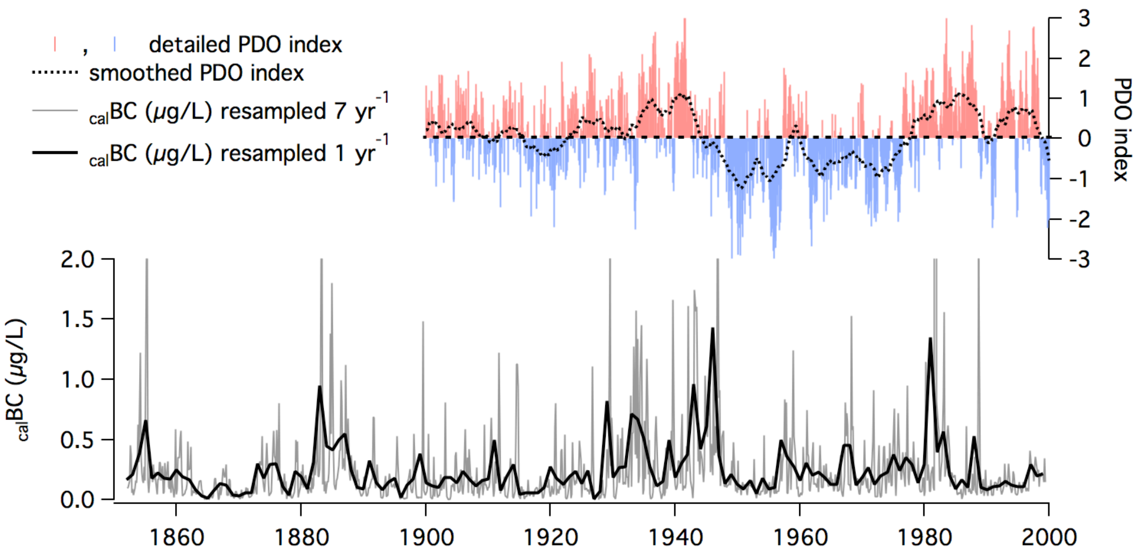

Figure 25 – Detailed and smoothed PDO indices based on sea surface temperature anomalies in the North Pacific (upper panel). PDO index data are from (Mantua et al., 1997), and downloadable at http://jisao.washington.edu/pdo/PDO.latest. The $_{cal}$BC record from the PR Col ice core is shown resampled to 7 yr^{-1} and 1 yr^{-1} resolution (lower panel).

However, the PDO cannot explain the entire BC signal given that relatively low BC concentrations are coincident with positive PDO phases, particularly in the 1990s. It is likely that some combination of changes in BC source and transport are responsible for the variations observed in the BC record from the PR Col ice core.

Comparison of Mt. Logan and Mt. Waddington BC Records.

Because of the geographical similarity, the Logan $_{cal}$BC record is briefly compared to a BC record from Mt. Waddington (3000 m.a.s.l.), British Columbia (figure 17). There may be some coincidence of elevated BC concentrations in the earlier part of each record, but similarities between the two are not obvious (Fig. 23). BC at

Mt. Waddington was attributed to a mix of Asian pollution, local forest fires, and proximity to Vancouver (Neff et al., 2012). It is possible that the BC record at Mt. Logan is influenced by all of these sources except for a nearby metropolitan center.

Climate Implications of the BC Record from Mt. Logan

BC affects the climate directly by absorbing solar radiation while entrained in the atmosphere and after deposition on glacier and snow surfaces. The ice core record of BC from Mt. Logan allows a general assessment of the climate impacts of BC deposited on glaciers and snow surfaces in the St. Elias Mountains. The maximum albedo reduction due to BC would have occurred at the time when BC concentrations are highest in the ice core record. For reasons related to sample treatments (discussed previously), BC losses in the ice core samples prevent quantitative determination of the maximum concentrations in the record. These concentrations may still be estimated based on the measurement of $_{cal}$BC in fresh ice samples; the highest $_{cal}$BC measured in the fresh ice samples was 20.3 μg/L, but most peak BC concentrations did not exceed 8 μg/L (figure 18). Although a linear relationship does not explain all of the differences between $_{cal}$BC in fresh and archived samples, it predicts a maximum concentration of 62.2 μg/L for an archived sample that was deposited at the PR Col in late 1946 ($_{cal}$BC = 13.9 μg/L, not shown in figure 20 due to resampling). The relationship also predicts a mean BC concentration of 1.6 μg/L. Any added impurities will reduce the albedo of glaciers and snowpacks and potentially trigger feedbacks associated with the metamorphosis of snow and ice crystals (Flanner et al., 2009), but the BC concentrations observed in the PR Col core are (except perhaps for select high concentration samples) not typically considered high enough to significantly reduce snow albedo. It is likely that the PR Col on Mt. Logan is located at high enough elevation and at great enough distance from major sources of BC that the annual accumulation at the site dilutes the BC load, minimizing the albedo reduction.

An important caveat with this simple interpretation is that $_{cal}$BC as measured and reported in this study is not directly comparable with BC concentrations and accompanying estimates of albedo reduction reported in other studies. $_{cal}$BC largely excludes particles > 500 nm, which have lower mass absorption cross sections and are less efficient at reducing albedo (see Chapter II for more details). Mie theory predicts that the smaller particles comprising the measurements of $_{cal}$BC are more efficient absorbers (Schwarz et al., 2013), thus $_{cal}$BC likely represents a measurement of the BC that is more optically (and climatically) relevant and may be associated with a greater reduction of albedo per unit concentration. Although quantitative determination of albedo reduction is not possible using the ice core record presented here, the record does indicate that the 1850s, 1880s, 1930s, 1940s, and 1980s were periods of time when albedo reduction due to BC was of highest magnitude at the PR Col and surrounding region.

The $_{cal}$BC record also indicates periods of time when atmospheric warming due to BC was greatest. Similar to albedo reduction, quantitative determination of the amount of atmospheric warming due to BC is not possible because true atmospheric BC concentrations cannot be determined from $_{cal}$BC. Nevertheless, changes in the record reflect qualitative changes in the amount of atmospheric BC and suggest that BC in the atmosphere was elevated during the 1850s, 1880s, 1930s, 1940s, and 1980s. During these periods, atmospheric BC likely had the greatest climatic effects in terms of its direct warming of the atmosphere, its cooling of the surface by dimming, and its indirect warming and cooling through its interaction with clouds.

Conclusions

A North Pacific BC record spanning AD 1852-1999 indicates that BC deposition at the PR Col on Mt. Logan (> 5300 m.a.s.l.) is controlled by complex factors, and the majority of the BC is likely attributable to forest fires that occurred in Alaska, the Yukon Territory, and Siberia. Industrial emissions from Asia are another possible origin of the BC, albeit with less influence than local and Siberian forest fires. Because scientific interest in the trans-Pacific transport of Asian pollutants persists (e.g., Hadley et al., 2007; Jaffe et al., 2003; Osterberg et al., 2008), it is important to emphasize that the BC signal recorded at Mt. Logan does not appear to be driven by Asian industrial emissions. This is despite the fact that Pb in the ice core was previously interpreted as having an Asian industrial source (Osterberg et al., 2008). Other Asian sources of BC also have less influence on the record but cannot be ruled out; these include the residential burning of coal and biofuels and the burning of land for agricultural purposes.

Periods of elevated BC, namely the 1850s, 1880s, 1930s, 1940s, and 1980s, indicate times when forest fires were larger and more frequent, or times when other sources of BC were more influential because of increases in emissions or enhanced delivery of BC to the PR Col due to atmospheric conditions. Although quantitative determination of the climate effect is not possible from the record, the periods of elevated BC correspond to times when the climate effects of BC were greatest, including the warming of the atmosphere and melting of snow and ice by direct radiative transfer, or through the indirect influence of BC particles on cloud-forming processes.

CHAPTER IV

CONCLUSIONS

In the last decade, black carbon (BC) has become recognized by the scientific community as a significant contributor to the recently observed global warming, but large uncertainties associated with BC prohibit fully understanding its role in the environment. The work presented in this study addressed analytical uncertainties related to the measurement of BC in snow and ice samples and uncertainties related to BC's spatial extent and temporal variability in the North Pacific over the period AD 1852-1999. The main results and implications are summarized in this concluding chapter.

Method experiments were conducted to inform the protocol for measuring BC concentrations in liquid samples using the Single Particle Soot Photometer (SP2) at Central Washington University (CWU). The protocol is summarized in Chapter II, and much of the experimentation is of interest to the wider SP2 community seeking to measure BC in liquid samples, especially the community that uses the CETAC ultrasonic nebulizer. The finding of widest interest is that the correction of BC measurements of liquid samples using gravimetrically prepared BC standards varies depending on the type of BC material chosen as a standard. The experiments presented in this manuscript suggest that Aquadag standards are preferred over BC standard materials that were used for the calibration of liquid sample measurements in previous studies (including Aquablack 162 and Cabojet 200). Further experimentation is needed to see if Fullerene Soot, a BC material accepted as a standard by the atmospheric SP2 community, is more appropriate than Aquadag for the calibration of liquid sample measurements.

Also of wider interest to the BC community are experimental results that highlight the importance of keeping samples frozen prior to SP2 analysis. Samples stored in the liquid phase at room temperature and in polypropylene vials exhibited up to 80% BC losses over a period of 18 days with losses of up to 30% after only 3 days. Samples stored in glass vials in a refrigerator were stable over the same length of time. These results may not apply to ice core measurements that use a continuous melter, but they are significant for investigators who measure BC concentrations in samples that have been previously melted, such as discrete snow and ice samples retrieved from remote field locations or archived samples. For information and findings from other experiments that explored sample treatment, sample nebulization, standard stability, system stability, and data processing, the reader is referred to Chapter II.

In addition to addressing analytical uncertainties related to the measurement of BC concentrations, a record of BC concentrations spanning AD 1852-1999 was developed using an ice core from the PR Col located on Mt. Logan in the Yukon Territory, Canada. The record indicates periods of elevated BC deposition (1850s, 1880s, 1930s, 1940s, and 1980s) indicative of higher atmospheric concentrations in the North Pacific region. Assessment of the possible sources of BC preserved in the ice core indicated that BC delivery to Mt. Logan is complex with multiple sources likely affecting the BC record at different times. Interpretation of empirical orthogonal function analysis suggested that the BC deposited at Mt. Logan was associated primarily with biomass burning, and secondarily with industrial emissions. Individual peaks in the BC record were linked to elevated BC emissions from forest fires because of associations with the forest fire tracers [K^+] and [NO_3^-]. Satellite imagery confirmed the boreal forests in Alaska, the Yukon Territory, and Siberia as possible source regions for BC from forest fire emissions. Comparison of the BC record with geographically similar glaciochemical, spatial-statistical, and sedimentological records of forest fires indicated that certain periods of elevated forest fire activity in the possible source regions were coincident with periods of elevated BC, although no record was identical to the BC record. Reasons for differences include differences in geographic location, differences in the chemical species measured, or complex factors affecting the transportation of BC including atmospheric circulation and precipitation in the region. Though forest fires were interpreted as the dominant source of BC captured at Mt. Logan, other sources could not be ruled out as contributing to the BC signal. Statistical analysis indicated an association between BC and industrial emissions, but long-term industrial trends were not evident in the BC record. Because scientific interest in the trans-Pacific transport of Asian pollutants persists, it is important to emphasize that the BC signal recorded at Mt. Logan does not appear to be driven by Asian industrial emissions. Since an Asian industrial signal is not apparent in the record, it is likely that other Asian emissions sources including residential emissions and open land burning for agricultural purposes are also secondary to more local biomass burning sources in terms of their contribution to the BC signal in the PR Col ice core.

With many potential sources of BC and complex factors controlling its deposition, it is difficult to attach a single causal explanation to periods of elevated BC in the record. Since the majority of changes in the BC signal are associated with biomass burning, periods of elevated BC in the record (1850s, 1880s, 1930s, 1940s, and 1980s) likely reflect times of increased forest fire activity in Alaska, the Yukon Territory, and Siberia. On the other hand, these periods may be indicative of times when conditions were appropriate to maximize BC transport from industrial emissions or other sources. Preliminary investigations suggest that elevated BC concentrations are associated with periods of positive PDO when westerly atmospheric circulation is enhanced. Future work will explore the degree to which large scale atmospheric changes may have affected BC transport to Mt. Logan in the past. Regardless of the reason, periods of elevated BC concentration in the ice core are indicative of elevated BC in the North Pacific atmosphere and elevated BC deposition to the PR Col and surrounding snow and ice. These are periods when the climate impacts of BC were greatest in the region surrounding Mt. Logan, including enhanced albedo reduction of glaciers and snowpacks in the St. Elias Mts. and enhanced atmospheric warming due to BC absorption and radiative transfer.

REFERENCES

Andreae, M. O., and Gelencser, A., 2006, Black carbon or brown carbon? The nature of light-absorbing carbonaceous aerosols: Atmospheric Chemistry and Physics, v. 6, p. 3131-3148.

Auffhammer, M., Ramanathan, V., and Vincent, J. R., 2006, Integrated model shows that atmospheric brown clouds and greenhouse gases have reduced rice harvests in India: Proceedings of the National Academy of Sciences of the United States of America, v. 103, no. 52, p. 19668-19672.

Bahadur, R., Russell, L. M., Jacobson, M. Z., Prather, K., Nenes, A., Adams, P., and Seinfeld, J. H., 2012, Importance of composition and hygroscopicity of BC particles to the effect of BC mitigation on cloud properties: Application to California conditions: Journal of Geophysical Research-Atmospheres, v. 117, p. 15.

Baumgardner, D., Popovicheva, O., Allan, J., Bernardoni, V., Cao, J., Cavalli, F., Cozic, J., Diapouli, E., Eleftheriadis, K., Genberg, P. J., Gonzalez, C., Gysel, M., John, A., Kirchstetter, T. W., Kuhlbusch, T. A. J., Laborde, M., Lack, D., Muller, T., Niessner, R., Petzold, A., Piazzalunga, A., Putaud, J. P., Schwarz, J., Sheridan, P., Subramanian, R., Swietlicki, E., Valli, G., Vecchi, R., and Viana, M., 2012, Soot reference materials for instrument calibration and intercomparisons: a workshop summary with recommendations: Atmospheric Measurement Techniques, v. 5, no. 8, p. 1869-1887.

Behling, H., Pillar, V. D., Orloic, L., and Bauermann, S. G., 2004, Late Quaternary Araucaria forest, grassland (Campos),fire and climate dynamics, studied by high-resolution pollen, charcoal and multivariate analysis of the Cambara do Sul core in southern Brazil: Palaeogeography Palaeoclimatology Palaeoecology, v. 203, no. 3-4, p. 277-297.

Berntsen, T. K., Karlsdottir, S., and Jaffe, D. A., 1999, Influence of Asian emissions on the composition of air reaching the North Western United States: Geophysical Research Letters, v. 26, no. 14, p. 2171-2174.

Bisiaux, M. M., Edwards, R., Heyvaert, A. C., Thomas, J. M., Fitzgerald, B., Susfalk, R. B., Schladow, S. G., and Thaw, M., 2011, Stormwater and fire as sources of black carbon nanoparticles to Lake Tahoe: Environmental Science & Technology, v. 45, p. 2065-2071.

Bisiaux, M. M., Edwards, R., McConnell, J. R., Albert, M. R., Anschutz, H., Neumann, T. A., Isaksson, E., and Penner, J. E., 2012a, Variability of black carbon deposition to the East Antarctic Plateau, 1800-2000 AD: Atmospheric Chemistry and Physics, v. 12, no. 8, p. 3799-3808.

Bisiaux, M. M., Edwards, R., McConnell, J. R., Curran, M. A. J., Van Ommen, T. D., Smith, A. M., Neumann, T. A., Pasteris, D. R., Penner, J. E., and Taylor, K., 2012b, Changes in black carbon deposition to Antarctica from two high-resolution ice core records, 1850-2000 AD: Atmospheric Chemistry and Physics, v. 12, no. 9, p. 4107-4115.

Bond, T. C., Bhardwaj, E., Dong, R., Jogani, R., Jung, S. K., Roden, C., Streets, D. G., and Trautmann, N. M., 2007, Historical emissions of black and organic carbon aerosol from energy-related combustion, 1850-2000: Global Biogeochemical Cycles, v. 21, no. 2.

Bond, T. C., Doherty, S. J., Fahey, D. W., Forster, P. M., Bernsten, T., DeAngelo, B. J., Flanner, M. G., Ghan, S., Karcher, B., Koch, D., Kinne, S., Kondo, Y., Quinn, P. K., Sarofim, M. C., Schultz, M. G., Schulz, M., Venkataraman, C., Zhang, H., Zhang, S., Bellouin, N., Guttikunda, S. K., Hopke, P. K., Jacobsen, M. Z., Kaiser, J. W., Klimont, Z., Lohmann, U., Schwartz, J. P., Shindell, D., Storelvmo, T., Warren, S. G., and Zender, C. S., 2013, Bounding the role of black carbon in the climate system: A scientific assessment.: Journal of Geophysical Research, v. in press.

Bond, T. C., Streets, D. G., Yarber, K. F., Nelson, S. M., Woo, J. H., and Klimont, Z., 2004, A technology-based global inventory of black and organic carbon emissions from combustion: Journal of Geophysical Research-Atmospheres, v. 109, no. D14.

Boparai, P., Lee, J. M., and Bond, T. C., 2008, Revisiting thermal-optical analyses of carbonaceous aerosol using a physical model: Aerosol Science and Technology, v. 42, no. 11, p. 930-U15.

Brandt, R. E., Warren, S. G., and Clarke, A. D., 2011, A controlled snowmaking experiment testing the relation between black carbon content and reduction of snow albedo: Journal of Geophysical Research, v. 116, no. D08109.

Budyko, M. I., 1969, The effect of solar radiation variations on the climate of the Earth: Tellus, v. 21, no. 5.

Carcaillet, C., Almquist, H., Asnong, H., Bradshaw, R. H. W., Carrion, J. S., Gaillard, M. J., Gajewski, K., Haas, J. N., Haberle, S. G., Hadorn, P., Muller, S. D., Richard, P. J. H., Richoz, I., Rosch, M., Goni, M. F. S., von Stedingk, H., Stevenson, A. C., Talon, B., Tardy, C., Tinner, W., Tryterud, E., Wick, L., and

Willis, K. J., 2002, Holocene biomass burning and global dynamics of the carbon cycle: Chemosphere, v. 49, no. 8, p. 845-863.

Chakrabarty, R. K., Garro, M. A., Wilcox, E. M., and Moosmuller, H., 2012, Strong radiative heating due to wintertime black carbon aerosols in the Brahmaputra River Valley: Geophysical Research Letters, v. 39, p. 5.

Chameides, W. L., Yu, H., Liu, S. C., Bergin, M., Zhou, X., Mearns, L., Wang, G., Kiang, C. S., Saylor, R. D., Luo, C., Huang, Y., Steiner, A., and Giorgi, F., 1999, Case study of the effects of atmospheric aerosols and regional haze on agriculture: An opportunity to enhance crop yields in China through emission controls?: Proceedings of the National Academy of Sciences of the United States of America, v. 96, no. 24, p. 13626-13633.

Chen, W. T., Lee, Y. H., Adams, P. J., Nenes, A., and Seinfeld, J. H., 2010, Will black carbon mitigation dampen aerosol indirect forcing?: Geophysical Research Letters, v. 37, p. 5.

Chow, J. C., Watson, J. G., Chen, L. W. A., Arnott, W. P., and Moosmuller, H., 2004, Equivalence of elemental carbon by thermal/optical reflectance and transmittance with different temperature protocols: Environmental Science & Technology, v. 38, no. 16, p. 4414-4422.

Chung, C. E., Ramanathan, V., and Decremer, D., 2012, Observationally constrained estimates of carbonaceous aerosol radiative forcing: Proceedings of the National Academy of Sciences of the United States of America, v. 109, no. 29, p. 11624-11629.

Chylek, P., Johnson, B., Damiano, P. A., Taylor, K. C., and Clement, P., 1995, Biomass burning record and black carbon in the GISP2 ice core: Geophysical Research Letters, v. 22, no. 2.

Chylek, P., Johnson, B., and Wu, H., 1992a, Black carbon concentration in a Greenland DYE-3 ice core: Geophysical Research Letters, v. 19, no. 19.

-, 1992b, Black carbon concentration in Byrd Station ice core - from 13,000 to 700 years before present: Annales Geophysicae-Atmospheres Hydrospheres and Space Sciences, v. 10, no. 8.

Eichler, A., Tinner, W., Brusch, S., Olivier, S., Papina, T., and Schwikowski, M., 2011, An ice-core based history of Siberian forest fires since AD 1250: Quaternary Science Reviews, v. 30, no. 9-10, p. 1027-1034.

Fauria, M. M., and Johnson, E. A., 2006, Large-scale climatic patterns control large lightning fire occurrence in Canada and Alaska forest regions: Journal of Geophysical Research-Biogeosciences, v. 111, no. G4.

-, 2008, Climate and wildfires in the North American boreal forest: Philosophical Transactions of the Royal Society B-Biological Sciences, v. 363, no. 1501, p. 2317-2329.

Feichter, J., and Stier, P., 2012, Assessment of black carbon radiative effects in climate models: Wiley Interdisciplinary Reviews-Climate Change, v. 3, no. 4, p. 359-370.

Filippov, A. V., Markus, M. W., and Roth, P., 1999, In-situ characterization of ultrafine particles by laser-induced incandescence: Sizing and particle structure determination: Journal of Aerosol Science, v. 30, no. 1, p. 71-87.

Fisher, D., Osterberg, E., Dyke, A., Dahl-Jensen, D., Demuth, M., Zdanowicz, C., Bourgeois, J., Koerner, R. M., Mayewski, P., Wake, C., Kreutz, K., Steig, E., Zheng, J., Yalcin, K., Goto-Azuma, K., Luckman, B., and Rupper, S., 2008, The Mt Logan Holocene-late Wisconsinan isotope record: Tropical Pacific-Yukon connections: Holocene, v. 18, no. 5, p. 667-677.

Fisher, D., Wake, C., Kreutz, K., Yalcin, K., Steig, E., Mayewski, P., Anderson, L., Zheng, J., Rupper, S., Zdanowicz, C., Demuth, M., Waszkiewicz, M., Dahl-Jensen, D., Goto-Azuma, K., Bourgeois, J., Koerner, R. M., Sekerka, J., Osterberg, E., Abbott, M. B., Finney, B. P., and Burns, S. J., 2004, Stable isotope records from Moung Logan, Eclipse ice cores and nearby Jellybean Lake. Water cycle of the North Pacific over 2000 years and over five vertical kilometers: sudden shifts and tropical connections: Géographie physique et Quaternaire, v. 58, no. 2-3.

Fisher, D. A., 2011, Connecting the Atlantic-sector and the north Pacific (Mt Logan) ice core stable isotope records during the Holocene: The role of El Nino: Holocene, v. 21, no. 7, p. 1117-1124.

Flanner, M. G., Zender, C. S., Hess, P. G., Mahowald, N. M., Painter, T. H., Ramanathan, V., and Rasch, P. J., 2009, Springtime warming and reduced snow cover from carbonaceous particles: Atmospheric Chemistry and Physics, v. 9, no. 7, p. 2481-2497.

Flanner, M. G., Zender, C. S., Randerson, J. T., and Rasch, P. J., 2007, Present-day climate forcing and response from black carbon in snow: Journal of Geophysical Research-Atmospheres, v. 112, no. D11.

Flannigan, M. D., Stocks, B. J., and Wotton, B. M., 2000, Climate change and forest fires: Science of the Total Environment, v. 262, no. 3, p. 221-229.

Ghan, S. J., Liu, X., Easter, R. C., Zaveri, R., Rasch, P. J., Yoon, J. H., and Eaton, B., 2012, Toward a Minimal Representation of Aerosols in Climate Models: Comparative Decomposition of Aerosol Direct, Semidirect, and Indirect Radiative Forcing: Journal of Climate, v. 25, no. 19, p. 6461-6476.

Gillett, N. P., Weaver, A. J., Zwiers, F. W., and Flannigan, M. D., 2004, Detecting the effect of climate change on Canadian forest fires: Geophysical Research Letters, v. 31, no. 18.

Grenfell, T. C., Doherty, S. J., Clarke, A. D., and Warren, S. G., 2011, Light absorption from particulate impurities in snow and ice determined by spectrophotometric analysis of filters: Applied Optics, v. 50, no. 14, p. 2037-2048.

Gysel, M., 2012, Scientist, Paul Scherrer Institut: Villigen, Switzerland.

-, 2013, Scientist, Paul Scherrer Institut: Villigen, Switzerland.

Gysel, M., Laborde, M., Olfert, J. S., Subramanian, R., and Grohn, A. J., 2011, Effective density of Aquadag and fullerene soot black carbon reference materials used for SP2 calibration: Atmospheric Measurement Techniques, v. 4, no. 12, p. 2851-2858.

Hadley, O. L., Corrigan, C. E., Kirchstetter, T. W., Cliff, S. S., and Ramanathan, V., 2010, Measured black carbon deposition on the Sierra Nevada snow pack and implication for snow pack retreat: Atmospheric Chemistry and Physics Discussions, v. 10, p. 10463-10485.

Hadley, O. L., and Kirchstetter, T. W., 2012, Black-carbon reduction of snow albedo: Nature Climate Change, v. 2, no. 6, p. 437-440.

Hadley, O. L., Ramanathan, V., Carmichael, G. R., Tang, Y., Corrigan, C. E., Roberts, G. C., and Mauger, G. S., 2007, Trans-Pacific transport of black carbon and fine aerosols (D < 2.5 mu m) into North America: Journal of Geophysical Research-Atmospheres, v. 112, no. D5.

Han, Y. M., Marlon, J. R., Cao, J. J., Jin, Z. D., and An, Z. S., 2012, Holocene linkages between char, soot, biomass burning and climate from Lake Daihai, China: Global Biogeochemical Cycles, v. 26, p. 9.

Hansen, J., and Nazarenko, L., 2004, Soot climate forcing via snow and ice albedos: Proceedings of the National Academy of Sciences of the United States of America, v. 101, no. 2, p. 423-428.

Hare, S. R., Mantua, N. J., and Francis, R. C., 1999, Inverse production regimes: Alaska and West Coast Pacific salmon: Fisheries, v. 24, no. 1, p. 6-14.

Heald, C. L., Jacob, D. J., Park, R. J., Alexander, B., Fairlie, T. D., Yantosca, R. M., and Chu, D. A., 2006, Transpacific transport of Asian anthropogenic aerosols and its impact on surface air quality in the United States: Journal of Geophysical Research-Atmospheres, v. 111, no. D14.

Hegg, D. A., Warren, S. G., Grenfell, T. C., Doherty, S. J., Larson, T. V., and Clarke, A. D., 2009, Source Attribution of Black Carbon in Arctic Snow: Environmental Science & Technology, v. 43, no. 11, p. 4016-4021.

Higuera, P. E., Brubaker, L. B., Anderson, P. M., Hu, F. S., and Brown, T. A., 2009, Vegetation mediated the impacts of postglacial climate change on fire regimes in the south-central Brooks Range, Alaska: Ecological Monographs, v. 79, no. 2, p. 201-219.

Holdsworth, G., Fogarasi, S., and Krouse, H. R., 1991, Variation of the stable isotopes of water with altitude in the Saint Elias Mountains of Canada: Journal of Geophysical Research-Atmospheres, v. 96, no. D4, p. 7483-7494.

Holdsworth, G., Higuchi, K., Zielinski, G. A., Mayewski, P. A., Wahlen, M., Deck, B., Chylek, P., Johnson, B., and Damiano, P., 1996, Historical biomass burning: Late 19th century pioneer agriculture revolution in northern hemisphere ice core data and its atmospheric interpretation: Journal of Geophysical Research-Atmospheres, v. 101, no. D18, p. 23317-23334.

Holdsworth, G., and Krouse, H. R., 2002, Altitudinal variation of the stable isotopes of snow in regions of high relief: Journal of Glaciology, v. 48, no. 160, p. 31-41.

Holdsworth, G., Krouse, H. R., and Peake, E., 1988, Trace-Acid Ion Content of Shallow Snow and Ice Cores from Mountain Sites in Western Canada: Annals of Glaciology, v. 10.

Holdsworth, G., Pourchet, M., Prantl, F. A., and Meyerhof, D. P., 1984, Radioactivity levels in a firn core from the Yukon Territory, Canada, CANADA: Atmospheric Environment, v. 18, no. 2, p. 461-466.

IPCC, 2007, Climate Change 2007: The Physical Science Basis. Contribution of Working Group I to the Fourth Assessment Report of the Intergovernmental Panel on Climate Change.

Jaffe, D., Mahura, A., Kelley, J., Atkins, J., Novelli, P. C., and Merrill, J., 1997, Impact of Asian emissions on the remote North Pacific atmosphere: Interpretation of CO data from Shemya, Guam, Midway and Mauna Loa: Journal of Geophysical Research-Atmospheres, v. 102, no. D23, p. 28627-28635.

Jaffe, D., McKendry, I., Anderson, T., and Price, H., 2003, Six 'new' episodes of trans-Pacific transport of air pollutants: Atmospheric Environment, v. 37, no. 3, p. 391-404.

Jenkins, M., 2011, Assessment of Black Carbon in Snow and Ice from the Tibetan Plateau and Pacific Northwest: Central Washington University.

Kang, S. C., Mayewski, P. A., and Yan, Y. P., 2005, A 290-a record of atmospheric circulation over the North Pacific from a Mt. Logan ice core, Yukon Territory: Acta Oceanologica Sinica, v. 24, no. 4, p. 81-90.

Kasischke, E. S., Williams, D., and Barry, D., 2002, Analysis of the patterns of large fires in the boreal forest region of Alaska: International Journal of Wildland Fire, v. 11, no. 2.

Kaspari, S., 2011, Assistant Professor, Central Washington University: Ellensburg, WA, USA.

Kaspari, S., Schwikowski, M., Gysel, M., Flanner, M. G., Kang, S., Hou, S., and Mayewski, P. A., 2011, Recent increase in black carbon concentrations from a Mt. Everest ice core spanning 1860-2000 AD: Geophysical Research Letters, v. 38.

Kawamura, K., Izawa, Y., Mochida, M., and Shiraiwa, T., 2012, Ice core records of biomass burning tracers (levoglucosan and dehydroabietic, vanillic and p-hydroxybenzoic acids) and total organic carbon for past 300 years in the Kamchatka Peninsula, Northeast Asia: Geochimica Et Cosmochimica Acta, v. 99.

Kelsey, E. P., Wake, C. P., Yalcin, K., and Kreutz, K., 2012, Eclipse Ice Core Accumulation and Stable Isotope Variability as an Indicator of North Pacific Climate: Journal of Climate, v. 25, no. 18, p. 6426-6440.

Keywood, M., Kanakidou, M., Stohl, A., Dentener, F., Grassi, G., Meyer, C. P., Torseth, K., Edwards, D., Thompson, A. M., Lohmann, U., and Burrows, J., 2013, Fire in the Air: Biomass Burning Impacts in a Changing Climate: Critical Reviews in Environmental Science and Technology, v. 43, no. 1, p. 40-83.

Kirchstetter, T. W., 2012, Staff Scientist, Lawrence Berkeley National Laboratory, Sustainable Energy Systems Group: Berkeley, CA, USA.

Kirchstetter, T. W., and Novakov, T., 2007, Controlled generation of black carbon particles from a diffusion flame and applications in evaluating black carbon measurement methods: Atmospheric Environment, v. 41, no. 9, p. 1874-1888.

Laborde, M., Mertes, P., Zieger, P., Dommen, J., Baltensperger, U., and Gysel, M., 2012, Sensitivity of the Single Particle Soot Photometer to different black carbon types: Atmospheric Measurement Techniques, v. 5, no. 5.

Larsen, C. P. S., Morris, W. A., and MacDonald, G. M., 2000, Records of geomagnetic secular variation since 1200 AD and the potential for chronological control of lake sediments in northern Alberta: Canadian Journal of Earth Sciences, v. 37, no. 12, p. 1711-1722.

Latif, M., and Barnett, T. P., 1996, Decadal climate variability over the North Pacific and North America: Dynamics and predictability: Journal of Climate, v. 9, no. 10, p. 2407-2423.

Lau, K. M., Kim, M. K., and Kim, K. M., 2006, Asian summer monsoon anomalies induced by aerosol direct forcing: the role of the Tibetan Plateau: Climate Dynamics, v. 26, no. 7-8, p. 855-864.

Lavanchy, V. M. H., Gaggeler, H. W., Schotterer, U., Schwikowski, M., and Baltensperger, U., 1999, Historical record of carbonaceous particle concentrations from a European high-alpine glacier (Colle Gnifetti, Switzerland): Journal of Geophysical Research-Atmospheres, v. 104, no. D17, p. 21227-21236.

Legrand, M., Deangelis, M., Staffelbach, T., Neftel, A., and Stauffer, B., 1992, Large perturbations of ammonium and organic-acids content in the Summit-Greenland ice core - fingerprint from forest fires: Geophysical Research Letters, v. 19, no. 5, p. 473-475.

Legrand, M., Preunkert, S., Schock, M., Cerqueira, M., Kasper-Giebl, A., Afonso, J., Pio, C., Gelencser, A., and Dombrowski-Etchevers, I., 2007, Major 20th century changes of carbonaceous aerosol components (EC, WinOC, DOC, HULIS, carboxylic acids, and cellulose) derived from Alpine ice cores: Journal of Geophysical Research-Atmospheres, v. 112, no. D23.

Liu, X., Xu, B., Yao, T., Wang, N., and Wu, G., 2008, Carbonaceous particles in Muztagh Ata ice core, West Kunlun Mountains, China: Chinese Science Bulletin, v. 53, no. 21.

Lynch, J. A., Hollis, J. L., and Hu, F. S., 2004, Climatic and landscape controls of the boreal forest fire regime: Holocene records from Alaska: Journal of Ecology, v. 92, no. 3, p. 477-489.

Mantua, N. J., and Hare, S. R., 2002, The Pacific decadal oscillation: Journal of Oceanography, v. 58, no. 1, p. 35-44.

Mantua, N. J., Hare, S. R., Zhang, Y., Wallace, J. M., and Francis, R. C., 1997, A Pacific interdecadal climate oscillation with impacts on salmon production: Bulletin of the American Meteorological Society, v. 78, no. 6, p. 1069-1079.

Marlon, J. R., Bartlein, P. J., Carcaillet, C., Gavin, D. G., Harrison, S. P., Higuera, P. E., Joos, F., Power, M. J., and Prentice, I. C., 2008, Climate and human influences on global biomass burning over the past two millennia: Nature Geoscience, v. 1, no. 10, p. 697-702.

McCarty, J. L., Ellicott, E. A., Romanenkov, V., Rukhovitch, D., and Koroleva, P., 2012, Multi-year black carbon emissions from cropland burning in the Russian Federation: Atmospheric Environment, v. 63.

McConnell, J. R., Edwards, R., Kok, G. L., Flanner, M. G., Zender, C. S., Saltzman, E. S., Banta, J. R., Pasteris, D. R., Carter, M. M., and Kahl, J. D. W., 2007, 20th-century industrial black carbon emissions altered arctic climate forcing: Science, v. 317, no. 5843, p. 1381-1384.

McCoy, V. M., and Burn, C. R., 2005, Potential alteration by climate change of the forest-fire regime in the Boreal forest of central Yukon Territory: Arctic, v. 58, no. 3, p. 276-285.

Meeker, L. D., and Mayewski, P. A., 2002, A 1400-year high-resolution record of atmospheric circulation over the North Atlantic and Asia: Holocene, v. 12, no. 3, p. 257-266.

Menon, S., Hansen, J., Nazarenko, L., and Luo, Y. F., 2002, Climate effects of black carbon aerosols in China and India: Science, v. 297, no. 5590, p. 2250-2253.

Ming, J., Cachier, H., Xiao, C., Qin, D., Kang, S., Hou, S., and Xu, J., 2008, Black carbon record based on a shallow Himalayan ice core and its climatic implications: Atmospheric Chemistry and Physics, v. 8, no. 5, p. 1343-1352.

Ming, J., Xiao, C. D., Cachier, H., Qin, D. H., Qin, X., Li, Z. Q., and Pu, J. C., 2009, Black Carbon (BC) in the snow of glaciers in west China and its potential effects on albedos: Atmospheric Research, v. 92, no. 1, p. 114-123.

Monaghan, M. C., and Holdsworth, G., 1990, The origin of non-sea-salt sulfate in the Mount Logan ice core: Nature, v. 343, no. 6255, p. 245-248.

Moore, G. W. K., Alverson, K., and Holdsworth, G., 2002a, Variability in the climate of the Pacific Ocean and North America as expressed in the Mount Logan ice core: Annals of Glaciology, Vol 35, v. 35, p. 423-429.

-, 2003, The impact that elevation has on the ENSO signal in precipitation records from the Gulf of Alaska region: Climatic Change, v. 59, no. 1-2, p. 101-121.

Moore, G. W. K., Holdsworth, G., and Alverson, K., 2001, Extra-tropical response to ENSO as Expressed in an ice core from the Saint Elias Mountain range: Geophysical Research Letters, v. 28, no. 18, p. 3457-3460.

-, 2002b, Climate change in the North Pacific region over the past three centuries: Nature, v. 420, no. 6914, p. 401-403.

Moteki, N., and Kondo, Y., 2007, Effects of mixing state on black carbon measurements by laser-induced incandescence: Aerosol Science and Technology, v. 41, no. 4, p. 398-417.

-, 2010, Dependence of Laser-Induced Incandescence on Physical Properties of Black Carbon Aerosols: Measurements and Theoretical Interpretation: Aerosol Science and Technology, v. 44, no. 8, p. 663-675.

Neff, P. D., Steig, E., Clark, D. H., McConnell, J. R., Pettit, E. C., and Menounos, B., 2012, Ice-core net snow accumulation and seasonal snow chemistry at a temperate-glacier site: Mount Waddington, southwest British Columbia, Canada.: Journal of Glaciology, v. 58, no. 212.

Novakov, T., Ramanathan, V., Hansen, J. E., Kirchstetter, T. W., Sato, M., Sinton, J. E., and Sathaye, J. A., 2003, Large historical changes of fossil-fuel black carbon aerosols: Geophysical Research Letters, v. 30, no. 6.

Ocko, I. B., Ramaswamy, V., Ginoux, P., Ming, Y., and Horowitz, L. W., 2012, Sensitivity of scattering and absorbing aerosol direct radiative forcing to physical climate factors: Journal of Geophysical Research-Atmospheres, v. 117, p. 13.

Ohata, S., 2013, Masters Candidate, University of Tokyo: Tokyo, Japan.

Ohata, S., Moteki, N., and Kondo, Y., 2011, Evaluation of a Method for Measurement of the Concentration and Size Distribution of Black Carbon Particles Suspended in Rainwater: Aerosol Science and Technology, v. 45, p. 1326-1336.

Ohata, S., Moteki, N., Schwartz, J. P., Fahey, D. W., and Kondo, Y., 2012, Abstract A431-07 Evaluations of the Method to Measure Black Carbon Particles Suspended in Rainwater and Snow Samples, American Geophysical Union 2012 Fall Meeting: San Francisco.

Osterberg, E., 2011, Research Assistant Professor, Dartmouth College: Hanover, NH, USA.

Osterberg, E., Mayewski, P., Kreutz, K., Fisher, D., Handley, M., Sneed, S., Zdanowicz, C., Zheng, J., Demuth, M., Waskiewicz, M., and Bourgeois, J., 2008, Ice core record of rising lead pollution in the North Pacific atmosphere: Geophysical Research Letters, v. 35, no. 5.

Osterberg, E. C., Handley, M. J., Sneed, S. B., Mayewski, P. A., and Kreutz, K. J., 2006, Continuous ice core melter system with discrete sampling for major ion, trace element, and stable isotope analyses: Environmental Science & Technology, v. 40, no. 10, p. 3355-3361.

Osterberg, E. C., Mayewski, P. A., Fisher, D. A., Kreutz, K. J., and Sneed, S., unpublished data.

Owega, S., Evans, G. J., Jervis, R. E., Fila, M., D'Souza, R., and Khan, B. U. Z., 2004, Long-range sources of Toronto particulate matter (PM2.5) identified by Aerosol Laser Ablation Mass Spectrometry (LAMS): Atmospheric Environment, v. 38, no. 33, p. 5545-5553.

Pacyna, J. M., and Pacyna, E. G., 2001, An assessment of global and regional emissions of trace metals to the atmosphere from anthropogenic sources worldwide: Environmental Reviews, v. 9, no. 4, p. 269-298.

Pere, J. C., Colette, A., Dubuisson, P., Bessagnet, B., Mallet, M., and Pont, V., 2012, Impacts of future air pollution mitigation strategies on the aerosol direct radiative forcing over Europe: Atmospheric Environment, v. 62, p. 451-460.

Pierce, J. L., Meyer, G. A., and Jull, A. J. T., 2004, Fire-induced erosion and millennialscale climate change in northern ponderosa pine forests: Nature, v. 432, no. 7013, p. 87-90.

Primbs, T., Simonich, S., Schmedding, D., Wilson, G., Jaffe, D., Takami, A., Kato, S., Hatakeyama, S., and Kajii, Y., 2007, Atmospheric outflow of anthropogenic semivolatile organic compounds from East Asia in spring 2004: Environmental Science & Technology, v. 41, no. 10, p. 3551-3558.

Qian, Y., Gustafson, W. I., Leung, L. R., and Ghan, S. J., 2009, Effects of soot-induced snow albedo change on snowpack and hydrological cycle in western United States based on Weather Research and Forecasting chemistry and regional climate simulations: Journal of Geophysical Research-Atmospheres, v. 114.

Qian, Y., Leung, L. R., Ghan, S. J., and Giorgi, F., 2003, Regional climate effects of aerosols over China: modeling and observation: Tellus Series B-Chemical and Physical Meteorology, v. 55, no. 4, p. 914-934.

Qu, X., and Hall, A., 2005, Surface contribution to planetary albedo variability in cryosphere regions: Journal of Climate, v. 18, no. 24, p. 5239-5252.

Ramanathan, V., and Carmichael, G., 2008, Global and regional climate changes due to black carbon: Nature Geoscience, v. 1, no. 4, p. 221-227.

Rehman, I. H., Ahmed, T., Praveen, P. S., Kar, A., and Ramanathan, V., 2011, Black carbon emissions from biomass and fossil fuels in rural India: Atmospheric Chemistry and Physics, v. 11, no. 14, p. 7289-7299.

Rupper, S., Steig, E. J., and Roe, G., 2004, The relationship between snow accumulation at Mt. Logan, Yukon, Canada, and climate variability in the North Pacific: Journal of Climate, v. 17, no. 24, p. 4724-4739.

Schmid, H., Laskus, L., Abraham, H. J., Baltensperger, U., Lavanchy, V., Bizjak, M., Burba, P., Cachier, H., Crow, D., Chow, J., Gnauk, T., Even, A., ten Brink, H. M., Giesen, K. P., Hitzenberger, R., Hueglin, C., Maenhaut, W., Pio, C., Carvalho, A., Putaud, J. P., Toom-Sauntry, D., and Puxbaum, H., 2001, Results of the "carbon conference" international aerosol carbon round robin test stage I: Atmospheric Environment, v. 35, no. 12, p. 2111-2121.

Schoennagel, T., Veblen, T. T., and Romme, W. H., 2004, The interaction of fire, fuels, and climate across rocky mountain forests: Bioscience, v. 54, no. 7, p. 661-676.

Schwarz, J., 2012, Research Scientist III, NOAA Earth System Research Laboratory: Boulder, CO, USA.

Schwarz, J. P., Doherty, S. J., Li, F., Ruggiero, S. T., Tanner, C. E., Perring, A. E., Gao, R. S., and Fahey, D. W., 2012, Assessing Single Particle Soot Photometer and Integrating Sphere/ Integrating Sandwich Spectrophotometer measurement techniques for quantifying black carbon concentration in snow: Atmospheric Measurement Techniques, v. 5, no. 11, p. 2581-2592.

Schwarz, J. P., Gao, R. S., Fahey, D. W., Thomson, D. S., Watts, L. A., Wilson, J. C., Reeves, J. M., Darbeheshti, M., Baumgardner, D. G., Kok, G. L., Chung, S. H., Schulz, M., Hendricks, J., Lauer, A., Karcher, B., Slowik, J. G., Rosenlof, K. H., Thompson, T. L., Langford, A. O., Loewenstein, M., and Aikin, K. C., 2006, Single-particle measurements of midlatitude black carbon and light-scattering aerosols from the boundary layer to the lower stratosphere: Journal of Geophysical Research-Atmospheres, v. 111, no. D16.

Schwarz, J. P., Gao, R. S., Perring, A. E., Spackman, J. R., and Fahey, D. W., 2013, Black carbon aerosol size in snow: Nature, in press.

Schwarz, J. P., Spackman, J. R., Gao, R. S., Perring, A. E., Cross, E. S., Onasch, T. B., Ahern, A., Wrobel, W., Davidovits, P., Olfert, J., Dubey, M. K., Mazzoleni, C., and Fahey, D. W., 2010, The Detection Efficiency of the Single Particle Soot Photometer: Aerosol Science and Technology, v. 44, p. 612-628.

Skiles, S. M., Painter, T. H., Deems, J. S., Bryant, A. C., and Landry, C. C., 2012, Dust radiative forcing in snow of the Upper Colorado River Basin: 2. Interannual variability in radiative forcing and snowmelt rates: Water Resources Research, v. 48, p. 11.

Slowik, J. G., Cross, E. S., Han, J. H., Davidovits, P., Onasch, T. B., Jayne, J. T., WilliamS, L. R., Canagaratna, M. R., Worsnop, D. R., Chakrabarty, R. K., Moosmuller, H., Arnott, W. P., Schwarz, J. P., Gao, R. S., Fahey, D. W., Kok, G. L., and Petzold, A., 2007, An inter-comparison of instruments measuring black carbon content of soot particles: Aerosol Science and Technology, v. 41, no. 3, p. 295-314.

Soja, A. J., Tchebakova, N. M., French, N. H. F., Flannigan, M. D., Shugart, H. H., Stocks, B. J., Sukhinin, A. I., Parfenova, E. I., Chapin, F. S., and Stackhouse, P. W., 2007, Climate-induced boreal forest change: Predictions versus current observations: Global and Planetary Change, v. 56, no. 3-4, p. 274-296.

Song, C. H., Ma, Y., Orsini, D., Kim, Y. P., and Weber, R. J., 2005, An investigation into the ionic chemical composition and mixing state of biomass burning particles recorded during TRACE-P P3B Flight#10: Journal of Atmospheric Chemistry, v. 51, no. 1, p. 43-64.

Stephens, M., Turner, N., and Sandberg, J., 2003, Particle identification by laser-induced incandescence in a solid-state laser cavity: Applied Optics, v. 42, no. 19, p. 3726-3736.

Sterle, K. M., McConnell, J. R., Dozier, J., Edwards, R., and Bisiaux, M., 2009, Black Carbon in the Eastern Sierra Nevada, AGU Fall Meeting.

Sterle, K. M., McConnell, J. R., Dozier, J., Edwards, R., and Flanner, M. G., 2012, Retention and radiative forcing of black carbon in Eastern Sierra Nevada snow: The Cryosphere Discussions, v. 6, p. 2247-2264.

Stocks, B. J., Fosberg, M. A., Lynham, T. J., Mearns, L., Wotton, B. M., Yang, Q., Jin, J. Z., Lawrence, K., Hartley, G. R., Mason, J. A., and McKenney, D. W., 1998, Climate change and forest fire potential in Russian and Canadian boreal forests: Climatic Change, v. 38, no. 1, p. 1-13.

Stocks, B. J., Mason, J. A., Todd, J. B., Bosch, E. M., Wotton, B. M., Amiro, B. D., Flannigan, M. D., Hirsch, K. G., Logan, K. A., Martell, D. L., and Skinner, W. R., 2002, Large forest fires in Canada, 1959-1997: Journal of Geophysical Research-Atmospheres, v. 108, no. D1.

Streets, D. G., Bond, T. C., Carmichael, G. R., Fernandes, S. D., Fu, Q., He, D., Klimont, Z., Nelson, S. M., Tsai, N. Y., Wang, M. Q., Woo, J. H., and Yarber, K. F., 2003, An inventory of gaseous and primary aerosol emissions in Asia in the year 2000: Journal of Geophysical Research-Atmospheres, v. 108, no. D21, p. 23.

Streets, D. G., Gupta, S., Waldhoff, S. T., Wang, M. Q., Bond, T. C., and Bo, Y. Y., 2001, Black carbon emissions in China: Atmospheric Environment, v. 35, no. 25, p. 4281-4296.

Subramanian, R., 2011, Research Scientist, Carnegie Mellon University: Pittsburgh, PA, USA.

United States Environmental Protection Agency, 2012, Report to Congress on Black Carbon.

Wang, R., Tao, S., Wang, W., Liu, J., Shen, H., Shen, G., Wang, B., Liu, X., Li, W., Huang, Y., Zhang, Y., Lu, Y., Chen, H., Chen, Y., Wang, C., Zhu, D., Wang, X., Li, B., Liu, W., and Ma, J., 2012, Black Carbon Emissions in China from 1949 to 2050: Environmental Science & Technology, v. 46, no. 14.

Warren, S. G., 1984, Impurities in snow: Effects on albedo and snowmelt (review): Annals of Glaciology, v. 5, p. 177-179.

Warren, S. G., and Wiscombe, W. J., 1985, Dirty snow after nuclear war: Nature, v. 313, p. 467-470.

Weber, M. G., and Stocks, B. J., 1998, Forest fires and sustainability in the boreal forests of Canada: Ambio, v. 27, no. 7, p. 545-550.

Wendl, I., 2011, Ph.D. Candidate, Paul Scherrer Institut: Villigen, Switzerland.

Whitlow, S. I., Mayewski, P., Dibb, J., Holdsworth, G., and Twickler, M., 1994, An ice-core-based record of biomass burning in the Arctic and Subactic, 1750-1980: Tellus, v. 46B, p. 234-242.

Xu, B.-Q., Wang, M., Joswiak, D. R., Cao, J.-J., Yao, T.-D., Wu, G.-J., Yang, W., and Zhao, H.-B., 2009a, Deposition of anthropogenic aerosols in a southeastern Tibetan glacier: Journal of Geophysical Research-Atmospheres, v. 114.

Xu, B. Q., Cao, J. J., Hansen, J., Yao, T. D., Joswia, D. R., Wang, N. L., Wu, G. J., Wang, M., Zhao, H. B., Yang, W., Liu, X. Q., and He, J. Q., 2009b, Black soot and the survival of Tibetan glaciers: Proceedings of the National Academy of Sciences of the United States of America, v. 106, no. 52, p. 22114-22118.

Yalcin, K., and Wake, C. P., 2001, Anthropogenic signals recorded in an ice core from Eclipse Icefield, Yukon Territory, Canada: Geophysical Research Letters, v. 28, no. 23, p. 4487-4490.

Yalcin, K., Wake, C. R., Kreutz, K. J., and Whitlow, S. I., 2006, A 1000-yr record of forest fire activity from Eclipse Icefield, Yukon, Canada: Holocene, v. 16, no. 2, p. 200-209.

Yasunari, T. J., Bonasoni, P., Laj, P., Fujita, K., Vuillermoz, E., Marinoni, A., Cristofanelli, P., Duchi, R., Tartari, G., and Lau, K. M., 2010, Estimated impact of black carbon deposition during pre-monsoon season from Nepal Climate Observatory - Pyramid data and snow albedo changes over Himalayan glaciers: Atmospheric Chemistry and Physics, v. 10, no. 14, p. 6603-6615.

Youn, D., Park, R. J., Jeong, J. I., Moon, B. K., Yeh, S. W., Kim, Y. H., Woo, J. H., Im, E. G., Jeong, J. H., Lee, S. J., and Song, C. K., 2011, Impacts of aerosols on regional meteorology due to Siberian forest fires in May 2003: Atmospheric Environment, v. 45, no. 7, p. 1407-1412.

Yukon Wildland Fire Management, Wildfire Statistics from 1950 to 2006, http://www.community.gov.yk.ca/firemanagement/sts46.html.

Zhou, C., Penner, J. E., Flanner, M. G., Bisiaux, M. M., Edwards, R., and McConnell, J. R., 2012, Transport of black carbon to polar regions: Sensitivity and forcing by black carbon: Geophysical Research Letters, v. 39.

APPENDIXES

APPENDIX A

NEBULIZER EFFICIENCY DATA

PSL Size	***220***	***356***	***505***	***771***	***1025***
Efficiency SCHG (%)	17.32	18.06	17.23	3.37	0.76
	18.75	18.68	17.49		
	18.22	19.13	17.95		
Efficiency SCLG (%)	19.63	17.70	18.00	3.37	0.75
	19.59	20.69	20.21	3.19	
	18.57	18.00	18.11	3.16	
Mean Efficiency (%)	18.68	18.71	18.17	3.27	0.75
Relative Efficiency	1.00	1.00	0.97	0.17	0.04

APPENDIX B

MASS-SIZE DISTRIBUTION DATA OF VARIOUS BC MATERIALS

Aquablack 162			*Cabojet 200*		
Mass Distribution (Dm/dlog D_{MEV}) (µg/L)	**Normalized Mass Distribution (µg/L)**	**Diameter (nm)**	**Mass Distribution (Dm/dlog D_{MEV}) (µg/L)**	**Normalized Mass Distribution (µg/L)**	**Diameter (nm)**
1.46	0.91	80.38	2.08	0.93	80.16
1.41	0.88	80.94	2.15	0.96	80.75
1.44	0.90	81.51	2.14	0.95	81.35
1.44	0.90	82.08	2.08	0.92	81.95
1.39	0.87	82.65	2.07	0.92	82.55
1.39	0.87	83.22	2.14	0.95	83.16
1.38	0.86	83.80	2.16	0.96	83.78
1.37	0.86	84.39	2.11	0.94	84.39
1.34	0.83	84.98	2.12	0.94	85.02
1.30	0.81	85.57	2.05	0.91	85.64
1.31	0.82	86.17	2.08	0.92	86.28
1.29	0.80	86.77	2.10	0.94	86.91
1.25	0.78	87.37	2.04	0.91	87.56
1.28	0.80	87.98	2.09	0.93	88.20
1.26	0.79	88.60	2.09	0.93	88.85
1.18	0.74	89.21	2.06	0.92	89.51
1.22	0.77	89.84	1.97	0.88	90.17
1.22	0.76	90.46	1.94	0.86	90.84
1.18	0.74	91.09	2.03	0.90	91.51
1.16	0.72	91.73	1.96	0.87	92.18
1.10	0.69	92.37	1.85	0.82	92.86
1.09	0.68	93.01	1.91	0.85	93.55
1.10	0.69	93.66	1.85	0.82	94.24
1.05	0.66	94.31	1.84	0.82	94.93
1.03	0.65	94.97	1.87	0.83	95.64
1.03	0.64	95.63	1.81	0.80	96.34
0.99	0.62	96.30	1.70	0.76	97.05
0.97	0.61	96.97	1.75	0.78	97.77
1.00	0.62	97.65	1.76	0.78	98.49
0.96	0.60	98.33	1.71	0.76	99.22
0.96	0.60	99.02	1.69	0.75	99.95
0.88	0.55	99.71	1.68	0.75	100.69

0.82	0.51	100.40	1.68	0.75	101.43
0.84	0.52	101.10	1.60	0.71	102.18
0.83	0.52	101.81	1.52	0.67	102.94
0.77	0.48	102.52	1.48	0.66	103.70
0.76	0.48	103.23	1.57	0.70	104.46
0.74	0.46	103.95	1.44	0.64	105.23
0.77	0.48	104.68	1.48	0.66	106.01
0.70	0.44	105.41	1.33	0.59	106.79
0.66	0.41	106.14	1.35	0.60	107.58
0.64	0.40	106.88	1.28	0.57	108.37
0.62	0.39	107.63	1.24	0.55	109.17
0.61	0.38	108.38	1.22	0.54	109.98
0.58	0.36	109.13	1.23	0.54	110.79
0.61	0.38	109.89	1.19	0.53	111.61
0.56	0.35	110.66	1.19	0.53	112.43
0.53	0.33	111.43	1.10	0.49	113.26
0.51	0.32	112.21	1.01	0.45	114.10
0.45	0.28	112.99	0.96	0.43	114.94
0.47	0.29	113.78	0.90	0.40	115.79
0.42	0.26	114.57	0.90	0.40	116.65
0.37	0.23	115.37	0.88	0.39	117.51
0.36	0.23	116.18	0.77	0.34	118.38
0.41	0.25	116.99	0.75	0.33	119.25
0.37	0.23	117.80	0.77	0.34	120.13
0.34	0.21	118.62	0.76	0.34	121.02
0.32	0.20	119.45	0.75	0.33	121.91
0.31	0.19	120.29	0.75	0.34	122.81
0.28	0.17	121.12	0.64	0.29	123.72
0.27	0.17	121.97	0.59	0.26	124.63
0.24	0.15	122.82	0.59	0.26	125.55
0.22	0.14	123.68	0.54	0.24	126.48
0.22	0.14	124.54	0.50	0.22	127.41
0.22	0.14	125.41	0.46	0.20	128.35
0.20	0.13	126.28	0.43	0.19	129.30
0.16	0.10	127.16	0.44	0.20	130.25
0.16	0.10	128.05	0.42	0.19	131.22
0.17	0.10	128.94	0.38	0.17	132.18
0.17	0.11	129.84	0.34	0.15	133.16
0.14	0.09	130.75	0.36	0.16	134.14
0.11	0.07	131.66	0.34	0.15	135.13
0.14	0.09	132.58	0.32	0.14	136.13
0.11	0.07	133.50	0.31	0.14	137.14

0.12	0.08	134.43	0.24	0.11	138.15
0.13	0.08	135.37	0.19	0.09	139.17
0.13	0.08	136.31	0.16	0.07	140.20
0.09	0.06	137.26	0.19	0.08	141.23
0.09	0.05	138.22	0.23	0.10	142.27
0.09	0.05	139.19	0.20	0.09	143.32
0.06	0.04	140.16	0.16	0.07	144.38
0.06	0.04	141.13	0.15	0.07	145.45
0.05	0.03	142.12	0.12	0.05	146.52
0.06	0.04	143.11	0.12	0.06	147.60
0.05	0.03	144.11	0.13	0.06	148.69
0.04	0.02	145.11	0.12	0.05	149.79
0.05	0.03	146.12	0.08	0.03	150.90
0.04	0.03	147.14	0.09	0.04	152.01
0.04	0.03	148.17	0.08	0.03	153.13
0.05	0.03	149.20	0.05	0.02	154.26
0.06	0.04	150.24	0.04	0.02	155.40
0.05	0.03	151.29	0.07	0.03	156.55
0.05	0.03	152.35	0.05	0.02	157.71
0.03	0.02	153.41	0.05	0.02	158.87
0.03	0.02	154.48	0.05	0.02	160.04
0.03	0.02	155.55	0.04	0.02	161.23
0.03	0.02	156.64	0.05	0.02	162.42
0.04	0.03	157.73	0.01	0.01	163.61
0.05	0.03	158.83	0.02	0.01	164.82
0.03	0.02	159.94	0.02	0.01	166.04
0.04	0.02	161.05	0.02	0.01	167.27
0.02	0.01	162.18	0.02	0.01	168.50
0.02	0.01	163.31	0.01	0.01	169.74
0.03	0.02	164.45	0.02	0.01	171.00
0.04	0.03	165.59	0.01	0.01	172.26
0.03	0.02	166.75	0.05	0.02	173.53
0.02	0.01	167.91	0.03	0.01	174.81
0.02	0.01	169.08	0.01	0.00	176.10
0.02	0.01	170.26	0.01	0.00	177.40
0.02	0.02	171.45	0.02	0.01	178.71
0.03	0.02	172.64	0.02	0.01	180.03
0.01	0.01	173.85	0.01	0.00	181.36
0.01	0.01	175.06			
0.02	0.01	176.28			
0.01	0.01	177.51			
0.01	0.00	178.75			

0.00	0.00	180.00			
0.01	0.00	181.25			
0.01	0.01	182.52			
0.01	0.00	183.79			
0.01	0.01	185.07			
0.01	0.01	186.36			
0.02	0.01	187.66			
0.02	0.01	188.97			
Flame Soot			***Aquadag***		
Mass Distribution (Dm/dlog D_{MEV}) (µg/L)	**Normalized Mass Distribution (µg/L)**	**Diameter (nm)**	**Mass Distribution (Dm/dlog D_{MEV}) (µg/L)**	**Normalized Mass Distribution (µg/L)**	**Diameter (nm)**
1.16	0.39	80.17	0.26	0.15	80.30
1.18	0.40	80.79	0.25	0.14	81.23
1.23	0.42	81.41	0.25	0.14	82.18
1.23	0.42	82.04	0.25	0.14	83.13
1.22	0.41	82.68	0.25	0.14	84.10
1.22	0.41	83.32	0.27	0.15	85.07
1.33	0.45	83.97	0.29	0.17	86.06
1.26	0.43	84.62	0.29	0.17	87.06
1.27	0.43	85.27	0.30	0.17	88.07
1.39	0.47	85.93	0.33	0.19	89.09
1.37	0.46	86.60	0.34	0.19	90.13
1.42	0.48	87.27	0.33	0.19	91.18
1.41	0.48	87.95	0.34	0.19	92.23
1.46	0.49	88.63	0.34	0.20	93.31
1.46	0.50	89.32	0.38	0.22	94.39
1.58	0.54	90.01	0.39	0.23	95.48
1.64	0.56	90.71	0.39	0.22	96.59
1.60	0.54	91.41	0.41	0.24	97.72
1.60	0.54	92.12	0.42	0.24	98.85
1.71	0.58	92.83	0.43	0.25	100.00
1.77	0.60	93.55	0.45	0.26	101.16
1.81	0.61	94.27	0.46	0.26	102.33
1.71	0.58	95.00	0.47	0.27	103.52
1.83	0.62	95.74	0.51	0.29	104.73
1.81	0.61	96.48	0.53	0.30	105.94
1.87	0.63	97.23	0.55	0.31	107.17
1.88	0.64	97.98	0.58	0.33	108.42

2.08	0.70	98.74	0.62	0.35	109.68
1.97	0.67	99.51	0.62	0.35	110.95
1.96	0.66	100.28	0.61	0.35	112.24
1.95	0.66	101.06	0.67	0.38	113.54
2.17	0.73	101.84	0.70	0.40	114.86
2.20	0.75	102.63	0.72	0.41	116.19
2.11	0.71	103.43	0.77	0.44	117.54
2.14	0.73	104.23	0.81	0.46	118.91
2.29	0.78	105.04	0.82	0.47	120.29
2.24	0.76	105.85	0.79	0.45	121.69
2.30	0.78	106.67	0.85	0.48	123.10
2.29	0.78	107.50	0.91	0.52	124.53
2.32	0.79	108.33	1.01	0.58	125.97
2.40	0.81	109.17	0.99	0.56	127.44
2.46	0.83	110.01	0.99	0.57	128.92
2.41	0.82	110.87	1.02	0.59	130.41
2.61	0.88	111.73	1.09	0.62	131.93
2.54	0.86	112.59	1.15	0.66	133.46
2.60	0.88	113.46	1.14	0.65	135.01
2.58	0.87	114.34	1.22	0.70	136.58
2.58	0.87	115.23	1.26	0.72	138.17
2.56	0.87	116.12	1.20	0.69	139.77
2.64	0.90	117.02	1.31	0.75	141.39
2.67	0.91	117.93	1.35	0.77	143.03
2.66	0.90	118.84	1.33	0.76	144.70
2.58	0.87	119.77	1.31	0.75	146.38
2.55	0.86	120.69	1.36	0.78	148.08
2.56	0.87	121.63	1.38	0.79	149.80
2.60	0.88	122.57	1.38	0.79	151.54
2.78	0.94	123.52	1.46	0.84	153.30
2.60	0.88	124.48	1.49	0.85	155.08
2.49	0.84	125.44	1.44	0.82	156.88
2.69	0.91	126.42	1.47	0.84	158.70
2.86	0.97	127.40	1.43	0.82	160.54
2.69	0.91	128.38	1.51	0.86	162.41
2.69	0.91	129.38	1.53	0.87	164.29
2.52	0.86	130.38	1.54	0.88	166.20
2.56	0.87	131.39	1.57	0.90	168.13
2.53	0.86	132.41	1.59	0.91	170.08
2.75	0.93	133.43	1.56	0.89	172.06
2.47	0.84	134.47	1.58	0.91	174.06
2.43	0.82	135.51	1.56	0.89	176.08

2.42	0.82	136.56	1.62	0.93	178.12
2.34	0.79	137.62	1.56	0.89	180.19
2.40	0.81	138.69	1.57	0.90	182.28
2.04	0.69	139.76	1.59	0.91	184.40
2.16	0.73	140.84	1.60	0.92	186.54
2.15	0.73	141.94	1.61	0.92	188.71
1.96	0.67	143.04	1.66	0.95	190.90
2.07	0.70	144.14	1.58	0.90	193.12
2.03	0.69	145.26	1.54	0.88	195.36
1.75	0.59	146.39	1.50	0.86	197.63
1.62	0.55	147.52	1.67	0.96	199.92
1.66	0.56	148.66	1.57	0.90	202.24
1.67	0.57	149.82	1.58	0.90	204.59
1.66	0.56	150.98	1.57	0.90	206.97
1.44	0.49	152.15	1.46	0.83	209.37
1.41	0.48	153.33	1.44	0.82	211.80
1.28	0.44	154.51	1.45	0.83	214.26
1.19	0.41	155.71	1.56	0.89	216.75
1.31	0.45	156.92	1.48	0.85	219.27
1.25	0.42	158.14	1.61	0.92	221.81
1.01	0.34	159.36	1.58	0.90	224.39
1.01	0.34	160.60	1.55	0.89	227.00
0.88	0.30	161.84	1.50	0.86	229.63
0.82	0.28	163.09	1.36	0.78	232.30
0.78	0.27	164.36	1.44	0.82	235.00
0.72	0.24	165.63	1.43	0.82	237.73
0.58	0.20	166.92	1.42	0.81	240.49
0.57	0.19	168.21	1.41	0.81	243.28
0.66	0.22	169.51	1.40	0.80	246.11
0.66	0.22	170.83	1.39	0.80	248.96
0.41	0.14	172.15	1.38	0.79	251.85
0.51	0.17	173.48	1.38	0.79	254.78
0.48	0.16	174.83	1.37	0.78	257.74
0.51	0.17	176.18	1.36	0.78	260.73
0.34	0.12	177.55	1.35	0.77	263.76
0.46	0.15	178.92	1.34	0.77	266.82
0.38	0.13	180.31	1.33	0.76	269.92
0.35	0.12	181.71	1.27	0.72	273.06
0.36	0.12	183.12	1.28	0.73	276.23
0.35	0.12	184.54	1.36	0.78	279.43
0.19	0.07	185.97	1.46	0.83	282.68
0.26	0.09	187.41	1.29	0.74	285.96

0.18	0.06	188.86	1.16	0.66	289.28
0.18	0.06	190.32	1.07	0.61	292.64
0.21	0.07	191.80	1.14	0.65	296.04
0.19	0.06	193.29	1.17	0.67	299.48
0.17	0.06	194.78	1.05	0.60	302.96
0.19	0.06	196.29	1.03	0.59	306.47
0.17	0.06	197.81	1.19	0.68	310.03
0.13	0.04	199.35	1.18	0.67	313.63
0.07	0.02	200.89	1.19	0.68	317.28
0.07	0.02	202.45	0.93	0.53	320.96
0.11	0.04	204.02	1.00	0.57	324.69
0.12	0.04	205.60	0.94	0.54	328.46
0.08	0.03	207.19	0.98	0.56	332.27
0.04	0.01	208.80	0.97	0.55	336.13
0.02	0.01	210.42	0.95	0.54	340.04
0.08	0.03	212.05	0.80	0.45	343.98
0.07	0.03	213.69	0.73	0.42	347.98
0.05	0.02	215.35	0.76	0.44	352.02
0.05	0.02	217.02	0.85	0.49	356.11
0.06	0.02	218.70	0.69	0.39	360.25
0.05	0.02	220.39	0.72	0.41	364.43
0.03	0.01	222.10	0.79	0.45	368.66
0.06	0.02	223.82	0.79	0.45	372.94
0.01	0.00	225.56	0.72	0.41	377.27
0.01	0.00	227.30	0.57	0.33	381.65
0.03	0.01	229.06	0.62	0.36	386.09
0.03	0.01	230.84	0.58	0.33	390.57
0.02	0.01	232.63	0.55	0.32	395.11
			0.71	0.40	399.69
			0.88	0.50	404.34
			0.82	0.47	409.03
			0.72	0.41	413.78
			0.46	0.26	418.59
			0.46	0.26	423.45
			0.44	0.25	428.36
			0.40	0.23	433.34
			0.51	0.29	438.37
			0.43	0.25	443.46
			0.54	0.31	448.61
			0.49	0.28	453.82
			0.59	0.34	459.09
			0.45	0.26	464.42

	0.27	0.15	469.82
	0.39	0.23	475.28
	0.53	0.30	480.79
	0.47	0.27	486.38
	0.36	0.20	492.03
	0.35	0.20	497.74
	0.47	0.27	503.52
	0.34	0.19	509.37
	0.20	0.11	515.28
	0.31	0.18	521.27
	0.20	0.12	526.95
	0.37	0.21	533.44
	0.44	0.25	539.64
	0.06	0.04	545.90
	0.11	0.06	552.24
	0.06	0.04	558.66
	0.11	0.06	565.15
	0.30	0.17	571.31
	0.37	0.21	578.35
	0.34	0.20	585.07
	0.15	0.09	591.86
	0.24	0.14	598.17
	0.11	0.06	605.68
	0.06	0.03	612.72
	0.00	0.00	619.84
	0.02	0.01	627.03
	0.84	0.48	634.32
	0.32	0.18	641.68
	0.06	0.03	649.14
	0.12	0.07	655.78
	0.15	0.08	664.30
	0.24	0.14	672.01
	0.72	0.41	679.14
	0.00	0.00	687.72
	0.00	0.00	695.70
	0.00	0.00	703.78
	0.00	0.00	711.95
	0.00	0.00	720.21
	0.32	0.18	728.58
	0.14	0.08	737.05
	0.83	0.48	745.61

Fullerene Soot			*BC in Snow*		
Mass Distribution (Dm/dlog D_{MEV}) (µg/L)	**Normalized Mass Distribution (µg/L)**	**Diameter (nm)**	**Mass Distribution (Dm/dlog D_{MEV}) (µg/L)**	**Normalized Mass Distribution (µg/L)**	**Diameter (nm)**
0.41	0.33	80.51	1.41	0.47	80.07
0.42	0.34	81.39	1.41	0.47	80.93
0.41	0.33	82.27	1.45	0.48	81.80
0.42	0.34	83.17	1.47	0.49	82.67
0.44	0.36	84.07	1.50	0.50	83.55
0.47	0.38	84.99	1.54	0.51	84.45
0.47	0.38	85.91	1.53	0.51	85.35
0.50	0.41	86.85	1.57	0.52	86.26
0.52	0.42	87.79	1.59	0.53	87.19
0.52	0.42	88.75	1.61	0.54	88.12
0.52	0.42	89.72	1.66	0.55	89.06
0.56	0.45	90.69	1.69	0.56	90.01
0.55	0.45	91.68	1.72	0.57	90.97
0.58	0.47	92.68	1.73	0.58	91.95
0.57	0.47	93.69	1.73	0.58	92.93
0.61	0.50	94.71	1.74	0.58	93.92
0.65	0.53	95.74	1.79	0.60	94.93
0.67	0.54	96.78	1.81	0.60	95.94
0.63	0.51	97.83	1.87	0.62	96.97
0.62	0.51	98.90	1.87	0.62	98.01
0.71	0.57	99.98	1.96	0.65	99.05
0.66	0.54	101.07	1.98	0.66	100.11
0.72	0.58	102.17	1.98	0.66	101.18
0.73	0.60	103.28	1.98	0.66	102.27
0.72	0.58	104.40	2.04	0.68	103.36
0.73	0.59	105.54	2.03	0.68	104.46
0.76	0.62	106.69	2.07	0.69	105.58
0.79	0.64	107.85	2.06	0.69	106.71
0.79	0.64	109.02	2.09	0.70	107.85
0.83	0.67	110.21	2.16	0.72	109.00
0.82	0.67	111.41	2.22	0.74	110.17
0.80	0.66	112.62	2.25	0.75	111.35
0.86	0.70	113.85	2.29	0.76	112.54
0.83	0.68	115.09	2.33	0.78	113.74
0.86	0.70	116.34	2.35	0.78	114.96
0.86	0.70	117.61	2.37	0.79	116.19

0.88	0.72	118.89	2.37	0.79	117.43
0.90	0.74	120.18	2.46	0.82	118.68
0.93	0.76	121.49	2.48	0.83	119.95
0.90	0.73	122.81	2.47	0.82	121.24
0.91	0.74	124.15	2.52	0.84	122.53
0.96	0.78	125.50	2.51	0.84	123.84
0.97	0.79	126.87	2.60	0.87	125.17
0.97	0.79	128.25	2.63	0.88	126.50
1.01	0.82	129.65	2.71	0.90	127.86
1.02	0.83	131.06	2.71	0.90	129.22
1.03	0.84	132.49	2.69	0.90	130.61
1.05	0.86	133.93	2.72	0.91	132.00
1.04	0.84	135.39	2.74	0.91	133.41
0.95	0.77	136.86	2.79	0.93	134.84
1.01	0.82	138.35	2.81	0.94	136.28
1.03	0.84	139.86	2.76	0.92	137.74
1.07	0.87	141.38	2.75	0.92	139.21
0.99	0.80	142.92	2.80	0.93	140.70
1.07	0.87	144.47	2.73	0.91	142.21
0.97	0.79	146.05	2.65	0.88	143.73
1.02	0.83	147.64	2.67	0.89	145.26
1.12	0.91	149.24	2.77	0.92	146.82
1.02	0.83	150.87	2.85	0.95	148.39
1.01	0.82	152.51	2.90	0.97	149.97
1.06	0.87	154.17	2.88	0.96	151.57
1.08	0.88	155.85	2.84	0.95	153.20
1.00	0.82	157.55	2.76	0.92	154.83
1.03	0.84	159.26	2.83	0.94	156.49
1.01	0.82	161.00	2.71	0.90	158.16
1.01	0.82	162.75	2.70	0.90	159.85
0.96	0.78	164.52	2.66	0.89	161.56
0.97	0.79	166.31	2.59	0.86	163.29
0.93	0.76	168.12	2.54	0.85	165.04
0.88	0.72	169.95	2.55	0.85	166.80
0.91	0.74	171.80	2.54	0.85	168.58
0.85	0.69	173.67	2.53	0.84	170.39
0.80	0.65	175.56	2.38	0.79	172.21
0.87	0.70	177.48	2.42	0.81	174.05
0.77	0.63	179.41	2.47	0.82	175.91
0.74	0.60	181.36	2.39	0.80	177.79
0.83	0.68	183.34	2.28	0.76	179.69
0.84	0.68	185.33	2.30	0.77	181.61

0.75	0.61	187.35	2.33	0.78	183.56
0.71	0.58	189.39	2.27	0.76	185.52
0.73	0.60	191.45	2.14	0.71	187.50
0.66	0.54	193.53	2.27	0.76	189.51
0.67	0.54	195.64	2.33	0.78	191.53
0.71	0.58	197.77	2.16	0.72	193.58
0.77	0.63	199.92	1.97	0.66	195.65
0.75	0.61	202.10	2.07	0.69	197.74
0.61	0.50	204.30	2.05	0.68	199.86
0.69	0.56	206.53	1.97	0.66	201.99
0.71	0.58	208.77	1.98	0.66	204.15
0.66	0.54	211.05	2.03	0.68	206.34
0.70	0.57	213.35	1.99	0.66	208.54
0.72	0.59	215.67	2.09	0.70	210.77
0.69	0.56	218.02	1.88	0.63	213.03
0.60	0.49	220.39	1.71	0.57	215.30
0.60	0.49	222.79	1.76	0.59	217.61
0.70	0.57	225.21	1.80	0.60	219.93
0.64	0.52	227.67	1.67	0.56	222.28
0.62	0.50	230.15	1.57	0.52	224.66
0.59	0.48	232.65	1.59	0.53	227.06
0.56	0.46	235.18	1.60	0.53	229.49
0.53	0.43	237.74	1.52	0.51	231.94
0.51	0.41	240.33	1.52	0.51	234.42
0.48	0.39	242.95	1.52	0.51	236.93
0.45	0.37	245.59	1.49	0.50	239.46
0.42	0.35	248.27	1.46	0.49	242.02
0.36	0.29	250.97	1.43	0.48	244.61
0.36	0.30	253.70	1.40	0.47	247.23
0.37	0.30	256.46	1.37	0.46	249.87
0.42	0.34	259.26	1.34	0.45	252.54
0.40	0.33	262.08	1.31	0.44	255.24
0.35	0.29	264.93	1.28	0.43	257.97
0.29	0.23	267.82	1.15	0.38	260.73
0.38	0.31	270.73	1.08	0.36	263.52
0.36	0.30	273.68	1.11	0.37	266.34
0.33	0.27	276.66	1.10	0.37	269.18
0.32	0.26	279.67	0.91	0.30	272.06
0.29	0.24	282.72	0.90	0.30	274.97
0.31	0.25	285.80	0.87	0.29	277.91
0.26	0.21	288.91	0.92	0.31	280.88
0.33	0.26	292.05	0.77	0.26	283.89

0.23	0.19	295.23	0.82	0.27	286.92
0.26	0.21	298.45	0.80	0.27	289.99
0.24	0.19	301.69	0.67	0.22	293.09
0.30	0.25	304.98	0.73	0.24	296.22
0.37	0.30	308.30	0.67	0.22	299.39
0.19	0.16	311.66	0.65	0.22	302.59
0.14	0.11	315.05	0.67	0.22	305.83
0.27	0.22	318.48	0.65	0.22	309.10
0.32	0.26	321.95	0.61	0.20	312.40
0.27	0.22	325.45	0.56	0.19	315.74
0.23	0.18	328.99	0.51	0.17	319.12
0.16	0.13	332.58	0.47	0.16	322.53
0.20	0.16	336.20	0.44	0.15	325.98
0.15	0.12	339.86	0.48	0.16	329.46
0.09	0.07	343.56	0.59	0.20	332.99
0.16	0.13	347.30	0.59	0.20	336.55
0.18	0.15	351.08	0.57	0.19	340.14
0.14	0.11	354.90	0.31	0.10	343.78
0.30	0.25	358.76	0.32	0.11	347.46
0.18	0.15	362.67	0.38	0.13	351.17
0.11	0.09	366.62	0.46	0.15	354.93
0.11	0.09	370.61	0.30	0.10	358.72
0.15	0.12	374.64	0.34	0.11	362.56
0.23	0.19	378.72	0.40	0.13	366.43
0.18	0.15	382.85	0.41	0.14	370.35
0.15	0.12	387.02	0.41	0.14	374.31
0.13	0.10	391.23	0.31	0.10	378.32
0.08	0.07	395.49	0.27	0.09	382.36
0.03	0.03	399.79	0.22	0.07	386.45
0.05	0.04	404.15	0.26	0.09	390.58
0.05	0.04	408.54	0.33	0.11	394.76
0.07	0.06	412.99	0.18	0.06	398.98
0.09	0.07	417.49	0.14	0.05	403.24
0.04	0.03	422.03	0.23	0.08	407.55
0.06	0.05	426.63	0.11	0.04	411.91
0.09	0.07	431.27	0.10	0.03	416.32
0.03	0.02	435.97	0.19	0.06	420.77
0.02	0.02	440.72	0.14	0.05	425.27
0.02	0.02	445.51	0.23	0.08	429.81
0.02	0.02	450.37	0.33	0.11	434.41
0.01	0.01	455.27	0.12	0.04	439.05
0.10	0.08	460.22	0.13	0.04	443.57

0.16	0.13	464.42	0.03	0.01	448.49
0.00	0.00	470.30	0.06	0.02	453.29
0.01	0.00	475.42	0.06	0.02	458.13
0.06	0.05	480.59	0.05	0.02	463.03
0.07	0.05	485.82	0.10	0.03	467.98
0.01	0.01	491.12	0.19	0.06	472.99
0.00	0.00	496.47	0.07	0.02	478.04
0.05	0.04	501.87	0.07	0.02	483.16
0.00	0.00	507.33	0.15	0.05	488.15
0.00	0.00	512.86	0.00	0.00	493.54
0.00	0.00	518.44	0.12	0.04	498.82
0.00	0.00	524.08	0.04	0.01	504.15
0.00	0.00	529.79	0.00	0.00	509.54
0.00	0.00	535.56	0.00	0.00	514.99
0.00	0.00	541.39	0.09	0.03	520.50
0.00	0.00	547.28	0.11	0.04	525.93
0.00	0.00	553.24	0.09	0.03	531.69
0.10	0.08	559.27	0.09	0.03	537.09
0.13	0.10	565.36	0.00	0.00	543.12
0.00	0.00	571.50	0.00	0.00	548.93
0.00	0.00	577.73	0.00	0.00	554.80
0.00	0.00	584.03	0.00	0.00	560.73
0.00	0.00	590.38	0.00	0.00	566.72
0.00	0.00	596.80	0.00	0.00	572.78
0.00	0.00	603.31	0.00	0.00	578.91
0.00	0.00	609.88	0.31	0.10	585.10
0.00	0.00	616.51	0.16	0.05	591.36
0.00	0.00	623.21	0.00	0.00	597.67
0.00	0.00	630.01	0.00	0.00	604.07
0.00	0.00	636.87	0.00	0.00	610.53
0.00	0.00	643.80	0.00	0.00	617.05
0.00	0.00	650.80	0.00	0.00	623.65
0.00	0.00	657.90	0.00	0.00	630.32
0.00	0.00	665.06	0.00	0.00	637.06
0.00	0.00	672.30	0.00	0.00	643.87
0.00	0.00	679.61	0.00	0.00	650.75
0.00	0.00	687.02	0.00	0.00	657.72
0.00	0.00	694.50	0.22	0.07	664.75
0.00	0.00	702.05	0.41	0.14	670.22
0.00	0.00	709.70			
0.00	0.00	717.43			
0.00	0.00	725.24			

0.00	0.00	733.13	
0.00	0.00	741.11	
0.00	0.00	749.19	
0.00	0.00	757.35	
0.04	0.03	765.58	
0.39	0.32	773.92	
0.20	0.16	782.35	

APPENDIX C

BC STANDARDS DATA

$_{meas}BC$ and $_{mass}BC$ units are μg/L.

Aquadag						
6/22/12	$_{meas}BC$	0.27	0.94	2.35	2.89	5.45
	$_{mass}BC$	0.52	2.05	5.19	7.26	11.75
6/25/12	$_{meas}BC$	0.17	0.91	1.71	2.70	4.25
	$_{mass}BC$	0.53	2.63	5.31	7.89	12.29
6/25/12	$_{meas}BC$	0.36	1.31	2.21	3.59	5.36
	$_{mass}BC$	0.54	2.36	4.61	7.55	10.79
6/29/12	$_{meas}BC$	0.15	0.86	1.58	2.20	4.25
	$_{mass}BC$	0.58	2.60	5.17	7.45	12.56
6/30/12	$_{meas}BC$	0.22	1.55	2.73	4.31	6.36
	$_{mass}BC$	0.46	2.72	5.19	7.43	12.18
7/4/12	$_{meas}BC$	0.36	1.36	3.08	4.30	6.62
	$_{mass}BC$	0.56	2.54	5.24	7.40	11.87
7/5/12	$_{meas}BC$	0.27	1.29	2.63	3.88	5.91
	$_{mass}BC$	0.52	2.51	5.19	7.64	12.64
7/10/12	$_{meas}BC$	0.28	0.99	2.29	3.60	4.69
	$_{mass}BC$	0.57	2.46	5.18	7.44	12.53
7/27/12	$_{meas}BC$	0.16	0.73	1.54	2.30	3.59
	$_{mass}BC$	0.49	2.35	5.20	7.24	10.99
4/26/13	$_{meas}BC$	0.17	0.76	1.14	2.43	3.24
	$_{mass}BC$	0.60	2.85	4.27	8.80	10.90
4/30/13	$_{meas}BC$	0.27	1.25	2.04	2.86	3.61
	$_{mass}BC$	0.67	2.88	5.52	7.41	12.11
5/1/13	$_{meas}BC$	0.19	0.75	1.19	1.56	2.88
	$_{mass}BC$	0.65	2.91	4.68	6.52	11.64
5/3/13	$_{meas}BC$	0.22	0.70	1.42	2.10	3.53
	$_{mass}BC$	0.67	2.37	4.48	6.38	10.62
5/8/13	$_{meas}BC$	0.30	0.93	2.37	3.05	3.31
	$_{mass}BC$	0.69	2.43	5.04	6.77	8.82
Flame Soot						
6/22/12	$_{meas}BC$	0.41	1.23	2.59	3.83	
	$_{mass}BC$	0.95	3.86	8.77	13.85	

	${}_{meas}BC$	0.17	0.74	1.54	2.00	3.61
6/25/12	${}_{mass}BC$	0.57	2.58	5.51	7.28	12.46
	${}_{meas}BC$	0.20	0.79	1.51	2.21	3.67
7/10/12	${}_{mass}BC$	0.56	2.47	5.19	7.38	11.23
	${}_{meas}BC$	0.17	0.78	1.66	2.13	3.51
7/27/12	${}_{mass}BC$	0.50	2.49	4.92	6.92	12.01
	${}_{meas}BC$	0.24	0.71	2.30	3.03	5.23
8/6/12	${}_{mass}BC$	0.54	2.52	5.02	7.31	12.81
Cabojet 200						
	${}_{meas}BC$	0.26	1.21	2.27	3.37	4.87
6/25/12	${}_{mass}BC$	0.70	3.18	6.24	9.70	15.15
	${}_{meas}BC$	0.16	0.68	1.24	2.24	2.67
7/13/12	${}_{mass}BC$	0.47	2.13	4.13	6.19	8.73
	${}_{meas}BC$	0.18	0.71	1.42	2.24	3.27
7/27/12	${}_{mass}BC$	0.49	2.25	4.44	6.41	9.87
	${}_{meas}BC$	0.31	1.40	2.51	3.30	5.09
8/6/12	${}_{mass}BC$	0.44	2.37	4.71	6.48	10.78
	${}_{meas}BC$	0.23	1.22	2.15	2.97	3.94
8/7/12	${}_{mass}BC$	0.43	2.44	4.96	6.96	10.60
Aquablack 162						
	${}_{meas}BC$	0.47	1.37	2.05	3.28	
6/29/12	${}_{mass}BC$	0.61	2.65	5.92	7.76	
	${}_{meas}BC$	0.15	0.68	1.15	1.62	2.57
7/13/12	${}_{mass}BC$	0.46	1.86	3.84	5.47	9.42
	${}_{meas}BC$	0.18	0.73	1.49	2.05	3.52
7/27/12	${}_{mass}BC$	0.38	1.86	3.58	5.11	9.69
	${}_{meas}BC$	0.24	0.95	1.78	2.37	3.32
8/7/12	${}_{mass}BC$	0.42	1.83	3.55	5.31	8.81
	${}_{meas}BC$	0.09	0.35	0.53	0.86	1.28
8/10/12	${}_{mass}BC$	0.38	1.79	3.48	5.64	8.97
Fullerene Soot						
	${}_{meas}BC$	0.20	0.77	1.85	2.74	3.63
4/26/13	${}_{mass}BC$	0.73	2.93	6.27	9.41	12.30
	${}_{meas}BC$	0.26	1.03	1.48	2.08	3.72
4/30/13	${}_{mass}BC$	0.74	3.13	5.42	7.73	12.64
5/1/13	${}_{meas}BC$	0.26	0.54	1.26	1.62	2.66

	$_{mass}BC$	0.59	2.62	5.24	6.80	11.42
5/3/13	$_{meas}BC$	0.22	0.68	1.01	2.32	3.09
	$_{mass}BC$	0.70	2.93	4.30	7.24	11.32
5/8/13	$_{meas}BC$	0.26	1.05	1.55	1.98	3.22
	$_{mass}BC$	0.62	2.67	3.95	5.73	8.72

APPENDIX D

STORAGE EXPERIMENT DATA

Sample	BC material	Vial Type	Storage Temp. (°C)	$_{meas}$BC after days in storage (indicated in italics) (µg/L)					
				0	*1*	*2*	*3*	*11*	*18*
1	Aquadag	polypropylene	2	1.39	1.49	1.46	1.30	1.47	1.28
2	Aquadag	polypropylene	2	1.36	1.46	1.39	1.32	1.48	1.29
3	Aquadag	polypropylene	25	1.32	1.54	1.39	1.19	0.62	0.29
4	Aquadag	polypropylene	25	1.39	1.54	1.43	1.07	0.59	0.26
5	Aquadag	polypropylene	2	4.97	4.74	4.93	4.37	4.57	4.14
6	Aquadag	polypropylene	2	4.86	4.82	5.11	4.37	4.70	4.44
7	Aquadag	polypropylene	25	4.59	4.90	4.54	3.77	3.11	1.55
8	Aquadag	polypropylene	25	5.24	5.16	4.76	3.75	3.62	1.81
9	Aquadag	polypropylene	2	6.26	6.61	7.05	5.92	6.14	5.48
10	Aquadag	polypropylene	2	7.04	6.67	6.89	6.03	6.30	6.01
11	Aquadag	polypropylene	25	7.10	6.98	6.28	4.94	4.81	3.90
12	Aquadag	polypropylene	25	7.26	6.93	6.16	5.14	4.82	4.56
13	BC in snow	polypropylene	2	2.43	2.81	2.78	2.84	2.74	2.64
14	BC in snow	polypropylene	2	2.51	2.91	2.57	2.71	2.75	2.59
15	BC in snow	polypropylene	25	2.26	2.53	2.25	1.89	1.00	0.68
16	BC in snow	polypropylene	25	2.51	2.52	2.47	1.77	0.94	0.51
17	Aquadag	glass	2	1.34	1.42	1.37	1.33	1.33	1.33
18	Aquadag	glass	2	1.34	1.39	1.35	1.27	1.32	1.35
19	Aquadag	glass	25	1.36	1.27	1.37	1.18	1.36	1.21
20	Aquadag	glass	25	1.63	1.63	1.53	1.33	1.43	1.38
21	Aquadag	glass	2	4.41	4.29	3.86	3.76	4.12	4.24
22	Aquadag	glass	2	4.87	4.89	4.51	4.02	4.17	4.36
23	Aquadag	glass	25	4.49	4.72	4.18	3.51	3.67	3.56
24	Aquadag	glass	25	4.67	4.60	4.51	3.90	4.19	4.28
25	Aquadag	glass	2	7.23	6.63	6.58	5.75	6.43	6.46
26	Aquadag	glass	2	6.80	6.71	6.62	5.65	5.96	6.53
27	Aquadag	glass	25	7.80	6.57	6.65	5.76	6.33	5.94
28	Aquadag	glass	25	6.45	6.68	6.37	5.78	6.45	6.01
29	BC in snow	glass	2	2.24	2.40	2.17	2.14	2.28	2.16
30	BC in	glass	2	2.48	2.66	2.67	2.53	2.66	2.67

	snow								
31	BC in snow	glass	25	2.25	2.47	2.15	2.05	2.22	2.03
32	BC in snow	glass	25	2.95	3.29	3.09	2.77	2.51	2.67

APPENDIX E

HIGH RESOLUTION ICE CORE DATA

Sample	Depth (m)	AD Year	$_{meas}$BC (µg/L)	$_{cal}$BC (µg/L)	Mean Background $_{cal}$BC (µg/L)	$_{cal}$BC Minus Background (µg/L)
6404	2.149	1999.42	0.081	0.186	0.038	0.148
6405	2.246	1999.32	0.190	0.437		0.399
6406	2.344	1999.22	0.116	0.267		0.229
6407	2.441	1999.12	0.047	0.108		0.070
6408	2.538	1999.02	0.122	0.280		0.242
6409	2.636	1998.92	0.115	0.264		0.226
6410	2.733	1998.83	0.094	0.216		0.178
6412	2.928	1998.63	0.135	0.310		0.272
6413	3.025	1998.53	0.068	0.156		0.118
6414	3.114	1998.44	0.039	0.090		0.052
6415	3.193	1998.36	0.120	0.276		0.238
6416	3.273	1998.28	0.125	0.288		0.250
6417	3.352	1998.20	0.130	0.298		0.260
6418	3.432	1998.12	0.098	0.226		0.188
6419	3.511	1998.04	0.100	0.231		0.193
6420	3.591	1997.95	0.182	0.418		0.380
6421	3.670	1997.86	0.168	0.387		0.349
6423	3.829	1997.66	0.062	0.144		0.106
6424	3.909	1997.57	0.093	0.214		0.176
6425	3.988	1997.47	0.118	0.272		0.234
6426	4.067	1997.37	0.141	0.323		0.285
6428	4.225	1997.18	0.180	0.413		0.375
6429	4.304	1997.10	0.054	0.124		0.086
6430	4.383	1997.00	0.283	0.650		0.612
6431	4.462	1996.92	0.124	0.285		0.247
6433	4.620	1996.75	0.049	0.113		0.075
6434	4.699	1996.66	0.032	0.074		0.036
6435	4.778	1996.58	0.064	0.148		0.110
6436	4.857	1996.49	0.053	0.121		0.083
6437	4.936	1996.41	0.068	0.157		0.119
6438	5.015	1996.34	0.036	0.082		0.044
6439	5.094	1996.25	0.060	0.137		0.099

6440	5.173	1996.17	0.094	0.215		0.177
6441	5.252	1996.08	0.061	0.140		0.102
6442	5.331	1996.00	0.072	0.165		0.127
6443	5.409	1995.92	0.081	0.186		0.148
6444	5.486	1995.83	0.081	0.186		0.148
6445	5.563	1995.76	0.046	0.107		0.069
6446	5.640	1995.67	0.046	0.106		0.068
6448	5.794	1995.52	0.036	0.082		0.045
6449	5.871	1995.43	0.065	0.150		0.112
6450	5.948	1995.35	0.060	0.137		0.099
6451	5.998	1995.29	0.096	0.220		0.182
6539	6.050	1995.24	0.077	0.177		0.139
6540	6.131	1995.16	0.065	0.149		0.111
6541	6.212	1995.07	0.044	0.102		0.064
6542	6.292	1994.98	0.032	0.073		0.036
6544	6.454	1994.70	0.040	0.092		0.054
6546	6.615	1994.40	0.176	0.404		0.366
6547	6.696	1994.26	0.065	0.150		0.112
6548	6.777	1994.12	0.039	0.090		0.052
6549	6.858	1993.99	0.043	0.099		0.061
6550	6.938	1993.89	0.068	0.156		0.119
6551	7.019	1993.79	0.024	0.055		0.017
6452	7.091	1993.71	0.083	0.192		0.154
6453	7.154	1993.63	0.104	0.239		0.201
6454	7.217	1993.55	0.193	0.445		0.407
6455	7.279	1993.48	0.064	0.147		0.109
6456	7.342	1993.40	0.119	0.274		0.236
6457	7.405	1993.32	0.062	0.143		0.105
6459	7.531	1993.17	0.065	0.149		0.111
6462	7.719	1992.94	0.145	0.334		0.296
6465	7.908	1992.72	0.026	0.060		0.022
6466	7.971	1992.66	0.050	0.115		0.077
6467	8.034	1992.59	0.045	0.103		0.065
6468	8.097	1992.51	0.040	0.091		0.054
6469	8.159	1992.44	0.026	0.061		0.023
6470	8.222	1992.37	0.050	0.114		0.076
6471	8.285	1992.29	0.041	0.095		0.057
6472	8.348	1992.22	0.071	0.163		0.125
6473	8.411	1992.15	0.099	0.227		0.189

6474	8.474	1992.08	0.113	0.260		0.222
6475	8.537	1992.00	0.089	0.206		0.168
6477	8.663	1991.76	0.050	0.114		0.076
6478	8.725	1991.62	0.077	0.176		0.139
6479	8.790	1991.50	0.077	0.177		0.139
6481	8.923	1991.24	0.082	0.188		0.150
6482	8.989	1991.10	0.034	0.079		0.041
6485	9.189	1990.73	0.100	0.229		0.191
6486	9.255	1990.60	0.043	0.100		0.062
6487	9.322	1990.49	0.052	0.119		0.081
6488	9.388	1990.36	0.086	0.199		0.161
6489	9.455	1990.25	0.040	0.092		0.054
6490	9.521	1990.13	0.035	0.081		0.043
322	9.365	1990.34	0.062	0.143	0.081	0.062
323	9.396	1990.29	0.126	0.289		0.208
324	9.427	1990.24	0.094	0.216		0.135
325	9.457	1990.20	0.103	0.237		0.156
326	9.488	1990.15	0.017	0.040	0.029	0.011
327	9.519	1990.10	0.018	0.040		0.011
328	9.549	1990.06	0.017	0.040		0.010
329	9.580	1990.01	0.067	0.153		0.124
330	9.610	1989.96	0.056	0.128		0.099
332	9.672	1989.87	0.050	0.114		0.085
333	9.702	1989.82	0.266	0.613		0.584
334	9.733	1989.78	0.102	0.235		0.206
335	9.764	1989.73	0.022	0.050		0.021
336	9.794	1989.68	0.031	0.071		0.042
337	9.825	1989.64	0.034	0.078		0.049
338	9.856	1989.59	0.022	0.050		0.021
339	9.886	1989.54	0.020	0.047		0.018
340	9.917	1989.50	0.035	0.080		0.050
341	9.948	1989.45	0.070	0.160		0.131
342	9.978	1989.40	0.115	0.264		0.234
344	10.040	1989.31	0.018	0.041		0.012
345	10.070	1989.26	0.030	0.070		0.041
346	10.101	1989.22	0.060	0.138		0.109
347	10.132	1989.17	0.037	0.085		0.056
348	10.162	1989.12	0.027	0.062		0.033
349	10.193	1989.08	0.031	0.071		0.042

350	10.224	1989.03	0.059	0.135		0.106
351	10.254	1988.98	0.069	0.159		0.129
353	10.316	1988.89	0.061	0.141		0.112
354	10.346	1988.84	0.134	0.307		0.278
355	10.377	1988.80	1.330	3.059		3.030
357	10.437	1988.71	0.962	2.214		2.184
358	10.466	1988.66	0.598	1.375		1.346
359	10.495	1988.62	0.381	0.876		0.847
360	10.523	1988.57	0.220	0.505	0.020	0.485
361	10.552	1988.53	0.025	0.057		0.037
362	10.581	1988.49	0.025	0.057		0.037
363	10.609	1988.44	0.014	0.033		0.013
364	10.638	1988.40	0.026	0.060		0.040
365	10.667	1988.36	0.040	0.092		0.072
366	10.695	1988.31	0.025	0.057		0.037
367	10.724	1988.27	0.046	0.105		0.085
369	10.781	1988.18	0.083	0.192		0.172
370	10.810	1988.14	0.265	0.609		0.588
371	10.839	1988.09	0.152	0.350		0.330
372	10.867	1988.05	0.069	0.159		0.139
376	10.982	1987.88	0.040	0.091		0.071
377	11.011	1987.83	0.044	0.101		0.081
378	11.039	1987.79	0.025	0.058		0.038
379	11.068	1987.74	0.156	0.359		0.339
381	11.125	1987.66	0.038	0.088		0.068
382	11.154	1987.61	0.049	0.113		0.092
383	11.183	1987.57	0.028	0.064		0.044
384	11.211	1987.53	0.025	0.057		0.037
385	11.240	1987.48	0.023	0.052		0.032
386	11.269	1987.44	0.031	0.072		0.052
387	11.297	1987.40	0.035	0.081		0.061
388	11.326	1987.35	0.028	0.065		0.045
389	11.355	1987.31	0.064	0.148		0.128
390	11.383	1987.26	0.034	0.078		0.058
391	11.412	1987.22	0.063	0.146		0.126
392	11.441	1987.18	0.029	0.067		0.047
393	11.471	1987.13	0.037	0.086		0.066
395	11.530	1987.04	0.177	0.407		0.387
396	11.559	1987.00	0.122	0.280		0.260

397	11.589	1986.95	0.027	0.062		0.042
398	11.618	1986.91	0.036	0.083		0.063
399	11.648	1986.86	0.022	0.052		0.032
400	11.677	1986.82	0.093	0.214		0.194
401	11.707	1986.77	0.164	0.377		0.357
402	11.736	1986.73	0.570	1.312		1.292
403	11.766	1986.68	0.141	0.324		0.304
404	11.795	1986.64	0.022	0.050		0.030
406	11.854	1986.55	0.026	0.060		0.040
407	11.884	1986.50	0.029	0.067		0.047
408	11.913	1986.46	0.044	0.101		0.081
409	11.943	1986.41	0.084	0.194		0.174
410	11.972	1986.37	0.129	0.296		0.276
411	12.002	1986.32	0.039	0.089		0.069
413	12.061	1986.23	0.012	0.029		0.009
414	12.090	1986.19	0.020	0.045		0.025
415	12.120	1986.14	0.030	0.069		0.049
416	12.149	1986.10	0.015	0.033		0.013
418	12.208	1986.01	0.010	0.023		0.003
421	12.297	1985.87	0.075	0.172		0.152
422	12.326	1985.83	0.053	0.122		0.102
423	12.356	1985.78	0.031	0.072		0.052
425	12.400	1985.50	0.051	0.117	0.023	0.094
426	12.445	1985.47	0.028	0.065		0.041
427	12.475	1985.42	0.033	0.077		0.053
428	12.505	1985.39	0.032	0.073		0.050
429	12.535	1985.35	0.028	0.065		0.042
431	12.595	1985.28	0.030	0.068		0.045
433	12.655	1985.21	0.033	0.075		0.052
434	12.685	1985.18	0.049	0.114		0.091
436	12.745	1985.11	0.057	0.130		0.107
437	12.775	1985.07	0.069	0.158		0.135
438	12.805	1985.04	0.082	0.189		0.165
439	12.835	1985.00	0.093	0.215		0.191
440	12.866	1984.95	0.024	0.055		0.032
441	12.896	1984.91	0.057	0.130		0.107
442	12.926	1984.86	0.137	0.314		0.291
443	12.956	1984.82	0.120	0.276		0.253
444	12.986	1984.77	0.037	0.085	0.033	0.053

446	13.046	1984.68	0.167	0.385		0.352
447	13.076	1984.63	0.158	0.363		0.330
448	13.106	1984.58	0.110	0.254		0.221
449	13.136	1984.54	0.041	0.095		0.062
450	13.166	1984.49	0.116	0.267		0.235
453	13.256	1984.35	0.079	0.183		0.150
455	13.316	1984.26	0.221	0.509		0.476
456	13.346	1984.22	0.044	0.101		0.069
458	13.406	1984.12	0.095	0.217		0.185
459	13.436	1984.08	0.054	0.125		0.093
460	13.466	1984.03	0.174	0.399		0.367
461	13.496	1983.99	0.123	0.282		0.250
462	13.526	1983.95	0.182	0.418		0.386
463	13.556	1983.92	0.470	1.082		1.049
464	13.586	1983.88	0.188	0.432		0.400
465	13.617	1983.85	0.055	0.126		0.093
466	13.647	1983.81	0.438	1.008		0.976
468	13.711	1983.74	0.148	0.341		0.309
469	13.743	1983.71	0.204	0.470		0.437
470	13.776	1983.66	0.278	0.639		0.606
471	13.809	1983.62	0.418	0.962		0.929
472	13.841	1983.59	0.139	0.319		0.286
473	13.874	1983.55	0.023	0.052		0.019
474	13.907	1983.51	0.051	0.118		0.085
475	13.939	1983.47	0.116	0.268		0.235
476	13.972	1983.44	0.161	0.370		0.338
477	14.005	1983.40	0.112	0.258		0.225
478	14.038	1983.35	0.101	0.232		0.199
479	14.070	1983.32	0.084	0.192		0.160
480	14.103	1983.28	0.087	0.200		0.167
481	14.136	1983.24	0.096	0.222		0.189
482	14.168	1983.20	0.172	0.395		0.362
483	14.201	1983.16	0.254	0.583		0.551
484	14.234	1983.13	1.213	2.791		2.759
485	14.266	1983.09	0.859	1.975		1.943
486	14.299	1983.05	0.541	1.244		1.211
487	14.332	1983.01	0.264	0.607	0.017	0.591
488	14.364	1982.96	0.368	0.846		0.829
489	14.397	1982.89	0.143	0.329		0.312

490	14.430	1982.84	0.150	0.345		0.328
491	14.463	1982.79	0.071	0.164		0.147
492	14.495	1982.71	0.135	0.310		0.293
493	14.528	1982.66	0.161	0.371		0.354
494	14.561	1982.61	0.031	0.071		0.054
495	14.593	1982.55	0.103	0.237		0.221
496	14.626	1982.48	0.071	0.163		0.147
497	14.659	1982.43	0.066	0.151		0.134
498	14.690	1982.38	0.107	0.245		0.229
499	14.721	1982.32	0.303	0.696		0.679
500	14.752	1982.27	0.266	0.613		0.596
501	14.783	1982.21	0.197	0.452	0.022	0.431
502	14.814	1982.16	0.298	0.686		0.665
503	14.845	1982.11	0.306	0.704		0.682
504	14.876	1982.04	0.256	0.589		0.567
505	14.907	1981.98	0.299	0.687		0.665
506	14.938	1981.93	0.695	1.600		1.578
507	14.969	1981.87	2.193	5.045		5.023
508	15.000	1981.81	4.307	9.907		9.886
510	15.061	1981.70	1.681	3.868		3.846
511	15.092	1981.65	0.087	0.200		0.178
512	15.123	1981.59	0.034	0.077		0.056
513	15.154	1981.54	0.033	0.076		0.055
514	15.185	1981.47	0.038	0.088		0.067
515	15.216	1981.41	0.033	0.076		0.054
516	15.247	1981.35	0.164	0.378		0.356
517	15.278	1981.30	0.099	0.227		0.205
518	15.309	1981.24	0.147	0.338		0.317
519	15.340	1981.19	0.097	0.222		0.201
520	15.370	1981.13	0.135	0.310		0.288
521	15.401	1981.07	0.041	0.094		0.072
522	15.432	1981.02	0.040	0.092		0.070
523	15.463	1980.96	0.038	0.089		0.067
524	15.494	1980.89	0.034	0.078		0.056
525	15.525	1980.83	0.044	0.102		0.080
526	15.556	1980.74	0.143	0.330		0.308
527	15.587	1980.67	0.069	0.158		0.136
528	15.618	1980.61	0.156	0.359		0.338
529	15.649	1980.54	0.134	0.309		0.287

530	15.680	1980.48	0.041	0.094		0.072
531	15.710	1980.41	0.029	0.066		0.044
532	15.741	1980.35	0.336	0.774		0.752
533	15.772	1980.28	0.863	1.984		1.963
534	15.802	1980.22	0.117	0.268		0.247
535	15.832	1980.15	0.012	0.027		0.005
536	15.862	1980.09	0.013	0.029		0.007
537	15.891	1980.02	0.024	0.055		0.033
538	15.921	1979.96	0.015	0.034		0.013
539	15.950	1979.91	0.109	0.250		0.229
540	15.980	1979.86	0.120	0.276		0.254
541	16.009	1979.80	0.030	0.070		0.048
542	16.039	1979.75	0.031	0.071		0.049
543	16.068	1979.70	0.157	0.360		0.339
544	16.098	1979.64	0.033	0.076		0.055
545	16.127	1979.59	0.019	0.043		0.021
546	16.157	1979.54	0.059	0.135		0.114
547	16.186	1979.48	0.031	0.071		0.050
548	16.216	1979.43	0.052	0.120		0.098
549	16.245	1979.38	0.020	0.047		0.025
550	16.275	1979.34	0.028	0.065		0.043
551	16.304	1979.29	0.044	0.102		0.080
552	16.334	1979.23	0.071	0.164		0.143
553	16.363	1979.18	0.092	0.211		0.189
554	16.393	1979.13	0.111	0.256		0.234
555	16.422	1979.07	0.135	0.310		0.288
556	16.452	1979.02	0.166	0.383		0.361
559	16.540	1978.89	0.035	0.081		0.060
560	16.570	1978.85	0.076	0.175		0.154
561	16.600	1978.81	0.137	0.314		0.293
562	16.629	1978.77	0.131	0.301		0.279
563	16.659	1978.73	0.107	0.246		0.224
564	16.688	1978.69	0.020	0.045		0.023
565	16.718	1978.65	0.095	0.219		0.198
566	16.747	1978.58	0.105	0.240		0.219
567	16.777	1978.52	0.064	0.148		0.126
568	16.806	1978.53	0.142	0.326		0.304
569	16.834	1978.49	0.100	0.230		0.209
570	16.862	1978.46	0.119	0.273		0.251

571	16.890	1978.42	0.203	0.466		0.444
572	16.917	1978.38	0.113	0.260		0.238
573	16.945	1978.35	0.129	0.298		0.276
574	16.972	1978.31	0.183	0.420		0.399
575	17.000	1978.27	0.262	0.603		0.581
576	17.027	1978.23	0.312	0.719		0.697
577	17.055	1978.20	0.108	0.249		0.227
578	17.082	1978.16	0.140	0.323		0.301
579	17.110	1978.12	0.185	0.426		0.404
580	17.138	1978.08	0.033	0.077		0.055
581	17.165	1978.04	0.421	0.968		0.946
582	17.193	1978.01	0.043	0.100		0.078
583	17.220	1977.97	0.017	0.039		0.017
584	17.248	1977.92	0.040	0.092		0.070
585	17.275	1977.88	0.041	0.093		0.071
586	17.303	1977.85	0.298	0.686		0.664
587	17.330	1977.80	0.104	0.240		0.218
588	17.358	1977.76	0.365	0.839		0.817
589	17.385	1977.71	0.060	0.138		0.117
590	17.413	1977.68	0.034	0.078	0.025	0.053
591	17.440	1977.64	0.104	0.240		0.215
592	17.468	1977.59	0.068	0.157		0.132
594	17.523	1977.52	0.033	0.075		0.050
595	17.551	1977.47	0.023	0.053		0.028
596	17.578	1977.42	0.149	0.343		0.318
597	17.606	1977.38	0.095	0.218		0.193
598	17.633	1977.35	0.142	0.327		0.302
599	17.661	1977.30	0.274	0.631		0.606
600	17.688	1977.26	0.773	1.779		1.754
601	17.716	1977.21	0.285	0.657		0.632
602	17.743	1977.18	0.264	0.607		0.582
603	17.771	1977.14	0.114	0.262		0.237
604	17.798	1977.09	0.094	0.216		0.191
605	17.825	1977.06	0.148	0.341		0.316
606	17.852	1977.02	0.236	0.543		0.518
607	17.878	1976.97	0.196	0.450		0.425
608	17.905	1976.92	0.043	0.099		0.073
609	17.932	1976.89	0.019	0.044		0.019
610	17.959	1976.84	0.036	0.083		0.058

611	17.986	1976.80	0.132	0.303		0.278
613	18.039	1976.72	0.059	0.137		0.112
614	18.066	1976.67	0.125	0.288		0.263
615	18.093	1976.64	0.215	0.494		0.469
616	18.120	1976.59	0.252	0.579		0.554
617	18.147	1976.55	0.083	0.191		0.166
618	18.174	1976.52	0.167	0.384		0.359
619	18.200	1976.47	0.203	0.466		0.441
620	18.227	1976.42	0.125	0.287		0.262
621	18.254	1976.39	0.032	0.073		0.048
622	18.281	1976.34	0.042	0.098		0.073
623	18.308	1976.30	0.079	0.181		0.156
624	18.335	1976.27	0.131	0.302		0.277
625	18.361	1976.22	0.052	0.120		0.095
626	18.388	1976.17	0.063	0.145		0.120
627	18.415	1976.14	0.068	0.155		0.130
628	18.442	1976.09	0.231	0.531		0.506
629	18.469	1976.05	0.172	0.395		0.370
630	18.495	1976.00	0.158	0.363		0.338
631	18.522	1975.96	0.085	0.195		0.170
632	18.549	1975.91	0.185	0.425		0.400
633	18.576	1975.85	0.132	0.304		0.278
634	18.603	1975.81	0.623	1.433		1.408
635	18.630	1975.76	0.164	0.378		0.353
636	18.656	1975.70	0.129	0.298		0.273
637	18.683	1975.67	0.227	0.521		0.496
638	18.710	1975.61	0.173	0.398		0.373
639	18.737	1975.56	0.032	0.073		0.048
640	18.764	1975.51	0.059	0.135		0.110
641	18.791	1975.46	0.014	0.033		0.008
642	18.817	1975.41	0.024	0.055		0.030
643	18.844	1975.37	0.025	0.057		0.032
644	18.871	1975.31	0.035	0.081		0.056
645	18.898	1975.26	0.151	0.348		0.323
646	18.926	1975.20	0.251	0.577		0.552
647	18.953	1975.17	0.538	1.237		1.212
648	18.980	1975.11	0.207	0.476		0.451
649	19.007	1975.06	0.094	0.215	0.023	0.192
650	19.034	1975.02	0.347	0.799		0.776

651	19.061	1974.97	0.077	0.177		0.154
652	19.089	1974.92	0.125	0.287		0.263
653	19.116	1974.86	0.030	0.069		0.046
654	19.143	1974.83	0.031	0.072		0.048
655	19.170	1974.78	0.059	0.136		0.113
656	19.197	1974.73	0.100	0.229		0.206
657	19.224	1974.69	0.032	0.073		0.050
658	19.252	1974.64	0.045	0.104		0.081
659	19.279	1974.59	0.079	0.181		0.158
660	19.306	1974.54	0.129	0.298		0.275
661	19.333	1974.51	0.178	0.409		0.386
662	19.360	1974.46	0.108	0.248		0.225
663	19.387	1974.41	0.511	1.175		1.152
664	19.415	1974.37	0.060	0.139		0.116
665	19.442	1974.32	0.042	0.098		0.074
666	19.469	1974.27	0.066	0.151		0.128
667	19.496	1974.22	0.116	0.267		0.244
668	19.523	1974.19	0.164	0.378		0.355
669	19.551	1974.14	0.183	0.420		0.397
670	19.578	1974.08	0.111	0.255		0.232
672	19.632	1974.00	0.045	0.104		0.080
673	19.659	1973.95	0.069	0.159		0.136
674	19.686	1973.90	0.031	0.071		0.048
676	19.714	1973.81	0.029	0.066		0.043
677	19.741	1973.76	0.079	0.181		0.158
678	19.768	1973.72	0.056	0.128		0.105
679	19.823	1973.68	0.115	0.265		0.242
680	19.851	1973.63	0.068	0.156		0.133
681	19.879	1973.58	0.156	0.359		0.336
682	19.907	1973.53	0.322	0.740		0.717
683	19.935	1973.49	0.348	0.801		0.778
684	19.963	1973.44	0.154	0.355		0.332
687	19.991	1973.29	0.094	0.216		0.193
688	20.074	1973.25	0.116	0.266		0.243
689	20.102	1973.20	0.023	0.052		0.029
690	20.130	1973.15	0.034	0.078		0.055
691	20.158	1973.10	0.018	0.041		0.018
692	20.186	1973.05	0.014	0.033		0.010
693	20.214	1973.02	0.018	0.041		0.018

694	20.241	1972.96	0.024	0.055		0.032
695	20.269	1972.89	0.027	0.062		0.039
696	20.297	1972.82	0.044	0.102		0.079
697	20.325	1972.76	0.074	0.171		0.148
698	20.353	1972.71	0.268	0.617		0.594
699	20.381	1972.64	0.296	0.681		0.658
700	20.409	1972.58	0.090	0.207		0.183
701	20.436	1972.51	0.072	0.166		0.143
702	20.464	1972.47	0.025	0.057		0.034
703	20.492	1972.40	0.014	0.032		0.009
704	20.520	1972.33	0.015	0.035		0.012
705	20.548	1972.27	0.023	0.054		0.031
706	20.576	1972.20	0.031	0.072		0.049
707	20.604	1972.16	0.017	0.038		0.015
708	20.632	1972.09	0.018	0.042		0.018
709	20.659	1972.02	0.014	0.033		0.010
710	20.687	1971.96	0.198	0.455		0.432
711	20.715	1971.90	0.319	0.735		0.712
712	20.743	1971.86	0.442	1.017		0.994
714	20.799	1971.73	0.220	0.507		0.484
715	20.826	1971.67	0.107	0.247		0.224
716	20.854	1971.63	0.127	0.292		0.269
717	20.881	1971.57	0.238	0.547		0.524
718	20.909	1971.51	0.061	0.140		0.117
719	20.936	1971.45	0.062	0.143		0.120
720	20.964	1971.41	0.039	0.089		0.066
721	20.991	1971.35	0.038	0.086		0.063
722	21.019	1971.29	0.039	0.089		0.066
723	21.046	1971.22	0.068	0.156		0.133
724	21.074	1971.18	0.032	0.074		0.051
725	21.101	1971.12	0.029	0.068		0.045
726	21.129	1971.06	0.046	0.107		0.084
727	21.156	1971.00	0.067	0.154		0.131
728	21.184	1970.98	0.032	0.073		0.050
729	21.211	1970.94	0.029	0.067		0.044
730	21.239	1970.90	0.069	0.158		0.135
731	21.266	1970.87	0.055	0.126		0.103
733	21.321	1970.81	0.158	0.363		0.340
734	21.349	1970.77	0.060	0.137		0.114

735	21.376	1970.74	0.042	0.098		0.075
736	21.404	1970.71	0.029	0.067		0.044
737	21.431	1970.68	0.053	0.122		0.099
738	21.459	1970.64	0.088	0.202		0.179
739	21.486	1970.61	0.128	0.294		0.271
740	21.514	1970.58	0.082	0.188		0.165
741	21.542	1970.55	0.119	0.274		0.251
742	21.569	1970.51	0.041	0.093		0.070
743	21.597	1970.48	0.073	0.167		0.144
744	21.624	1970.45	0.113	0.260		0.237
745	21.652	1970.42	0.490	1.128		1.105
746	21.679	1970.38	0.244	0.560		0.537
747	21.707	1970.35	0.014	0.033		0.010
748	21.734	1970.32	0.025	0.058		0.035
749	21.762	1970.29	0.074	0.170		0.147
750	21.789	1970.25	0.119	0.274		0.251
751	21.817	1970.21	0.128	0.293		0.270
752	21.844	1970.19	0.148	0.341	0.031	0.310
753	21.871	1970.15	0.019	0.044		0.014
754	21.898	1970.12	0.059	0.136		0.106
755	21.925	1970.08	0.036	0.082		0.051
756	21.952	1970.06	0.041	0.095		0.065
757	21.979	1970.02	0.100	0.230		0.200
758	22.006	1969.99	0.037	0.084		0.053
759	22.033	1969.96	0.047	0.108		0.078
760	22.060	1969.92	0.124	0.285		0.254
762	22.114	1969.86	0.064	0.147		0.117
763	22.141	1969.82	0.129	0.296		0.265
764	22.168	1969.78	0.037	0.086		0.055
765	22.195	1969.76	0.022	0.050		0.020
766	22.222	1969.72	0.047	0.107		0.077
767	22.249	1969.68	0.024	0.055		0.025
768	22.276	1969.65	0.040	0.091	0.034	0.058
770	22.330	1969.58	0.041	0.093		0.060
771	22.357	1969.55	0.034	0.079		0.045
772	22.384	1969.52	0.028	0.064		0.030
773	22.411	1969.48	0.060	0.138		0.104
774	22.438	1969.44	0.140	0.323		0.289
775	22.465	1969.42	0.034	0.079		0.045

776	22.492	1969.38	0.033	0.076		0.043
777	22.519	1969.34	0.037	0.086		0.052
778	22.546	1969.30	0.059	0.135		0.101
779	22.572	1969.28	0.085	0.196		0.162
780	22.599	1969.24	0.170	0.390		0.356
781	22.626	1969.20	0.040	0.093		0.059
782	22.653	1969.18	0.066	0.152		0.118
783	22.680	1969.14	0.120	0.276		0.243
784	22.707	1969.10	0.099	0.229		0.195
785	22.734	1969.08	0.066	0.152		0.119
786	22.761	1969.04	0.161	0.369		0.336
787	22.788	1969.00	0.032	0.073		0.039
788	22.814	1968.97	0.080	0.184		0.151
789	22.839	1968.94	0.039	0.091		0.057
790	22.864	1968.82	0.150	0.346		0.312
791	22.889	1968.74	0.104	0.239		0.206
792	22.913	1968.69	0.062	0.142		0.108
793	22.938	1968.62	0.307	0.706		0.672
795	22.988	1968.49	0.068	0.157		0.123
796	23.013	1968.44	0.214	0.493		0.460
797	23.038	1968.36	0.624	1.435		1.402
798	23.062	1968.31	0.900	2.071		2.037
799	23.087	1968.23	0.289	0.664		0.630
800	23.112	1968.18	0.046	0.106		0.072
801	23.137	1968.10	0.021	0.048		0.014
802	23.162	1968.05	0.030	0.070		0.036
803	23.187	1967.98	0.088	0.203		0.169
804	23.212	1967.93	0.112	0.258		0.225
805	23.236	1967.87	0.030	0.069		0.035
806	23.261	1967.82	0.080	0.185		0.151
807	23.286	1967.76	0.120	0.276		0.242
808	23.311	1967.71	0.130	0.298		0.264
809	23.336	1967.64	1.060	2.439		2.406
810	23.361	1967.60	0.353	0.812		0.778
811	23.385	1967.53	0.111	0.256		0.223
812	23.410	1967.49	0.034	0.079		0.045
813	23.435	1967.42	0.056	0.128		0.094
814	23.460	1967.38	0.619	1.424		1.390
815	23.485	1967.33	0.632	1.455		1.421

816	23.510	1967.27	0.199	0.457		0.424
817	23.534	1967.22	0.133	0.306		0.272
818	23.559	1967.16	0.139	0.319		0.285
819	23.584	1967.11	0.058	0.134		0.100
820	23.609	1967.04	0.025	0.058		0.025
821	23.634	1967.00	0.018	0.042		0.008
822	23.659	1966.93	0.043	0.099		0.065
823	23.683	1966.88	0.032	0.074		0.041
824	23.708	1966.80	0.027	0.062		0.028
825	23.733	1966.75	0.048	0.110		0.077
826	23.758	1966.68	0.051	0.118		0.084
827	23.783	1966.63	0.072	0.166		0.132
828	23.809	1966.55	0.265	0.610		0.576
829	23.836	1966.48	0.102	0.234		0.201
830	23.863	1966.43	0.043	0.099		0.066
831	23.890	1966.35	0.092	0.212		0.178
832	23.917	1966.28	0.026	0.060		0.026
833	23.944	1966.23	0.037	0.085		0.052
834	23.970	1966.15	0.049	0.114		0.080
835	23.997	1966.08	0.045	0.103		0.070
836	24.024	1966.03	0.114	0.262		0.228
837	24.051	1965.99	0.120	0.276		0.243
838	24.078	1965.96	0.045	0.105		0.071
839	24.105	1965.93	0.072	0.166		0.132
840	24.132	1965.80	0.059	0.135	0.026	0.110
841	24.159	1965.73	0.114	0.262		0.236
844	24.240	1965.57	0.020	0.045		0.019
845	24.267	1965.51	0.026	0.060		0.034
846	24.294	1965.47	0.034	0.079		0.054
847	24.321	1965.41	0.051	0.117		0.091
848	24.348	1965.35	0.040	0.092		0.067
849	24.375	1965.31	0.112	0.257		0.231
850	24.402	1965.24	0.065	0.150		0.124
851	24.429	1965.18	0.056	0.130		0.104
852	24.456	1965.12	0.079	0.182		0.157
853	24.483	1965.07	0.101	0.232		0.207
854	24.510	1965.02	0.074	0.170		0.145
855	24.537	1964.98	0.045	0.104		0.078
856	24.564	1964.95	0.189	0.436		0.410

858	24.618	1964.88	0.036	0.082		0.057
859	24.645	1964.85	0.047	0.107		0.082
860	24.672	1964.81	0.038	0.088		0.062
861	24.699	1964.78	0.029	0.067		0.041
862	24.726	1964.74	0.025	0.056		0.031
863	24.750	1964.72	0.108	0.248		0.222
864	24.774	1964.69	0.179	0.412		0.386
865	24.797	1964.65	0.033	0.076		0.051
866	24.821	1964.63	0.069	0.159		0.134
867	24.844	1964.60	0.040	0.093		0.067
868	24.867	1964.57	0.063	0.144		0.119
869	24.891	1964.54	0.052	0.120		0.095
870	24.914	1964.52	0.052	0.120		0.094
871	24.937	1964.48	0.145	0.333		0.307
872	24.961	1964.46	0.059	0.136		0.110
873	24.984	1964.43	0.095	0.218		0.192
874	25.007	1964.40	0.033	0.075		0.049
875	25.031	1964.37	0.175	0.403		0.377
876	25.054	1964.35	0.080	0.184		0.159
877	25.077	1964.31	0.026	0.059		0.033
878	25.101	1964.28	0.413	0.950		0.924
879	25.124	1964.26	0.134	0.308		0.282
880	25.147	1964.22	0.164	0.377		0.351
881	25.171	1964.20	0.080	0.184		0.158
882	25.194	1964.17	0.089	0.205		0.180
883	25.217	1964.14	0.077	0.177		0.152
884	25.252	1964.11	0.082	0.189		0.163
886	25.287	1964.05	0.058	0.132		0.107
887	25.311	1964.02	0.081	0.187		0.162
889	25.357	1963.95	0.106	0.244		0.219
890	25.381	1963.92	0.079	0.181		0.156
891	25.404	1963.89	0.058	0.133		0.108
892	25.427	1963.84	0.331	0.762		0.737
893	25.451	1963.80	0.063	0.144		0.118
894	25.474	1963.77	0.029	0.066		0.041
895	25.497	1963.72	0.100	0.230		0.204
896	25.521	1963.69	0.049	0.113		0.087
898	25.567	1963.61	0.101	0.231		0.206
899	25.591	1963.57	0.034	0.079		0.053

900	25.614	1963.54	0.021	0.049		0.023
901	25.637	1963.50	0.060	0.138		0.112
902	25.661	1963.46	0.378	0.869		0.843
903	25.684	1963.43	0.042	0.096		0.070
904	25.707	1963.38	0.066	0.153	0.024	0.129
905	25.731	1963.34	0.106	0.245		0.221
906	25.755	1963.30	0.095	0.218		0.195
908	25.804	1963.23	0.457	1.052		1.029
909	25.828	1963.18	0.135	0.311		0.287
911	25.878	1963.10	0.040	0.092		0.068
912	25.902	1963.07	0.063	0.146		0.122
913	25.927	1963.02	0.035	0.080		0.056
915	25.976	1962.94	0.031	0.071		0.047
916	26.001	1962.90	0.111	0.256		0.232
917	26.025	1962.86	0.111	0.254		0.231
918	26.050	1962.83	0.072	0.165		0.141
919	26.074	1962.79	0.065	0.149		0.125
920	26.099	1962.75	0.054	0.124		0.100
921	26.124	1962.71	0.083	0.190		0.166
922	26.148	1962.67	0.032	0.073		0.049
923	26.173	1962.63	0.039	0.091		0.067
924	26.197	1962.59	0.058	0.133		0.110
925	26.222	1962.56	0.042	0.097		0.073
926	26.246	1962.51	0.155	0.356		0.332
927	26.271	1962.48	0.061	0.141		0.117
928	26.296	1962.44	0.085	0.195		0.172
929	26.320	1962.40	0.062	0.143		0.119
930	26.345	1962.37	0.065	0.151		0.127
931	26.369	1962.32	0.052	0.121		0.097
932	26.394	1962.29	0.088	0.202		0.179
933	26.419	1962.24	0.056	0.129		0.106
934	26.443	1962.21	0.052	0.119		0.095
935	26.468	1962.16	0.250	0.575		0.551
936	26.492	1962.13	0.261	0.600		0.576
937	26.517	1962.08	0.271	0.624		0.600
938	26.542	1962.05	0.166	0.383		0.359
939	26.566	1962.00	0.146	0.335		0.312
940	26.591	1961.97	0.217	0.499		0.476
941	26.615	1961.92	0.116	0.267		0.243

942	26.640	1961.88	0.248	0.570		0.546
943	26.665	1961.85	0.060	0.139		0.115
944	26.689	1961.80	0.039	0.089		0.065
945	26.714	1961.77	0.041	0.093		0.070
946	26.738	1961.72	0.037	0.086		0.063
948	26.788	1961.63	0.073	0.168		0.144
949	26.813	1961.60	0.047	0.107		0.083
950	26.837	1961.55	0.042	0.097		0.073
952	26.887	1961.47	0.080	0.184		0.161
953	26.911	1961.43	0.277	0.638		0.614
954	26.936	1961.38	0.095	0.219		0.195
955	26.961	1961.35	0.180	0.413		0.389
956	26.986	1961.30	0.034	0.079		0.055
957	27.010	1961.27	0.127	0.292		0.268
958	27.035	1961.22	0.375	0.864		0.840
959	27.060	1961.18	0.432	0.993		0.969
961	27.109	1961.10	0.184	0.424		0.400
963	27.159	1961.02	0.155	0.356		0.333
964	27.183	1960.98	0.088	0.202		0.178
965	27.208	1960.90	0.101	0.233		0.210
967	27.258	1960.79	0.246	0.567		0.543
968	27.282	1960.74	0.098	0.226		0.203
970	27.332	1960.62	0.238	0.547		0.523
972	27.381	1960.50	0.042	0.097		0.074
973	27.406	1960.43	0.043	0.099		0.075
974	27.431	1960.38	0.027	0.062		0.038
975	27.455	1960.31	0.025	0.058		0.034
976	27.480	1960.26	0.023	0.054		0.030
977	27.505	1960.21	0.038	0.088		0.064
979	27.554	1960.10	0.031	0.071		0.047
980	27.579	1960.02	0.022	0.050		0.026
981	27.604	1959.98	0.019	0.044		0.020
984	27.678	1959.84	0.024	0.056		0.032
985	27.703	1959.80	0.033	0.076		0.052
986	27.727	1959.75	0.023	0.054		0.030
987	27.752	1959.71	0.092	0.211	0.032	0.178
988	27.777	1959.65	0.046	0.106		0.074
989	27.802	1959.62	0.059	0.135		0.102
990	27.826	1959.56	0.034	0.078		0.045

991	27.851	1959.53	0.060	0.138		0.105
992	27.876	1959.47	0.035	0.080		0.047
993	27.900	1959.44	0.173	0.397		0.365
994	27.925	1959.38	0.085	0.196		0.164
995	27.950	1959.35	0.107	0.246		0.213
996	27.975	1959.31	0.176	0.405		0.373
998	28.024	1959.22	0.183	0.420		0.388
999	28.049	1959.16	0.358	0.823		0.790
1000	28.074	1959.13	0.142	0.326		0.294
1001	28.098	1959.07	0.413	0.950		0.917
1002	28.123	1959.04	0.453	1.043		1.011
1003	28.148	1958.98	0.751	1.727		1.694
1004	28.172	1958.93	0.438	1.008		0.975
1005	28.197	1958.86	0.172	0.397		0.364
1006	28.222	1958.82	0.170	0.390		0.358
1007	28.247	1958.75	0.099	0.228		0.196
1008	28.271	1958.70	0.215	0.496		0.463
1009	28.296	1958.64	0.056	0.130		0.097
1010	28.321	1958.59	0.065	0.149		0.117
1011	28.346	1958.52	0.021	0.048		0.016
1012	28.370	1958.48	0.066	0.152		0.119
1013	28.395	1958.41	0.534	1.227		1.195
1014	28.420	1958.36	0.099	0.227		0.195
1015	28.444	1958.32	0.209	0.482		0.450
1016	28.469	1958.25	0.170	0.391		0.358
1017	28.494	1958.20	0.055	0.126		0.094
1018	28.519	1958.14	0.029	0.067	0.042	0.025
1019	28.534	1958.10	0.025	0.057		0.015
1020	28.550	1958.06	0.047	0.108		0.066
1021	28.566	1958.02	0.023	0.053		0.011
1022	28.590	1957.98	0.054	0.125		0.083
1024	28.637	1957.90	0.167	0.384		0.342
1025	28.660	1957.86	0.373	0.859		0.817
1026	28.683	1957.83	0.583	1.342		1.300
1027	28.707	1957.78	0.257	0.591		0.550
1028	28.730	1957.74	0.100	0.230		0.188
1030	28.777	1957.66	0.247	0.568		0.526
1031	28.801	1957.62	0.514	1.183		1.141
1032	28.824	1957.59	0.552	1.270		1.228

1033	28.848	1957.53	0.218	0.502		0.460
1034	28.871	1957.50	0.037	0.085		0.043
1035	28.894	1957.47	0.052	0.120		0.079
1036	28.918	1957.41	0.349	0.803		0.761
1038	28.965	1957.34	0.111	0.256		0.214
1039	28.988	1957.29	0.125	0.288		0.246
1040	29.012	1957.26	0.207	0.475		0.433
1041	29.035	1957.21	0.136	0.313		0.271
1043	29.082	1957.14	0.047	0.109		0.067
1045	29.129	1957.05	0.269	0.618		0.577
1046	29.152	1957.01	0.249	0.574		0.532
1047	29.176	1956.96	0.068	0.158		0.116
1048	29.199	1956.93	0.066	0.153	0.015	0.137
1050	29.246	1956.84	0.073	0.167		0.152
1051	29.270	1956.80	0.128	0.295		0.279
1053	29.316	1956.71	0.027	0.062		0.047
1054	29.340	1956.67	0.032	0.075		0.059
1055	29.363	1956.64	0.032	0.074		0.058
1057	29.410	1956.55	0.043	0.099		0.083
1059	29.457	1956.45	0.068	0.156		0.141
1060	29.481	1956.41	0.021	0.048		0.032
1061	29.504	1956.37	0.023	0.053		0.038
1062	29.528	1956.33	0.024	0.055		0.039
1063	29.551	1956.29	0.030	0.070		0.054
1065	29.598	1956.20	0.043	0.099		0.084
1066	29.621	1956.16	0.073	0.169		0.153
1067	29.645	1956.12	0.086	0.198		0.183
1068	29.668	1956.07	0.040	0.092		0.077
1070	29.715	1955.98	0.019	0.044		0.029
1072	29.762	1955.89	0.018	0.041		0.026
1073	29.785	1955.83	0.029	0.067		0.051
1074	29.809	1955.78	0.089	0.205		0.190
1075	29.832	1955.74	0.100	0.229		0.214
1077	29.879	1955.63	0.030	0.070		0.055
1079	29.914	1955.55	0.075	0.172		0.157
1080	29.950	1955.48	0.042	0.096		0.081
1081	29.973	1955.43	0.041	0.095		0.079
1082	29.996	1955.37	0.015	0.033		0.018
1083	30.020	1955.33	0.013	0.031		0.016

1084	30.043	1955.28	0.011	0.026		0.011
1085	30.067	1955.22	0.030	0.070		0.054
1086	30.090	1955.17	0.080	0.185		0.170
1087	30.114	1955.13	0.081	0.187		0.171
1088	30.137	1955.07	0.057	0.131		0.116
1089	30.161	1955.02	0.046	0.107		0.091
1090	30.184	1954.98	0.050	0.116		0.101
1091	30.207	1954.93	0.056	0.129		0.114
1092	30.231	1954.90	0.076	0.176		0.160
1093	30.254	1954.86	0.019	0.045		0.029
1094	30.278	1954.81	0.041	0.094		0.079
1095	30.301	1954.78	0.035	0.080		0.065
1096	30.325	1954.75	0.030	0.069	0.017	0.052
1098	30.372	1954.66	0.025	0.057		0.040
1099	30.395	1954.61	0.036	0.082		0.065
1101	30.417	1954.57	0.047	0.109		0.091
1102	30.439	1954.54	0.079	0.182		0.165
1103	30.460	1954.51	0.074	0.170		0.153
1104	30.482	1954.47	0.025	0.058		0.041
1107	30.546	1954.36	0.025	0.057		0.040
1108	30.568	1954.32	0.019	0.043		0.026
1109	30.589	1954.29	0.026	0.060		0.042
1110	30.611	1954.25	0.911	2.096		2.079
1111	30.632	1954.22	0.156	0.358		0.341
1112	30.653	1954.19	0.073	0.168		0.151
1113	30.675	1954.15	0.032	0.074		0.057
1114	30.696	1954.10	0.046	0.106		0.089
1115	30.718	1954.07	0.071	0.162		0.145
1116	30.739	1954.03	0.037	0.084		0.067
1117	30.761	1954.00	0.034	0.078		0.061
1118	30.782	1953.96	0.026	0.060		0.042
1119	30.804	1953.92	0.054	0.125		0.107
1120	30.825	1953.86	0.022	0.050		0.033
1121	30.846	1953.82	0.038	0.088		0.070
1122	30.868	1953.78	0.040	0.091		0.074
1123	30.889	1953.74	0.026	0.059		0.042
1124	30.911	1953.70	0.020	0.045		0.028
1125	30.932	1953.66	0.017	0.039		0.022
1126	30.954	1953.62	0.036	0.082		0.065

1127	30.975	1953.56	0.022	0.051		0.034
1128	31.007	1953.52	0.023	0.053		0.036
1130	31.039	1953.44	0.039	0.089		0.072
1131	31.061	1953.40	0.025	0.057		0.039
1132	31.082	1953.36	0.019	0.045		0.027
1133	31.104	1953.32	0.044	0.101		0.084
1134	31.125	1953.26	0.017	0.040		0.023
1135	31.147	1953.22	0.080	0.185		0.168
1136	31.168	1953.18	0.037	0.085		0.067
1137	31.190	1953.14	0.026	0.060		0.043
1139	31.233	1953.06	0.013	0.030		0.013
1140	31.254	1953.02	0.010	0.022		0.005
1143	31.318	1952.91	0.052	0.120		0.103
1147	31.383	1952.82	0.026	0.060	0.019	0.041
1148	31.404	1952.79	0.038	0.087		0.068
1149	31.426	1952.75	0.016	0.037		0.017
1150	31.447	1952.72	0.057	0.132		0.113
1151	31.468	1952.69	0.400	0.920		0.901
1152	31.490	1952.66	0.236	0.544		0.524
1153	31.511	1952.63	0.036	0.083		0.064
1154	31.533	1952.60	0.062	0.143		0.124
1155	31.554	1952.57	0.041	0.094		0.075
1156	31.576	1952.52	0.045	0.104		0.084
1157	31.597	1952.49	0.040	0.091		0.072
1158	31.619	1952.46	0.045	0.103		0.083
1159	31.640	1952.43	0.025	0.058		0.039
1160	31.661	1952.40	0.094	0.216		0.197
1161	31.683	1952.37	0.174	0.401		0.382
1162	31.704	1952.34	0.054	0.124		0.105
1163	31.726	1952.30	0.025	0.059		0.040
1164	31.747	1952.27	0.076	0.176		0.157
1165	31.769	1952.24	0.065	0.149		0.130
1166	31.790	1952.21	0.032	0.075		0.056
1167	31.812	1952.18	0.056	0.128		0.109
1168	31.833	1952.15	0.044	0.102		0.083
1169	31.854	1952.12	0.016	0.037		0.018
1170	31.876	1952.07	0.164	0.377		0.358
1171	31.897	1952.04	0.147	0.339		0.320
1172	31.919	1952.01	0.028	0.064		0.045

1173	31.940	1951.98	0.017	0.040		0.021
1174	31.961	1951.95	0.058	0.134		0.115
1175	31.982	1951.92	0.016	0.038		0.018
1176	32.003	1951.89	0.033	0.077		0.058
1177	32.024	1951.85	0.011	0.025		0.006
1178	32.045	1951.81	0.154	0.354		0.334
1179	32.065	1951.77	0.078	0.179		0.160
1180	32.086	1951.74	0.071	0.163		0.143
1181	32.107	1951.71	0.051	0.117		0.098
1182	32.128	1951.68	0.037	0.085		0.066
1183	32.148	1951.65	0.033	0.076		0.056
1184	32.169	1951.61	0.021	0.048		0.029
1185	32.190	1951.58	0.017	0.040		0.021
1186	32.211	1951.55	0.027	0.063	0.017	0.046
1187	32.232	1951.52	0.027	0.063		0.046
1188	32.252	1951.48	0.019	0.044		0.027
1189	32.273	1951.45	0.072	0.167		0.150
1190	32.294	1951.42	0.037	0.085		0.068
1191	32.315	1951.39	0.046	0.105		0.088
1192	32.335	1951.34	0.023	0.052		0.035
1193	32.356	1951.31	0.025	0.059		0.042
1195	32.398	1951.24	0.071	0.162		0.145
1196	32.419	1951.21	0.143	0.329		0.313
1197	32.439	1951.18	0.091	0.209		0.192
1198	32.460	1951.15	0.057	0.132		0.115
1199	32.481	1951.11	0.019	0.044		0.027
1200	32.502	1951.08	0.062	0.143		0.126
1201	32.522	1951.05	0.058	0.135		0.118
1202	32.543	1951.02	0.020	0.047		0.030
1203	32.564	1950.98	0.062	0.142		0.125
1204	32.585	1950.95	0.037	0.084		0.067
1205	32.606	1950.89	0.044	0.101		0.084
1206	32.626	1950.86	0.052	0.119		0.102
1207	32.647	1950.82	0.048	0.111		0.094
1208	32.668	1950.79	0.154	0.355		0.338
1209	32.689	1950.75	0.047	0.109		0.092
1210	32.709	1950.72	0.027	0.063		0.046
1211	32.730	1950.68	0.047	0.108		0.091
1212	32.751	1950.65	0.066	0.151		0.134

1213	32.772	1950.61	0.018	0.042		0.025
1214	32.793	1950.58	0.029	0.067		0.050
1215	32.813	1950.54	0.018	0.041		0.024
1216	32.834	1950.51	0.018	0.042		0.025
1217	32.855	1950.47	0.096	0.222		0.205
1218	32.876	1950.42	0.051	0.118		0.101
1219	32.896	1950.39	0.030	0.069		0.052
1220	32.917	1950.35	0.027	0.063		0.046
1221	32.938	1950.32	0.013	0.029		0.012
1222	32.959	1950.28	0.053	0.123		0.106
1223	32.980	1950.25	0.072	0.165		0.148
1224	33.000	1950.21	0.036	0.083		0.066
1225	33.021	1950.18	0.054	0.123		0.107
1226	33.042	1950.14	0.046	0.106		0.089
1227	33.063	1950.11	0.329	0.757		0.740
1228	33.084	1950.07	0.169	0.388		0.371
1229	33.104	1950.04	0.029	0.067		0.050
1230	33.125	1949.98	0.018	0.041		0.024
1231	33.146	1949.94	0.034	0.079		0.062
1232	33.167	1949.90	0.077	0.177		0.160
1233	33.187	1949.86	0.041	0.094		0.077
1234	33.208	1949.82	0.032	0.073		0.056
1235	33.229	1949.78	0.069	0.159		0.142
1236	33.250	1949.75	0.069	0.160		0.143
1237	33.271	1949.71	0.022	0.051		0.034
1238	33.291	1949.67	0.016	0.036		0.019
1239	33.312	1949.63	0.023	0.054		0.037
1240	33.333	1949.59	0.085	0.195		0.178
1241	33.354	1949.55	0.053	0.121		0.104
1242	33.374	1949.51	0.138	0.318		0.301
1243	33.395	1949.45	0.242	0.556		0.539
1244	33.416	1949.41	0.231	0.530		0.513
1245	33.437	1949.37	0.215	0.495		0.478
1246	33.458	1949.33	0.150	0.345		0.328
1247	33.478	1949.29	0.035	0.081		0.064
1248	33.499	1949.25	0.097	0.224		0.207
1251	33.561	1949.14	0.101	0.232		0.215
1252	33.582	1949.10	0.240	0.553		0.536
1253	33.603	1949.06	0.195	0.448		0.431

1254	33.624	1949.02	0.084	0.194		0.177
1255	33.645	1948.98	0.047	0.107		0.090
1256	33.665	1948.90	0.094	0.216		0.199
1257	33.686	1948.85	0.040	0.092		0.075
1258	33.707	1948.80	0.044	0.101		0.084
1259	33.728	1948.76	0.154	0.354		0.337
1260	33.748	1948.71	0.061	0.139		0.122
1261	33.769	1948.66	0.044	0.101		0.084
1262	33.790	1948.61	0.053	0.121		0.104
1263	33.811	1948.56	0.075	0.173		0.156
1264	33.832	1948.51	0.062	0.142		0.125
1265	33.852	1948.46	0.066	0.152		0.135
1266	33.873	1948.41	0.051	0.117		0.100
1267	33.894	1948.37	0.046	0.106		0.089
1268	33.915	1948.32	0.023	0.053		0.036
1269	33.936	1948.24	0.076	0.175	0.048	0.127
1270	33.956	1948.20	0.212	0.487		0.439
1271	33.977	1948.15	0.030	0.068		0.020
1272	33.998	1948.10	0.057	0.132		0.083
1273	34.019	1948.05	0.141	0.323		0.275
1274	34.039	1948.00	0.038	0.088		0.040
1275	34.060	1947.97	0.043	0.100		0.052
1276	34.081	1947.94	0.021	0.049		0.001
1277	34.102	1947.91	0.021	0.048		0.000
1278	34.123	1947.88	0.033	0.076		0.028
1279	34.143	1947.84	0.017	0.040		-0.008
1280	34.164	1947.81	0.026	0.061		0.013
1281	34.185	1947.78	0.341	0.784		0.736
1282	34.206	1947.73	0.383	0.881		0.832
1283	34.226	1947.70	0.328	0.755		0.707
1284	34.247	1947.67	0.163	0.375		0.327
1285	34.268	1947.64	0.087	0.201		0.153
1286	34.289	1947.61	0.102	0.235		0.187
1287	34.310	1947.58	0.085	0.196		0.148
1288	34.330	1947.55	0.063	0.144		0.096
1289	34.351	1947.52	0.589	1.355		1.307
1290	34.372	1947.48	0.625	1.437		1.389
1291	34.393	1947.45	0.056	0.129		0.081
1292	34.413	1947.42	0.031	0.072		0.024

1293	34.434	1947.39	0.073	0.167		0.119
1294	34.455	1947.34	0.056	0.129		0.081
1295	34.476	1947.31	0.026	0.061		0.013
1296	34.497	1947.28	0.111	0.254		0.206
1297	34.517	1947.25	0.087	0.200		0.152
1298	34.538	1947.22	0.058	0.133		0.085
1299	34.559	1947.19	0.355	0.817		0.769
1300	34.580	1947.16	0.690	1.586		1.538
1301	34.600	1947.13	0.280	0.644		0.596
1302	34.621	1947.09	0.344	0.791		0.742
1303	34.642	1947.06	0.199	0.457		0.409
1304	34.663	1947.03	0.123	0.283		0.235
1305	34.684	1947.00	0.233	0.535		0.487
1307	34.726	1946.93	1.183	2.721		2.673
1308	34.747	1946.90	6.061	13.943		13.894
1309	34.768	1946.87	4.345	9.994		9.946
1310	34.789	1946.85	1.035	2.381		2.333
1311	34.810	1946.82	0.281	0.646		0.598
1312	34.831	1946.79	0.387	0.890		0.841
1313	34.852	1946.76	0.407	0.936		0.888
1314	34.873	1946.73	0.206	0.474		0.426
1316	34.915	1946.68	0.103	0.236		0.188
1317	34.936	1946.63	0.243	0.559	0.095	0.464
1318	34.957	1946.61	0.303	0.696		0.601
1319	34.978	1946.58	0.323	0.742		0.647
1320	34.999	1946.55	0.132	0.304		0.209
1321	35.020	1946.52	0.157	0.361		0.266
1322	35.041	1946.49	0.053	0.122		0.027
1323	35.062	1946.46	0.102	0.234		0.139
1324	35.083	1946.44	0.270	0.620		0.525
1325	35.104	1946.41	0.402	0.926		0.831
1326	35.125	1946.38	0.498	1.145		1.049
1327	35.146	1946.34	0.086	0.199		0.103
1328	35.167	1946.31	0.087	0.201		0.106
1329	35.188	1946.28	0.060	0.137		0.042
1330	35.209	1946.25	0.074	0.169		0.074
1331	35.230	1946.23	0.277	0.637		0.542
1332	35.251	1946.20	1.101	2.534		2.439
1333	35.272	1946.17	1.411	3.247		3.151

1334	35.293	1946.14	0.325	0.747		0.652
1335	35.314	1946.11	0.133	0.305		0.210
1336	35.335	1946.08	0.202	0.465		0.370
1337	35.356	1946.04	0.057	0.131		0.036
1338	35.377	1946.01	0.084	0.194		0.099
1339	35.398	1945.98	0.212	0.487		0.392
1340	35.419	1945.94	0.135	0.311		0.215
1341	35.440	1945.91	0.095	0.218		0.123
1342	35.461	1945.87	0.114	0.263		0.168
1343	35.482	1945.83	0.445	1.024		0.928
1344	35.503	1945.79	0.310	0.712		0.617
1345	35.524	1945.75	0.220	0.507		0.412
1346	35.545	1945.71	0.093	0.214		0.119
1347	35.566	1945.66	0.089	0.204		0.109
1348	35.587	1945.62	0.036	0.084		-0.012
1349	35.608	1945.58	0.140	0.323		0.227
1350	35.629	1945.55	0.364	0.838		0.743
1351	35.650	1945.51	1.196	2.751		2.656
1352	35.671	1945.47	0.692	1.593		1.498
1353	35.692	1945.43	0.198	0.455		0.360
1354	35.713	1945.40	0.108	0.248		0.153
1355	35.734	1945.36	0.225	0.517		0.422
1357	35.776	1945.26	0.643	1.478		1.383
1358	35.797	1945.23	0.394	0.905		0.810
1359	35.818	1945.19	0.239	0.549		0.454
1361	35.860	1945.11	0.284	0.654		0.558
1362	35.881	1945.08	0.317	0.729		0.634
1363	35.902	1945.04	0.225	0.519		0.423
1364	35.923	1945.00	0.552	1.270		1.175
1365	35.944	1944.97	0.416	0.956		0.861
1366	35.965	1944.92	0.397	0.914		0.818
1367	35.986	1944.89	0.135	0.312		0.216
1368	36.007	1944.86	0.144	0.331		0.235
1369	36.028	1944.83	0.530	1.218		1.123
1370	36.049	1944.80	1.304	2.999		2.903
1371	36.070	1944.77	0.122	0.281		0.185
1372	36.091	1944.73	0.098	0.226		0.131
1373	36.112	1944.70	0.155	0.356		0.261
1374	36.133	1944.67	0.219	0.504		0.409

1375	36.154	1944.63	0.120	0.277		0.182
1376	36.175	1944.59	0.079	0.183		0.088
1377	36.196	1944.56	0.129	0.298		0.203
1378	36.217	1944.53	0.066	0.151		0.056
1379	36.238	1944.50	0.132	0.304	0.086	0.217
1380	36.259	1944.47	0.044	0.100		0.014
1381	36.280	1944.44	0.040	0.093		0.007
1382	36.301	1944.41	0.153	0.351		0.265
1383	36.322	1944.38	0.218	0.502		0.415
1384	36.343	1944.34	0.458	1.054		0.968
1385	36.364	1944.31	0.166	0.381		0.295
1386	36.385	1944.27	0.081	0.187		0.101
1387	36.406	1944.23	0.157	0.362		0.276
1388	36.427	1944.20	0.180	0.414		0.328
1389	36.448	1944.17	0.063	0.145		0.058
1390	36.469	1944.14	0.117	0.268		0.182
1391	36.490	1944.11	0.559	1.287		1.201
1392	36.511	1944.08	0.156	0.359		0.272
1393	36.532	1944.05	0.093	0.214		0.127
1394	36.553	1944.02	0.084	0.193		0.107
1395	36.574	1943.98	0.043	0.099		0.012
1396	36.595	1943.94	0.245	0.564		0.478
1397	36.616	1943.91	0.468	1.077		0.991
1398	36.637	1943.88	0.186	0.429		0.343
1399	36.658	1943.84	0.091	0.209		0.123
1400	36.679	1943.81	0.211	0.484		0.398
1401	36.700	1943.78	0.125	0.287		0.201
1402	36.721	1943.75	0.068	0.156		0.069
1403	36.742	1943.72	0.064	0.147		0.061
1404	36.763	1943.69	0.285	0.656		0.570
1405	36.784	1943.66	0.263	0.605		0.519
1406	36.805	1943.61	0.593	1.364		1.278
1407	36.826	1943.58	0.206	0.474		0.388
1408	36.847	1943.55	0.286	0.659		0.573
1409	36.868	1943.52	0.581	1.337		1.251
1410	36.889	1943.48	1.350	3.106		3.020
1411	36.910	1943.45	0.893	2.054		1.968
1412	36.931	1943.42	0.412	0.948		0.861
1413	36.952	1943.39	0.404	0.929		0.843

1414	36.973	1943.36	0.720	1.657		1.570
1415	36.994	1943.33	0.315	0.724		0.637
1416	37.015	1943.28	1.564	3.598		3.512
1417	37.036	1943.25	0.402	0.925		0.839
1418	37.057	1943.22	0.853	1.963		1.877
1419	37.078	1943.19	0.741	1.705		1.619
1420	37.099	1943.16	1.765	4.061		3.975
1421	37.121	1943.13	0.496	1.142		1.055
1422	37.142	1943.09	0.173	0.398		0.312
1423	37.163	1943.06	0.103	0.236		0.150
1424	37.184	1943.03	0.080	0.185		0.099
1425	37.205	1943.00	0.088	0.203		0.117
1426	37.226	1942.94	0.165	0.380		0.294
1427	37.247	1942.91	0.032	0.075		-0.012
1428	37.268	1942.87	0.032	0.073		-0.013
1429	37.289	1942.83	0.040	0.092		0.006
1430	37.310	1942.79	0.073	0.168		0.082
1431	37.331	1942.75	0.078	0.179		0.093
1432	37.352	1942.72	0.052	0.118		0.032
1433	37.373	1942.68	0.038	0.088		0.002
1434	37.394	1942.64	0.159	0.365		0.279
1435	37.415	1942.60	0.082	0.189		0.103
1436	37.435	1942.57	0.088	0.202		0.116
1437	37.455	1942.53	0.078	0.181		0.094
1438	37.475	1942.49	0.064	0.147		0.061
1439	37.495	1942.45	0.152	0.349		0.263
1441	37.534	1942.38	0.069	0.158		0.072
1442	37.554	1942.34	0.051	0.117		0.031
1443	37.574	1942.30	0.048	0.110		0.023
1444	37.594	1942.26	0.041	0.095		0.009
1445	37.614	1942.23	0.626	1.440		1.354
1446	37.634	1942.19	2.091	4.809		4.723
1447	37.654	1942.15	0.340	0.782		0.696
1448	37.674	1942.11	0.180	0.414		0.328
1449	37.693	1942.08	0.156	0.360		0.273
1450	37.713	1942.04	0.169	0.389		0.302
1451	37.733	1942.00	0.127	0.293		0.207
1452	37.753	1941.96	0.143	0.330		0.243
1453	37.773	1941.92	0.090	0.208		0.122

1454	37.793	1941.88	0.393	0.905		0.819
1455	37.813	1941.84	0.216	0.497		0.410
1456	37.833	1941.80	0.163	0.376		0.289
1457	37.852	1941.76	0.068	0.157		0.070
1458	37.872	1941.72	0.117	0.269		0.182
1459	37.892	1941.68	0.062	0.143		0.057
1460	37.912	1941.64	0.141	0.324	0.052	0.272
1461	37.932	1941.60	0.033	0.076		0.024
1462	37.952	1941.56	0.046	0.105		0.053
1463	37.972	1941.52	0.081	0.187		0.135
1464	37.992	1941.48	0.036	0.082		0.030
1465	38.012	1941.44	0.093	0.214		0.162
1466	38.031	1941.40	0.088	0.202	0.040	0.161
1467	38.051	1941.36	0.060	0.138		0.097
1468	38.071	1941.32	0.031	0.072		0.032
1469	38.091	1941.28	0.086	0.199		0.158
1470	38.111	1941.24	0.038	0.088		0.048
1471	38.131	1941.20	0.041	0.094		0.053
1472	38.151	1941.16	0.107	0.245		0.205
1473	38.171	1941.12	0.406	0.934		0.893
1474	38.190	1941.08	0.733	1.686		1.646
1475	38.210	1941.04	0.467	1.075		1.035
1476	38.230	1941.00	0.141	0.325		0.285
1477	38.250	1940.96	0.082	0.189		0.148
1478	38.270	1940.92	0.048	0.110		0.070
1479	38.290	1940.88	0.041	0.095		0.054
1480	38.310	1940.84	0.058	0.134		0.094
1481	38.330	1940.80	0.142	0.326		0.285
1482	38.349	1940.76	0.135	0.311		0.271
1483	38.369	1940.73	0.141	0.324		0.284
1484	38.389	1940.69	0.066	0.152		0.112
1485	38.409	1940.65	0.288	0.663		0.623
1486	38.429	1940.61	0.263	0.604		0.564
1487	38.449	1940.57	0.095	0.218		0.178
1488	38.469	1940.53	0.114	0.263		0.222
1489	38.489	1940.49	0.094	0.217		0.177
1490	38.508	1940.45	0.113	0.260		0.219
1491	38.528	1940.41	0.050	0.115		0.074
1492	38.548	1940.37	0.054	0.123		0.083

1493	38.568	1940.33	0.059	0.136		0.096
1494	38.588	1940.29	0.056	0.129		0.088
1495	38.608	1940.25	0.068	0.155		0.115
1496	38.628	1940.22	0.056	0.129		0.089
1497	38.648	1940.18	0.043	0.098		0.057
1500	38.707	1940.06	0.146	0.335		0.294
1501	38.727	1940.02	0.059	0.137		0.096
1502	38.747	1939.99	0.063	0.145		0.104
1503	38.767	1939.96	0.048	0.111		0.070
1505	38.807	1939.90	0.057	0.131		0.091
1506	38.827	1939.87	0.100	0.230		0.189
1507	38.846	1939.84	0.131	0.301	0.036	0.265
1508	38.866	1939.81	0.154	0.355		0.319
1510	38.906	1939.76	0.123	0.283		0.247
1511	38.926	1939.73	0.172	0.396		0.359
1512	38.946	1939.70	1.532	3.524		3.488
1514	38.986	1939.64	0.198	0.456		0.420
1515	39.005	1939.61	0.133	0.307		0.271
1516	39.025	1939.59	0.124	0.284		0.248
1517	39.045	1939.56	0.160	0.368		0.332
1518	39.065	1939.53	0.113	0.261		0.224
1519	39.085	1939.51	0.110	0.253		0.217
1520	39.105	1939.49	0.341	0.783		0.747
1521	39.125	1939.46	0.325	0.747		0.710
1522	39.145	1939.43	0.463	1.065		1.029
1523	39.164	1939.40	0.130	0.299		0.263
1524	39.184	1939.37	0.120	0.277		0.241
1525	39.204	1939.34	0.201	0.463		0.427
1527	39.244	1939.29	0.101	0.232		0.196
1528	39.264	1939.26	0.086	0.198		0.162
1529	39.284	1939.23	0.085	0.196		0.160
1530	39.323	1939.20	0.067	0.154	0.021	0.133
1533	39.363	1939.11	0.500	1.150		1.129
1534	39.383	1939.09	0.126	0.290		0.269
1535	39.403	1939.06	0.716	1.648		1.627
1536	39.423	1939.03	0.336	0.774		0.753
1537	39.443	1939.00	0.060	0.137		0.116
1539	39.473	1938.93	0.032	0.073		0.052
1540	39.502	1938.89	0.076	0.175		0.154

1542	39.542	1938.82	0.048	0.110		0.089
1544	39.582	1938.75	0.020	0.046		0.025
1547	39.642	1938.65	0.127	0.292		0.271
1549	39.681	1938.58	0.301	0.692		0.672
1551	39.721	1938.51	0.068	0.156		0.135
1553	39.761	1938.44	0.016	0.037		0.016
1555	39.801	1938.37	0.045	0.104		0.083
1557	39.840	1938.30	0.017	0.039		0.018
1561	39.918	1938.16	0.136	0.313		0.293
1564	39.976	1938.05	0.073	0.168		0.147
1566	40.015	1938.00	0.013	0.031		0.010
1568	40.053	1937.90	0.011	0.025		0.004
1570	40.092	1937.80	0.010	0.023		0.002
1572	40.130	1937.71	0.043	0.098		0.077
1574	40.169	1937.61	0.022	0.050		0.030
1576	40.207	1937.51	0.099	0.227		0.207
1578	40.246	1937.41	0.081	0.186		0.165
1584	40.361	1937.15	0.142	0.327		0.307
1588	40.438	1936.96	0.560	1.288		1.267
1590	40.477	1936.89	0.275	0.632		0.611
1592	40.515	1936.82	0.149	0.342		0.322
1594	40.554	1936.76	0.049	0.113		0.092
1596	40.592	1936.69	0.045	0.104		0.084
1598	40.631	1936.62	0.299	0.687		0.666
1600	40.669	1936.55	0.024	0.055		0.035
1604	40.746	1936.40	0.059	0.136		0.116
1606	40.785	1936.35	0.019	0.043		0.022
1608	40.823	1936.27	0.018	0.041		0.021
1610	40.862	1936.20	0.005	0.012		-0.008
1612	40.900	1936.13	0.015	0.035		0.014
1616	40.977	1935.98	0.043	0.100		0.079
1618	41.016	1935.90	0.185	0.426		0.405
1620	41.054	1935.84	0.262	0.603		0.583
1622	41.093	1935.76	0.097	0.222		0.201
1624	41.131	1935.67	0.106	0.244		0.223
1626	41.170	1935.59	0.161	0.370		0.349
1628	41.208	1935.51	1.040	2.393		2.373
1630	41.247	1935.43	0.327	0.752		0.731
1632	41.285	1935.35	0.064	0.146		0.126

1634	41.324	1935.29	0.094	0.216		0.195
1636	41.363	1935.20	0.088	0.202		0.181
1638	41.401	1935.12	0.483	1.112		1.092
1640	41.440	1935.04	0.037	0.085		0.064
1642	41.478	1934.96	0.012	0.027		0.006
1644	41.517	1934.88	0.012	0.027		0.006
1646	41.555	1934.80	0.071	0.164		0.143
1648	41.594	1934.74	0.246	0.565		0.544
1651	41.651	1934.62	0.062	0.143		0.122
1653	41.690	1934.54	1.324	3.046		3.025
1655	41.728	1934.46	0.449	1.034		1.013
1657	41.767	1934.38	0.134	0.308		0.287
1659	41.805	1934.30	0.120	0.276		0.256
1661	41.844	1934.24	0.041	0.095		0.075
1663	41.882	1934.16	0.094	0.217		0.196
1665	41.921	1934.08	0.033	0.077		0.056
1667	41.959	1934.00	1.283	2.952		2.931
1669	41.998	1933.94	0.147	0.337		0.317
1671	42.036	1933.89	0.105	0.241		0.220
1673	42.075	1933.83	0.141	0.325		0.305
1675	42.114	1933.79	0.289	0.665		0.645
1677	42.152	1933.74	0.984	2.264		2.243
1679	42.191	1933.68	0.548	1.260		1.239
1681	42.210	1933.63	0.341	0.785		0.764
1683	42.248	1933.57	0.099	0.227		0.206
1685	42.287	1933.51	0.065	0.150		0.129
1687	42.325	1933.47	0.670	1.542		1.521
1689	42.364	1933.42	0.633	1.456		1.435
1691	42.402	1933.36	0.294	0.676		0.655
1693	42.441	1933.31	0.412	0.947		0.926
1695	42.479	1933.25	0.079	0.182		0.161
1697	42.518	1933.19	0.206	0.474		0.454
1699	42.556	1933.14	0.799	1.838		1.817
1700	42.575	1933.13	0.170	0.392	0.016	0.376
1702	42.613	1933.07	0.024	0.055		0.039
1704	42.651	1933.01	0.057	0.132		0.116
1706	42.689	1932.95	0.071	0.163		0.147
1708	42.727	1932.88	0.206	0.474		0.458
1710	42.765	1932.83	0.612	1.407		1.391

1713	42.822	1932.72	0.063	0.145	0.019	0.126
1715	42.859	1932.66	0.035	0.080		0.061
1717	42.897	1932.59	0.087	0.199		0.180
1719	42.935	1932.53	0.022	0.050		0.031
1721	42.973	1932.47	0.042	0.096		0.077
1723	43.011	1932.40	0.148	0.339		0.320
1725	43.049	1932.33	0.044	0.102		0.083
1727	43.087	1932.26	0.052	0.120		0.101
1729	43.125	1932.21	0.324	0.745		0.726
1731	43.163	1932.14	0.094	0.216		0.197
1733	43.200	1932.07	0.052	0.120		0.101
1735	43.238	1932.00	0.070	0.161		0.142
1737	43.276	1931.90	0.072	0.165		0.146
1739	43.314	1931.83	0.074	0.171		0.152
1741	43.352	1931.73	0.055	0.126		0.107
1743	43.390	1931.63	0.267	0.615		0.596
1746	43.418	1931.46	0.140	0.321		0.302
1748	43.447	1931.40	0.087	0.201		0.182
1750	43.504	1931.30	0.286	0.658		0.639
1752	43.560	1931.20	0.116	0.266		0.247
1753	43.579	1931.15	0.084	0.193		0.174
1755	43.617	1931.05	0.056	0.130		0.111
1757	43.655	1930.98	0.081	0.186		0.167
1759	43.693	1930.88	0.340	0.781		0.762
1761	43.731	1930.78	0.066	0.152		0.133
1763	43.769	1930.68	0.042	0.097		0.078
1765	43.807	1930.58	0.034	0.078		0.059
1767	43.845	1930.50	0.009	0.021		0.002
1769	43.883	1930.40	0.014	0.032		0.013
1771	43.920	1930.30	0.016	0.036		0.017
1773	43.958	1930.20	0.018	0.042		0.023
1775	43.996	1930.10	0.023	0.053		0.034
1777	44.034	1930.03	0.323	0.743		0.724
1779	44.072	1929.94	0.120	0.275		0.256
1781	44.110	1929.86	0.409	0.940		0.921
1783	44.148	1929.78	0.287	0.659		0.640
1785	44.186	1929.73	0.036	0.082		0.063
1787	44.205	1929.65	0.217	0.500		0.481
1788	44.224	1929.61	0.492	1.133		1.114

1790	44.280	1929.53	2.028	4.665	0.104	4.561
1792	44.318	1929.45	0.146	0.337	0.030	0.307
1795	44.375	1929.35	0.071	0.163		0.134
1798	44.432	1929.24	0.121	0.279		0.250
1801	44.489	1929.12	0.470	1.082		1.053
1802	44.508	1929.08	0.020	0.045		0.016
1805	44.565	1928.98	0.102	0.234		0.205
1807	44.602	1928.89	0.045	0.103		0.074
1809	44.640	1928.81	0.012	0.029		-0.001
1811	44.678	1928.72	0.011	0.024		-0.005
1813	44.716	1928.64	0.057	0.132		0.103
1815	44.754	1928.57	0.016	0.037		0.007
1817	44.792	1928.49	0.027	0.063		0.034
1819	44.830	1928.40	0.034	0.079		0.049
1821	44.868	1928.32	0.151	0.347		0.317
1823	44.906	1928.26	0.037	0.086		0.056
1825	44.943	1928.17	0.018	0.042		0.013
1828	45.000	1928.04	0.016	0.037		0.008
1830	45.038	1927.94	0.019	0.044		0.014
1832	45.057	1927.83	0.039	0.090		0.061
1834	45.114	1927.74	0.008	0.019		-0.011
1836	45.152	1927.63	0.007	0.017		-0.013
1839	45.209	1927.46	0.006	0.014	0.017	-0.004
1841	45.247	1927.34	0.006	0.013		-0.004
1843	45.266	1927.26	0.009	0.021		0.003
1845	45.322	1927.14	0.009	0.021		0.004
1847	45.360	1927.03	0.005	0.011		-0.007
1849	45.397	1926.93	0.028	0.065		0.047
1851	45.435	1926.86	0.231	0.532		0.515
1853	45.472	1926.76	0.687	1.580		1.562
1855	45.510	1926.67	0.149	0.342		0.325
1857	45.547	1926.57	0.099	0.228		0.211
1859	45.585	1926.50	0.069	0.158		0.141
1861	45.622	1926.40	0.019	0.043		0.026
1863	45.660	1926.31	0.048	0.111		0.094
1865	45.678	1926.23	0.013	0.030		0.013
1864	45.697	1926.26	0.021	0.049	0.022	0.027
1866	45.725	1926.19	0.059	0.136		0.114
1868	45.753	1926.10	0.020	0.046		0.024

1869	45.800	1926.05	0.018	0.042		0.020
1871	45.847	1925.97	0.062	0.142		0.121
1873	45.903	1925.84	0.034	0.079		0.057
1876	45.922	1925.70	0.070	0.160		0.138
1877	45.960	1925.65	0.049	0.114		0.092
1879	45.997	1925.54	0.038	0.086		0.065
1881	46.035	1925.45	0.176	0.406		0.384
1883	46.072	1925.35	0.066	0.151		0.130
1885	46.110	1925.24	0.118	0.272		0.250
1887	46.147	1925.14	0.045	0.104		0.082
1889	46.222	1925.03	0.013	0.029		0.008
1893	46.260	1924.89	0.089	0.204		0.183
1895	46.297	1924.82	0.166	0.383		0.361
1897	46.335	1924.78	0.463	1.066		1.045
1899	46.372	1924.70	0.046	0.106		0.085
1901	46.410	1924.63	0.033	0.077		0.055
1903	46.447	1924.56	0.155	0.357		0.336
1905	46.485	1924.49	0.044	0.102		0.080
1907	46.522	1924.44	0.017	0.039		0.017
1909	46.560	1924.39	0.180	0.414		0.392
1911	46.578	1924.30	0.131	0.302	0.062	0.239
1913	46.635	1924.23	0.074	0.171	0.040	0.131
1915	46.672	1924.18	0.049	0.112		0.072
1917	46.710	1924.11	0.106	0.245		0.205
1919	46.747	1924.04	0.047	0.108		0.068
1921	46.785	1923.96	0.149	0.344	0.069	0.274
1923	46.822	1923.89	0.076	0.176		0.106
1925	46.860	1923.80	0.076	0.175		0.105
1927	46.897	1923.74	0.137	0.315		0.246
1929	46.935	1923.63	0.055	0.127		0.058
1931	46.953	1923.57	0.346	0.795		0.726
1933	46.991	1923.48	0.044	0.101		0.031
1935	47.047	1923.39	0.054	0.125		0.056
1937	47.141	1923.30	0.030	0.068		-0.001
1942	47.160	1923.11	0.239	0.549		0.480
1944	47.178	1923.02	0.021	0.049	0.020	0.029
1946	47.197	1922.98	0.047	0.109		0.089
1948	47.216	1922.90	0.047	0.107		0.087
1950	47.291	1922.84	0.015	0.035		0.015

1952	47.328	1922.77	0.009	0.022		0.001
1954	47.366	1922.72	0.015	0.034		0.013
1957	47.422	1922.62	0.011	0.024		0.004
1959	47.460	1922.56	0.013	0.029		0.009
1962	47.516	1922.48	0.011	0.024		0.004
1964	47.553	1922.41	0.023	0.053		0.032
1966	47.591	1922.34	0.009	0.021		0.001
1968	47.628	1922.28	0.551	1.266		1.246
1970	47.666	1922.23	0.172	0.395		0.375
1972	47.703	1922.16	0.021	0.048		0.028
1974	47.741	1922.10	0.014	0.031		0.011
1976	47.778	1922.03	0.019	0.043		0.023
1978	47.816	1921.97	0.112	0.257		0.236
1981	47.872	1921.82	0.302	0.696		0.675
1983	47.907	1921.75	0.184	0.423		0.403
1985	47.942	1921.63	0.046	0.106		0.085
1987	47.976	1921.55	0.043	0.099		0.078
1989	48.010	1921.45	0.066	0.151		0.131
1991	48.043	1921.37	0.055	0.126		0.106
1993	48.077	1921.29	0.022	0.051		0.031
1995	48.094	1921.18	0.082	0.188		0.168
1997	48.144	1921.11	0.014	0.032		0.011
1999	48.178	1921.03	0.030	0.068		0.048
2001	48.211	1920.93	0.014	0.033		0.013
2004	48.239	1920.81	1.016	2.336		2.316
2006	48.268	1920.73	0.070	0.162		0.142
2007	48.296	1920.69	0.055	0.127		0.106
2012	48.396	1920.50	0.017	0.039		0.018
2014	48.430	1920.40	0.041	0.093		0.073
2016	48.464	1920.33	0.077	0.177		0.156
2018	48.497	1920.26	0.039	0.090		0.070
2020	48.531	1920.17	0.031	0.071		0.051
2022	48.565	1920.10	0.018	0.041		0.021
2024	48.598	1920.00	0.011	0.026		0.006
2026	48.632	1919.93	0.039	0.090		0.070
2028	48.666	1919.86	0.022	0.052		0.031
2029	48.674	1919.82	0.044	0.100		0.080
2030	48.682	1919.77	0.090	0.208		0.187
2033	48.754	1919.66	0.070	0.162		0.141

2035	48.791	1919.57	0.041	0.094		0.074
2037	48.827	1919.48	0.106	0.245		0.224
2039	48.864	1919.41	0.016	0.037		0.016
2041	48.900	1919.32	0.056	0.128		0.108
2043	48.936	1919.25	0.085	0.196		0.176
2046	48.991	1919.11	0.028	0.064		0.043
2048	49.027	1919.02	0.035	0.082		0.061
2050	49.045	1918.93	0.018	0.042		0.021
2052	49.082	1918.79	0.011	0.025		0.005
2053	49.118	1918.72	0.017	0.039		0.019
2055	49.154	1918.62	0.036	0.083		0.063
2057	49.191	1918.48	0.095	0.218		0.197
2060	49.245	1918.29	0.030	0.069		0.048
2063	49.300	1918.10	0.034	0.078		0.057
2067	49.373	1917.88	0.054	0.124		0.104
2073	49.482	1917.56	0.038	0.087		0.066
2075	49.518	1917.44	0.023	0.054		0.033
2077	49.555	1917.35	0.024	0.055		0.035
2079	49.591	1917.24	0.015	0.034		0.014
2081	49.627	1917.12	0.044	0.102		0.082
2083	49.664	1917.03	0.042	0.097		0.076
2085	49.700	1916.94	0.018	0.040		0.020
2087	49.736	1916.82	0.049	0.113		0.092
2089	49.773	1916.71	0.010	0.022		0.002
2091	49.809	1916.59	0.029	0.066		0.046
2093	49.845	1916.50	0.105	0.241		0.220
2095	49.882	1916.38	0.031	0.072		0.052
2097	49.918	1916.26	0.026	0.060		0.040
2099	49.955	1916.18	0.020	0.046		0.025
2101	49.991	1916.06	0.026	0.060		0.040
2103	50.027	1915.95	0.012	0.027		0.007
2107	50.100	1915.77	0.023	0.052		0.032
2109	50.136	1915.69	0.067	0.155		0.134
2111	50.173	1915.59	0.016	0.036		0.016
2114	50.227	1915.44	0.064	0.148		0.127
2119	50.318	1915.21	0.013	0.030		0.009
2121	50.355	1915.13	0.012	0.028		0.008
2123	50.391	1915.03	0.025	0.057		0.036
2126	50.446	1914.88	0.499	1.147		1.127

2134	50.595	1914.44	0.123	0.282		0.262
2136	50.634	1914.32	0.034	0.078		0.058
2138	50.672	1914.21	0.015	0.034		0.013
2140	50.711	1914.09	0.010	0.022		0.002
2143	50.769	1913.93	0.072	0.165		0.145
2145	50.807	1913.84	0.173	0.399		0.379
2147	50.846	1913.76	0.123	0.284		0.263
2149	50.884	1913.69	0.102	0.235		0.214
2151	50.923	1913.60	0.146	0.335		0.315
2153	50.962	1913.51	0.224	0.515		0.495
2155	51.010	1913.42	0.025	0.058		0.037
2158	51.058	1913.29	0.084	0.194		0.173
2160	51.097	1913.20	0.015	0.034		0.014
2164	51.174	1913.04	0.010	0.022		0.002
2165	51.193	1913.00	0.022	0.051		0.031
2167	51.232	1912.93	0.028	0.064		0.044
2170	51.290	1912.83	0.013	0.031		0.011
2173	51.348	1912.72	0.025	0.058		0.038
2176	51.406	1912.64	0.042	0.096		0.076
2178	51.444	1912.57	0.117	0.270		0.249
2180	51.518	1912.43	0.020	0.047		0.026
2182	51.633	1912.24	0.091	0.209		0.189
2185	51.693	1912.14	0.049	0.112		0.092
2187	51.733	1912.07	0.028	0.064		0.043
2189	51.773	1912.00	0.019	0.044		0.023
2191	51.813	1911.93	0.069	0.160		0.139
2193	51.853	1911.86	0.121	0.277		0.257
2195	51.873	1911.78	1.571	3.614		3.594
2197	51.893	1911.73	0.324	0.744		0.724
2199	51.973	1911.66	0.114	0.263		0.243
2201	52.013	1911.59	0.097	0.223		0.203
2203	52.053	1911.53	0.144	0.330		0.310
2205	52.093	1911.46	0.173	0.398		0.378
2207	52.134	1911.39	0.044	0.102		0.082
2211	52.174	1911.25	0.096	0.221		0.200
2213	52.249	1911.20	0.097	0.223		0.202
2214	52.267	1911.15	0.193	0.443		0.423
2217	52.304	1911.07	0.079	0.181	0.020	0.160
2219	52.359	1911.00	0.027	0.063		0.042

2221	52.377	1910.94	0.018	0.042		0.021
2223	52.432	1910.87	0.010	0.024		0.003
2225	52.468	1910.79	0.044	0.101		0.081
2227	52.505	1910.73	0.046	0.105		0.085
2229	52.541	1910.65	0.160	0.368		0.348
2231	52.577	1910.58	0.356	0.820		0.799
2236	52.669	1910.40	0.036	0.082		0.062
2238	52.705	1910.35	0.080	0.183		0.163
2241	52.760	1910.23	0.053	0.122		0.102
2245	52.833	1910.10	0.050	0.115		0.094
2247	52.869	1910.02	0.058	0.134		0.114
2250	52.924	1909.92	0.018	0.041		0.021
2252	52.960	1909.84	0.022	0.050		0.029
10001	52.987	1909.81	0.095	0.219	0.046	0.174
10003	53.014	1909.75	0.037	0.086		0.040
10005	53.048	1909.67	0.128	0.295		0.250
10007	53.083	1909.61	0.086	0.199		0.153
10009	53.100	1909.53	0.044	0.102		0.057
10011	53.127	1909.47	0.239	0.550		0.505
10013	53.154	1909.41	0.348	0.800		0.754
10015	53.222	1909.33	0.079	0.182		0.136
10017	53.256	1909.27	0.038	0.087		0.042
10019	53.291	1909.20	0.028	0.064		0.019
10021	53.308	1909.14	0.037	0.085		0.039
10023	53.360	1909.06	0.052	0.120		0.075
10025	53.395	1909.00	0.076	0.174		0.128
10027	53.430	1908.93	0.231	0.532		0.486
10029	53.464	1908.88	0.062	0.144		0.098
10031	53.482	1908.81	0.035	0.080		0.035
10033	53.516	1908.76	0.065	0.150		0.105
10035	53.551	1908.69	0.049	0.112		0.067
10037	53.595	1908.64	0.026	0.061		0.015
10039	53.639	1908.58	0.020	0.045		0.000
10041	53.676	1908.53	0.029	0.066		0.020
10043	53.712	1908.46	0.068	0.157		0.112
10045	53.724	1908.37	0.120	0.276		0.231
10047	53.737	1908.32	0.040	0.093		0.047
10049	53.749	1908.27	0.031	0.070		0.025
10051	53.858	1908.20	0.029	0.066		0.021

10053	53.895	1908.15	0.245	0.564		0.519
10055	53.919	1908.08	0.035	0.080		0.035
10057	53.944	1908.01	0.023	0.054		0.008
10059	53.968	1907.97	0.118	0.270		0.225
10061	53.993	1907.92	0.118	0.272		0.226
10063	54.017	1907.84	0.076	0.175		0.130
10065	54.114	1907.79	0.047	0.109		0.064
10067	54.151	1907.72	0.023	0.054		0.008
10069	54.160	1907.66	0.036	0.084		0.038
10071	54.169	1907.59	0.078	0.180		0.134
10073	54.222	1907.54	0.038	0.088		0.042
10075	54.275	1907.48	0.041	0.094		0.048
10077	54.328	1907.41	0.024	0.056		0.011
10079	54.381	1907.34	0.207	0.476		0.430
10081	54.419	1907.28	0.038	0.087	0.037	0.050
10083	54.458	1907.21	0.026	0.060		0.023
10085	54.497	1907.15	0.092	0.212		0.174
10087	54.516	1907.10	0.144	0.331		0.293
10089	54.560	1907.04	0.351	0.808		0.770
10091	54.603	1906.98	0.083	0.191		0.154
10093	54.647	1906.88	0.035	0.080		0.043
10095	54.690	1906.80	0.029	0.067		0.029
10097	54.729	1906.72	0.254	0.583		0.546
10099	54.768	1906.64	0.126	0.290		0.252
10101	54.806	1906.56	0.100	0.230		0.192
10103	54.826	1906.50	0.076	0.174		0.137
10105	54.869	1906.40	0.159	0.366		0.328
10107	54.913	1906.34	0.304	0.700		0.662
10109	54.961	1906.26	0.235	0.541		0.504
10111	55.000	1906.18	0.062	0.142		0.105
10113	55.019	1906.10	0.056	0.128		0.091
10115	55.058	1906.02	0.027	0.062		0.024
10117	55.077	1905.96	0.036	0.082		0.045
10119	55.097	1905.90	0.056	0.129		0.091
10121	55.104	1905.81	0.035	0.080		0.043
10123	55.111	1905.75	0.058	0.134		0.097
10125	55.119	1905.69	0.201	0.463		0.426
10127	55.126	1905.63	0.125	0.288		0.251
10129	55.134	1905.57	0.137	0.316		0.279

10131	55.141	1905.51	0.094	0.217		0.179
10133	55.149	1905.45	0.046	0.105		0.068
10135	55.156	1905.39	0.036	0.082		0.045
10137	55.164	1905.33	0.029	0.066		0.028
10139	55.171	1905.27	0.045	0.104		0.066
10141	55.178	1905.21	0.059	0.136		0.098
10143	55.186	1905.16	0.066	0.153		0.115
10145	55.193	1905.10	0.081	0.186		0.149
10147	55.696	1905.03	0.147	0.339		0.302
10149	55.735	1904.97	0.079	0.181		0.144
10151	55.774	1904.83	0.306	0.703		0.666
10153	55.793	1904.70	0.071	0.163		0.125
10155	55.851	1904.57	0.033	0.075		0.038
10157	55.890	1904.43	0.096	0.221		0.183
10159	55.928	1904.33	0.063	0.146		0.108
10161	55.966	1904.18	0.074	0.171		0.133
10163	56.004	1904.07	0.041	0.094		0.056
10165	56.041	1903.99	0.018	0.041		0.003
10167	56.079	1903.86	0.016	0.037		-0.001
10169	56.116	1903.81	0.014	0.033		-0.005
10171	56.154	1903.70	0.022	0.050		0.013
10173	56.163	1903.64	0.016	0.037		-0.001
10175	56.228	1903.52	0.018	0.041	0.031	0.010
10177	56.266	1903.44	0.024	0.055		0.024
10179	56.303	1903.36	0.030	0.069		0.038
10181	56.316	1903.25	0.145	0.333		0.302
10183	56.328	1903.18	0.594	1.366		1.335
10185	56.341	1903.11	0.143	0.329		0.298
10187	56.453	1903.02	0.088	0.203		0.172
10189	56.491	1902.94	0.041	0.095		0.064
10191	56.509	1902.86	0.025	0.058		0.027
10193	56.565	1902.80	0.112	0.258		0.226
10195	56.603	1902.72	0.102	0.235		0.204
10197	56.640	1902.64	0.022	0.050		0.019
10199	56.678	1902.56	0.035	0.080		0.049
10201	56.715	1902.50	0.143	0.329		0.297
10203	56.753	1902.42	0.082	0.188		0.156
10205	56.771	1902.32	0.038	0.087		0.056
10207	56.821	1902.16	0.019	0.045		0.013

10209	56.922	1902.08	0.043	0.098		0.067
10211	56.958	1902.00	0.020	0.046		0.015
10213	56.993	1901.94	0.032	0.073		0.042
10215	57.006	1901.89	0.024	0.054		0.023
10217	57.018	1901.79	0.016	0.037		0.006
10219	57.059	1901.70	0.091	0.209		0.178
10221	57.100	1901.65	0.135	0.311		0.280
10223	57.171	1901.56	0.057	0.132		0.100
10225	57.207	1901.50	0.030	0.070		0.039
10227	57.243	1901.42	0.021	0.049		0.018
10229	57.278	1901.33	0.177	0.407		0.376
10231	57.314	1901.27	0.168	0.386		0.354
10233	57.349	1901.19	0.043	0.100		0.069
10235	57.367	1901.13	0.024	0.054		0.023
10237	57.403	1901.04	0.018	0.042		0.011
10239	57.447	1900.99	0.014	0.033		0.001
10241	57.492	1900.89	0.016	0.037		0.006
10243	57.527	1900.80	0.044	0.101		0.069
10245	57.563	1900.73	0.105	0.242		0.211
10247	57.599	1900.64	0.055	0.126		0.095
10249	57.634	1900.57	0.063	0.145		0.113
10251	57.670	1900.48	0.074	0.171		0.140
10253	57.705	1900.41	0.404	0.929		0.898
10255	57.723	1900.32	0.033	0.077		0.046
10257	57.759	1900.25	0.036	0.083		0.052
10260	57.812	1900.11	0.067	0.155		0.124
10261	57.848	1900.07	0.024	0.055		0.024
10263	57.865	1900.00	0.035	0.079		0.048
10267	57.954	1899.82	0.041	0.094	0.018	0.076
10271	58.026	1899.64	0.042	0.096		0.078
10273	58.035	1899.55	1.226	2.820		2.802
10275	58.043	1899.46	0.025	0.057		0.039
10277	58.132	1899.36	0.013	0.029		0.011
10280	58.159	1899.18	0.014	0.033		0.015
10282	58.186	1899.10	0.020	0.046		0.028
10284	58.269	1899.00	0.016	0.037		0.019
10286	58.306	1898.88	0.014	0.033		0.015
10288	58.325	1898.73	0.019	0.045		0.027
10290	58.371	1898.58	0.013	0.030		0.012

10292	58.418	1898.42	0.037	0.084		0.066
10294	58.455	1898.31	0.085	0.196		0.178
10296	58.492	1898.15	0.344	0.790		0.772
10298	58.529	1898.06	0.063	0.144		0.126
10300	58.566	1897.94	0.041	0.095		0.077
10302	58.603	1897.86	0.028	0.065		0.047
10304	58.640	1897.78	0.020	0.047		0.029
10306	58.659	1897.69	0.058	0.132		0.114
10308	58.696	1897.63	0.031	0.071		0.053
10310	58.752	1897.55	0.060	0.139		0.121
10312	58.771	1897.47	0.161	0.371		0.353
10314	58.798	1897.38	0.047	0.107		0.089
10316	58.826	1897.33	0.094	0.215		0.197
10318	58.902	1897.24	0.066	0.153		0.135
10320	58.922	1897.16	0.099	0.228		0.210
10322	58.984	1897.08	0.016	0.036		0.018
10324	59.025	1896.97	0.011	0.026		0.008
10326	59.072	1896.81	0.014	0.031		0.013
10330	59.119	1896.56	0.011	0.025		0.007
10332	59.195	1896.47	0.014	0.032		0.014
10334	59.233	1896.34	0.037	0.085		0.067
10336	59.271	1896.22	0.016	0.038		0.020
10338	59.310	1896.09	0.012	0.027		0.009
10340	59.348	1895.97	0.014	0.032		0.014
10342	59.386	1895.88	0.010	0.022		0.004
10344	59.424	1895.76	0.020	0.046		0.028
10346	59.462	1895.64	0.096	0.220		0.202
10348	59.500	1895.52	0.270	0.622		0.604
10350	59.538	1895.39	0.185	0.427		0.408
10352	59.576	1895.27	0.066	0.151		0.133
10354	59.614	1895.18	0.063	0.145		0.127
10356	59.652	1895.06	0.046	0.106		0.088
10358	59.690	1894.92	0.069	0.160		0.141
10360	59.730	1894.81	0.055	0.127		0.109
10362	59.769	1894.62	0.054	0.123		0.105
10364	59.808	1894.46	0.075	0.172		0.154
10366	59.828	1894.27	0.092	0.211		0.193
10368	59.848	1894.15	0.105	0.242		0.224
10370	59.927	1894.00	0.049	0.114		0.096

10372	59.967	1893.88	0.019	0.044		0.026
10376	60.039	1893.59	0.112	0.258		0.240
10378	60.086	1893.47	0.062	0.143		0.125
10379	60.125	1893.41				
10380	60.135	1893.37	0.06	0.14		0.12
10381	60.145	1893.32				
10382	60.185	1893.26				
10383	60.195	1893.21	0.03	0.06		0.04
10384	60.205	1893.15	0.02	0.05		0.03
10385	60.244	1893.09				
10386	60.264	1893.03	0.01	0.03		0.01
10387	60.284	1892.98				
10388	60.344	1892.92	0.01	0.02		0.01
2254	60.405	1892.78	0.05	0.12		0.10
2256	60.465	1892.59	0.06	0.13		0.11
2258	60.526	1892.35	0.02	0.04		0.02
2260	60.567	1892.25	0.18	0.41		0.39
2262	60.588	1892.09	0.04	0.08		0.06
2264	60.608	1891.97	0.07	0.15		0.13
2267	60.703	1891.78	0.30	0.70		0.68
2269	60.795	1891.64	0.31	0.70		0.68
2272	60.858	1891.47	0.06	0.15		0.13
2274	60.900	1891.36	0.10	0.23		0.21
2276	60.942	1891.25	0.06	0.15		0.13
2281	61.047	1890.97	0.03	0.07		0.05
2283	61.068	1890.90	0.07	0.16		0.14
2285	61.131	1890.83	0.04	0.09		0.07
2287	61.152	1890.69	0.02	0.05		0.03
2289	61.173	1890.59	0.02	0.05		0.03
2291	61.309	1890.52	0.02	0.05		0.03
2293	61.342	1890.34	0.07	0.17		0.15
2296	61.457	1890.19	0.13	0.31		0.29
2298	61.545	1890.10	0.02	0.04		0.02
2302	61.609	1889.98	0.05	0.11		0.09
2304	61.673	1889.89	0.03	0.06		0.04
2306	61.716	1889.80	0.02	0.05		0.03
2308	61.759	1889.73	0.02	0.04		0.02
2310	61.802	1889.66	0.03	0.08		0.06
2312	61.823	1889.57	0.02	0.04		0.02

2314	61.934	1889.39	0.08	0.19		0.16
2316	62.046	1889.21	0.10	0.22		0.20
2318	62.092	1889.13	0.05	0.12		0.10
2320	62.139	1889.05	0.14	0.32		0.30
2322	62.185	1888.94	0.04	0.10		0.08
2324	62.232	1888.83	0.05	0.10		0.08
2326	62.278	1888.69	0.10	0.22		0.20
2328	62.325	1888.54	0.22	0.50		0.48
2330	62.371	1888.43	0.05	0.11		0.09
2332	62.418	1888.29	0.13	0.30		0.27
2334	62.464	1888.14	0.15	0.33		0.31
2336	62.511	1888.03	0.20	0.45		0.43
2338	62.557	1887.93	0.08	0.19		0.17
2340	62.604	1887.84	0.07	0.17		0.15
2342	62.651	1887.75	0.03	0.07		0.05
2344	62.721	1887.64	0.54	1.23		1.21
2346	62.763	1887.56	0.13	0.30		0.28
2348	62.804	1887.47	0.33	0.76		0.74
2350	62.846	1887.40	0.10	0.24		0.22
2352	62.888	1887.33	0.13	0.30		0.28
2354	62.930	1887.25	0.24	0.54		0.52
2356	62.951	1887.16	1.01	2.32		2.30
2358	62.971	1887.11	0.21	0.47		0.45
2360	63.055	1887.02	0.10	0.23		0.21
2362	63.097	1886.94	0.07	0.15		0.13
2364	63.138	1886.87	0.23	0.52		0.50
2366	63.180	1886.80	0.11	0.26		0.24
2369	63.243	1886.69	0.12	0.28		0.26
2371	63.297	1886.57	0.50	1.16		1.14
2373	63.351	1886.50	0.43	0.98		0.96
2375	63.405	1886.39	0.46	1.06		1.03
2377	63.445	1886.31	0.13	0.30		0.28
2379	63.485	1886.24	0.14	0.32		0.30
2381	63.525	1886.17	0.21	0.47		0.45
2384	63.585	1886.06	0.08	0.19		0.17
2386	63.625	1885.98	0.17	0.40		0.38
2388	63.665	1885.89	0.06	0.13		0.11
2390	63.705	1885.81	0.11	0.25		0.23
2393	63.765	1885.68	0.04	0.09		0.07

2395	63.805	1885.60	0.04	0.09		0.07
2397	63.845	1885.51	0.07	0.15		0.13
2399	63.885	1885.43	0.04	0.10		0.07
2401	63.925	1885.34	0.04	0.08		0.06
2403	63.965	1885.26	0.10	0.22		0.20
2405	64.005	1885.11	0.29	0.66		0.64
2407	64.028	1885.02	1.13	2.60		2.58
2409	64.051	1884.93	0.12	0.28		0.26
2412	64.150	1884.80	0.60	1.38		1.36
2414	64.210	1884.70	0.62	1.42		1.40
2416	64.249	1884.61	0.20	0.47		0.45
2418	64.289	1884.52	0.12	0.28		0.26
2420	64.329	1884.43	0.10	0.22		0.20
2422	64.368	1884.34	0.10	0.22		0.20
2424	64.408	1884.25	0.04	0.08		0.06
2426	64.448	1884.16	0.10	0.23		0.21
2428	64.487	1884.07	0.03	0.07		0.05
2432	64.566	1883.87	0.09	0.22		0.19
2434	64.606	1883.77	0.04	0.09		0.07
2436	64.646	1883.67	0.04	0.08		0.06
2438	64.685	1883.56	0.63	1.44		1.42
2440	64.725	1883.49	0.06	0.15		0.13
2443	64.785	1883.33	2.16	4.96		4.94
2446	64.844	1883.18	0.22	0.52		0.50
2448	64.884	1883.08	0.12	0.28		0.25
2450	64.923	1882.98	0.12	0.28		0.26
2452	64.963	1882.91	0.06	0.14		0.12
2454	65.003	1882.84	0.12	0.27		0.25
2456	65.042	1882.76	0.07	0.16		0.14
2458	65.082	1882.69	0.12	0.27		0.25
2460	65.122	1882.62	0.35	0.81		0.79
2462	65.161	1882.55	0.32	0.74		0.72
2465	65.221	1882.44	0.11	0.25		0.23
2467	65.260	1882.36	0.06	0.14		0.12
2469	65.300	1882.29	0.11	0.26		0.24
2471	65.340	1882.22	0.12	0.27		0.25
2473	65.379	1882.15	0.25	0.58		0.56
2475	65.419	1882.07	0.06	0.14		0.12
10392	65.459	1881.88	0.04	0.10	0.03	0.07

10394	65.483	1881.77	0.11	0.25		0.22
10396	65.507	1881.66	0.05	0.12		0.09
10398	65.532	1881.55	0.02	0.04		0.02
10400	65.682	1881.45	0.06	0.14		0.12
10402	65.725	1881.33	0.05	0.12		0.10
10404	65.768	1881.23	0.03	0.07		0.04
10406	65.811	1881.13	0.04	0.09		0.07
10408	65.854	1881.00	0.04	0.09		0.07
10410	65.897	1880.92	0.12	0.27		0.24
10412	65.940	1880.84	0.02	0.05		0.02
10414	65.983	1880.73	0.10	0.22		0.20
10416	66.026	1880.67	0.15	0.35		0.32
10418	66.069	1880.57	0.05	0.12		0.10
10420	66.112	1880.33	0.16	0.36		0.33
10422	66.170	1880.22	0.08	0.18		0.15
10424	66.227	1880.16	0.04	0.10		0.08
10426	66.306	1880.08	0.10	0.22		0.19
10428	66.346	1880.00	0.12	0.28		0.25
10430	66.365	1879.87	0.04	0.08		0.06
10432	66.385	1879.79	0.04	0.08		0.06
10434	66.464	1879.68	0.03	0.07		0.04
10436	66.504	1879.56	0.01	0.03		0.01
10438	66.544	1879.44	0.30	0.68		0.65
10440	66.563	1879.32	0.10	0.24		0.21
10442	66.623	1879.21	0.28	0.63		0.61
10444	66.662	1879.09	0.11	0.25		0.22
10446	66.702	1878.98	0.03	0.07		0.05
10448	66.742	1878.89	0.05	0.10		0.08
10450	66.781	1878.81	0.03	0.07		0.04
10452	66.821	1878.72	0.02	0.04		0.02
10454	66.861	1878.64	0.02	0.05		0.02
10456	66.900	1878.55	0.01	0.03		0.01
10458	66.940	1878.47	0.02	0.04		0.01
10460	66.960	1878.38	0.03	0.06		0.04
10462	67.019	1878.30	0.04	0.10		0.07
10464	67.059	1878.21	0.02	0.04		0.02
10466	67.098	1878.13	0.02	0.06		0.03
10468	67.138	1878.04	0.06	0.15		0.12
10470	67.177	1877.96	0.04	0.10		0.07

10472	67.217	1877.88	0.04	0.09		0.06
10474	67.257	1877.80	0.02	0.04		0.01
10476	67.296	1877.72	0.01	0.03		0.00
10478	67.336	1877.64	0.02	0.04		0.01
10480	67.376	1877.56	0.15	0.35		0.32
10482	67.415	1877.50	0.05	0.11		0.09
10484	67.455	1877.42	0.06	0.14		0.11
10486	67.494	1877.34	0.04	0.08		0.06
10488	67.534	1877.26	0.18	0.41		0.38
10490	67.574	1877.18	0.05	0.12		0.10
10493	67.633	1877.06	0.04	0.08		0.06
10495	67.673	1876.97	0.02	0.05		0.03
10497	67.713	1876.83	0.08	0.18		0.15
10499	67.753	1876.69	0.08	0.19		0.16
10502	67.813	1876.48	0.37	0.85		0.83
10504	67.853	1876.34	0.05	0.11		0.09
10506	67.873	1876.21	0.29	0.67		0.64
10508	67.933	1876.07	0.10	0.24		0.21
10510	67.973	1875.95	0.18	0.42		0.39
10512	68.013	1875.84	0.14	0.32		0.29
10514	68.053	1875.74	0.17	0.39		0.36
10516	68.093	1875.63	0.24	0.54		0.52
10518	68.132	1875.53	0.30	0.70		0.67
10520	68.172	1875.42	0.12	0.28		0.26
10522	68.212	1875.32	0.03	0.08		0.05
10524	68.253	1875.18	0.03	0.07		0.05
10526	68.298	1875.08	0.04	0.08		0.06
10528	68.342	1874.96	0.02	0.05		0.03
10530	68.386	1874.83	0.03	0.06		0.03
10532	68.430	1874.72	0.11	0.25		0.22
10534	68.475	1874.58	0.16	0.36		0.34
10536	68.519	1874.47	0.22	0.50		0.47
10538	68.563	1874.33	0.09	0.21		0.18
10540	68.607	1874.22	0.03	0.08		0.05
10542	68.652	1874.11	0.05	0.11		0.09
10544	68.696	1873.97	0.07	0.16		0.13
10546	68.740	1873.85	0.09	0.22		0.19
10548	68.784	1873.71	0.33	0.76		0.73
10550	68.828	1873.59	0.08	0.19		0.16

10552	68.873	1873.47	0.15	0.35		0.32
10554	68.917	1873.32	0.13	0.30		0.27
10556	68.961	1873.21	0.12	0.27		0.24
10558	68.972	1873.07	0.16	0.37		0.34
10560	68.983	1872.93	0.03	0.07		0.04
10562	69.091	1872.79	0.03	0.08		0.05
10564	69.112	1872.64	0.08	0.18		0.15
10566	69.174	1872.46	0.03	0.06		0.04
10568	69.216	1872.32	0.04	0.09		0.06
10570	69.258	1872.18	0.03	0.07		0.04
10572	69.300	1872.04	0.02	0.06		0.03
10574	69.342	1871.93	0.03	0.06		0.03
10576	69.383	1871.85	0.02	0.05		0.02
10578	69.425	1871.74	0.02	0.05		0.02
10580	69.467	1871.65	0.02	0.04		0.02
10582	69.509	1871.57	0.04	0.08		0.05
10584	69.550	1871.48	0.05	0.12		0.09
10586	69.592	1871.39	0.06	0.13		0.10
10588	69.634	1871.30	0.03	0.06		0.03
10590	69.676	1871.20	0.08	0.17		0.15
10592	69.720	1871.11	0.03	0.06		0.04
10594	69.745	1870.97	0.03	0.08		0.05
10596	69.820	1870.85	0.03	0.06		0.04
10598	69.845	1870.72	0.02	0.04		0.02
10600	69.921	1870.59	0.02	0.03		0.01
10602	69.971	1870.46	0.05	0.12		0.09
10604	70.021	1870.33	0.02	0.04		0.02
10606	70.071	1870.21	0.01	0.03		0.00
10608	70.122	1870.08	0.02	0.04		0.01
10610	70.172	1869.95	0.03	0.07		0.05
10612	70.222	1869.83	0.01	0.03		0.00
10614	70.272	1869.72	0.04	0.10		0.07
10616	70.323	1869.59	0.04	0.09		0.07
2479	70.373	1869.34	0.02	0.05	0.03	0.02
2482	70.488	1869.20	0.02	0.04		0.01
2484	70.529	1869.10	0.02	0.05		0.02
2486	70.570	1869.00	0.04	0.10		0.06
2488	70.611	1868.88	0.02	0.05		0.02
2490	70.652	1868.76	0.02	0.05		0.02

2492	70.693	1868.64	0.07	0.15		0.12
2494	70.734	1868.52	0.13	0.29		0.26
2496	70.774	1868.39	0.03	0.06		0.02
2498	70.815	1868.24	0.04	0.10		0.07
2500	70.856	1868.12	0.02	0.05		0.02
2502	70.897	1868.00	0.20	0.47		0.44
2504	70.938	1867.86	0.06	0.13		0.10
2506	70.979	1867.72	0.11	0.25		0.22
2510	71.061	1867.45	0.13	0.30		0.27
2512	71.102	1867.31	0.03	0.08		0.04
2514	71.153	1867.14	0.03	0.06		0.03
2516	71.193	1867.00	0.08	0.19		0.15
2518	71.233	1866.90	0.02	0.05		0.01
2520	71.240	1866.75	0.02	0.04		0.00
2522	71.247	1866.60	0.05	0.12		0.09
2524	71.253	1866.45	0.03	0.06		0.03
2525	71.433	1866.40	0.09	0.21		0.18
2531	71.518	1866.08	0.08	0.18		0.15
2533	71.581	1865.98	0.03	0.07		0.04
2536	71.666	1865.80	0.02	0.05		0.01
2539	71.729	1865.66	0.02	0.05		0.02
2541	71.772	1865.56	0.05	0.11		0.07
2543	71.814	1865.44	0.02	0.04		0.00
2545	71.856	1865.34	0.02	0.04		0.00
2547	71.898	1865.27	0.02	0.05		0.01
2549	71.941	1865.15	0.01	0.03		-0.01
2551	71.982	1865.05	0.01	0.03		-0.01
2553	72.032	1864.94	0.02	0.03		0.00
2555	72.081	1864.74	0.03	0.06		0.03
2557	72.129	1864.62	0.02	0.04		0.00
2558	72.153	1864.53				
2559	72.177	1864.47	0.03	0.08		0.04
2560	72.201	1864.41				
2561	72.224	1864.32	0.03	0.06		0.02
2562	72.248	1864.26				
2563	72.272	1864.18	0.05	0.11		0.08
2565	72.296	1864.06	0.04	0.08		0.05
2567	72.381	1863.95	0.08	0.17	0.01	0.16
2570	72.465	1863.64	0.05	0.13		0.11

2572	72.550	1863.45	0.04	0.09		0.08
2574	72.591	1863.34	0.04	0.08		0.07
2576	72.633	1863.24	0.02	0.05		0.03
2578	72.674	1863.13	0.03	0.06		0.05
2580	72.716	1863.00	0.04	0.09		0.08
2582	72.757	1862.89	0.03	0.06		0.05
2584	72.799	1862.77	0.04	0.10		0.08
2586	72.840	1862.66	0.03	0.07		0.06
2588	72.881	1862.54	0.03	0.07		0.06
2590	72.923	1862.43	0.01	0.03		0.02
2592	72.964	1862.29	0.28	0.65		0.63
2594	72.985	1862.17	0.09	0.20		0.19
2596	73.047	1862.06	0.11	0.26		0.25
2598	73.089	1861.96	0.12	0.27		0.25
2600	73.130	1861.89	0.31	0.71		0.70
2602	73.172	1861.81	0.08	0.19		0.18
2605	73.234	1861.70	0.04	0.10		0.09
2608	73.396	1861.39	0.03	0.07		0.05
2610	73.558	1861.09	0.01	0.02		0.00
2612	73.604	1861.00	0.03	0.06		0.05
2615	73.671	1860.80	0.25	0.59		0.57
2617	73.764	1860.52	0.16	0.36		0.35
2619	73.856	1860.17	0.02	0.04		0.03
2621	73.896	1860.03	0.02	0.05		0.04
2623	73.917	1859.93	0.03	0.07		0.06
2625	73.977	1859.84	0.46	1.06		1.05
2627	73.997	1859.76	0.05	0.11		0.10
2629	74.058	1859.67	0.01	0.02		0.01
2631	74.098	1859.58	0.02	0.04		0.02
2633	74.138	1859.49	0.03	0.06		0.05
2635	74.178	1859.40	0.05	0.11		0.10
2637	74.219	1859.31	0.11	0.25		0.24
2639	74.259	1859.22	0.04	0.10		0.09
2641	74.299	1859.13	0.02	0.05		0.03
2643	74.340	1859.04	0.08	0.19		0.18
2645	74.380	1858.95	0.09	0.20		0.19
2647	74.420	1858.85	0.01	0.03		0.02
2649	74.460	1858.74	0.06	0.13		0.11
2651	74.501	1858.64	0.09	0.22		0.20

2653	74.541	1858.54	0.21	0.48		0.46
2655	74.581	1858.44	0.04	0.09		0.08
2657	74.622	1858.33	0.02	0.05		0.03
2659	74.662	1858.23	0.24	0.56		0.55
2661	74.703	1858.13	0.06	0.13		0.12
2663	74.745	1858.00	0.02	0.05		0.03
2665	74.786	1857.87	0.03	0.07		0.05
2667	74.827	1857.74	0.15	0.34		0.33
2669	74.868	1857.61	0.07	0.15		0.14
2671	74.909	1857.48	0.13	0.31		0.30
2673	74.950	1857.35	0.17	0.39		0.37
2675	74.991	1857.23	0.06	0.15		0.13
2677	75.032	1857.10	0.11	0.24		0.23
2679	75.073	1856.98	0.06	0.13		0.12
2681	75.114	1856.88	0.02	0.04		0.03
2683	75.155	1856.76	0.04	0.09		0.07
2685	75.196	1856.66	0.17	0.40		0.39
2687	75.237	1856.56	0.05	0.12		0.10
2689	75.278	1856.46	0.08	0.19		0.18
2691	75.319	1856.37	0.07	0.17		0.16
2693	75.361	1856.27	0.18	0.41		0.40
2695	75.402	1856.17	0.03	0.07		0.06
2697	75.443	1856.07	0.12	0.28		0.27
2699	75.484	1855.97	0.11	0.26		0.25
2704	75.586	1855.69	0.02	0.05		0.04
2707	75.648	1855.54	0.04	0.10		0.09
2709	75.689	1855.44	0.08	0.18		0.16
2712	75.751	1855.28	1.81	4.17		4.15
2715	75.812	1855.13	0.15	0.35		0.32
2716	75.833	1855.08	0.09	0.21	0.03	0.17
2717	75.853	1855.03	0.06	0.15		0.12
2719	75.894	1854.93	0.16	0.37		0.34
2721	75.935	1854.82	0.09	0.20		0.17
2723	75.976	1854.73	0.08	0.18		0.15
2725	76.018	1854.64	0.03	0.07		0.04
2727	76.059	1854.56	0.12	0.28		0.25
2729	76.100	1854.47	0.07	0.16		0.13
2731	76.141	1854.38	0.19	0.44		0.41
2734	76.202	1854.24	0.12	0.28		0.25

2736	76.243	1854.16	0.78	1.80		1.77
2738	76.284	1854.07	0.17	0.39		0.36
2740	76.326	1853.96	0.11	0.25		0.22
2742	76.367	1853.87	0.41	0.95		0.92
2744	76.408	1853.79	0.13	0.30		0.27
2746	76.449	1853.70	0.12	0.28		0.25
2749	76.510	1853.57	0.04	0.10		0.07
2751	76.551	1853.49	0.11	0.25		0.22
2753	76.592	1853.40	0.05	0.12		0.09
2755	76.634	1853.32	0.06	0.13		0.11
2757	76.675	1853.21	0.02	0.04		0.02
2760	76.736	1853.09	0.04	0.09		0.07
2762	76.777	1853.00	0.05	0.11		0.10
2764	76.818	1852.91	0.03	0.07		0.05
2767	76.880	1852.77	0.14	0.32		0.31
2769	76.921	1852.68	0.20	0.47		0.45
2774	77.024	1852.45	0.04	0.09		0.07
2776	77.065	1852.34	0.05	0.12		0.10
2778	77.106	1852.25	0.05	0.11		0.09
2783	77.208	1852.02	0.04	0.08	0.02	0.07

APPENDIX F

FRESH ICE DATA

Sample	Length (cm)	Depth (m)	Adjust-ed Depth (m)	$_{meas}$BC (µg/L)	$_{cal}$BC (µg/L)	Mean Back-ground from LBC Blanks (µg/L)	$_{cal}$BC Minus Back-ground (µg/L)
LBC-1	5	12.425	12.425	0.121	0.279	0.036	0.242
LBC-2	5	12.475	12.475	0.114	0.261		0.225
LBC-3	5	12.525	12.525	0.150	0.345		0.308
LBC-4	5	12.575	12.575	0.186	0.429		0.392
LBC-5	5	12.625	12.625	0.090	0.207		0.171
LBC-6	5	12.675	12.675	0.150	0.345		0.308
LBC-7	5	12.725	12.725	0.217	0.500		0.463
LBC-8	4	12.770	12.770	0.264	0.608		0.572
LBC-9	5	12.815	12.815	0.263	0.605		0.569
LBC-10	4	12.860	12.860	0.037	0.085		0.049
LBC-11	4	12.900	12.900	0.528	1.214		1.177
LBC-12	5	12.968	12.988	0.236	0.542		0.506
LBC-13	5	13.018	13.038	0.321	0.739		0.703
LBC-14	4	13.063	13.083	0.333	0.766		0.730
LBC-15	5	13.108	13.128	0.385	0.886		0.850
LBC-16	4	13.153	13.173	0.164	0.378		0.342
LBC-17	4	13.193	13.213	0.120	0.276		0.240
LBC-18	4	13.233	13.253	0.282	0.649		0.612
LBC-19	5	13.278	13.318	0.776	1.785		1.748
LBC-20	4	13.323	13.363	0.253	0.581		0.545
LBC-21	6	13.373	13.413	0.321	0.739		0.703
LBC-22	5	13.428	13.488	0.520	1.197		1.161
LBC-23	5	13.478	13.538	1.987	4.570		4.534
LBC-24	4.5	13.526	13.586	1.102	2.536		2.499
LBC-25	4.5	13.571	13.631	0.113	0.259		0.223
LBC-26	5	13.687	13.687	0.152	0.349	0.043	0.306
LBC-27	4.5	13.735	13.735	0.355	0.816		0.772
LBC-28	4.5	13.780	13.780	0.951	2.188		2.145
LBC-29	6	13.832	13.832	0.423	0.973		0.929
LBC-30	5	13.887	13.887	0.086	0.198		0.154

LBC-31	5	13.937	13.937	0.107	0.246		0.202
LBC-32	5	13.987	13.987	0.187	0.430		0.387
LBC-33	5	14.037	14.037	0.148	0.340		0.296
LBC-34	5	14.087	14.087	0.158	0.365		0.321
LBC-35	4.5	14.135	14.135	0.162	0.372		0.328
LBC-36	4.5	14.180	14.180	0.503	1.157		1.113
LBC-37	5	14.257	14.197	3.839	8.832		8.788
LBC-38	5	14.307	14.247	5.205	11.974		11.931
LBC-39	5	14.357	14.317	2.239	5.149		5.106
LBC-40	5	14.407	14.367	0.958	2.203		2.159
LBC-41	5	14.457	14.437	0.740	1.702		1.659
LBC-42	5	14.507	14.487	0.793	1.823		1.780
LBC-43	4	14.552	14.532	0.921	2.120		2.076
LBC-44	4	14.592	14.572	0.383	0.880		0.837
LBC-45	4	14.632	14.612	0.534	1.229		1.185
LBC-46	5	15.195	15.195	2.584	5.944		5.901
LBC-48	5	15.285	15.285	0.644	1.481		1.438
LBC-49	4	15.330	15.330	0.579	1.333		1.289
LBC-50	4	15.370	15.370	0.532	1.225		1.181
LBC-51	4	15.410	15.410	0.303	0.697		0.654
LBC-52	4	15.450	15.450	0.367	0.844		0.801
LBC-53	4	15.490	15.490	0.126	0.290		0.246
LBC-54	3.5	15.528	15.528	0.310	0.713		0.670
LBC-55	4	15.565	15.565	0.304	0.700		0.656
LBC-56	4	15.605	15.605	0.375	0.862		0.819
LBC-57	4	15.645	15.645	0.333	0.766		0.723
LBC-58	4	15.685	15.705	0.066	0.152		0.109
LBC-59	5	15.813	15.793	0.157	0.360		0.317
LBC-60	5	15.863	15.863	0.042	0.096		0.052
LBC-61	5	15.913	15.913	0.283	0.651		0.608
LBC-62	5	15.963	15.963	0.348	0.801		0.757
LBC-63	4	16.008	16.008	0.099	0.228		0.185
LBC-64	4	16.048	16.048	0.567	1.303		1.260
LBC-65	4.5	16.091	16.091	0.557	1.281		1.237
LBC-67	5	16.188	16.238	0.041	0.093		0.050
LBC-68	5	16.238	16.288	0.073	0.167		0.124
LBC-69	5	16.288	16.338	0.293	0.673		0.630
LBC-70	5	16.338	16.388	0.338	0.778		0.735
LBC-71	5	16.388	16.438	0.431	0.991		0.947

LBC-72	5	16.438	16.488	0.459	1.057		1.013
LBC-73	5	16.488	16.536	0.438	1.008		0.965
LBC-74	4.5	16.536	16.581	0.590	1.357		1.313
LBC-75	4.5	16.581	16.643	0.570	1.311		1.268
LBC-76	4	16.623	16.683	0.629	1.448		1.404
LBC-77	4	16.663	16.723	0.759	1.745		1.702
LBC-78	4	16.703	16.826	0.670	1.540		1.497
LBC-79	5	16.846	16.876	0.455	1.046		1.003
LBC-80	5	16.896	16.926	0.428	0.985		0.942
LBC-81	5	16.946	16.996	1.099	2.528		2.484
LBC-82	5	16.996	17.046	1.150	2.645		2.601
LBC-83	5	17.046	17.091	0.355	0.816		0.772
LBC-84	4	17.091	17.136	0.558	1.284		1.240
LBC-85	5	17.136	17.186	1.845	4.243	0.062	4.181
LBC-86	5	17.186	17.231	1.964	4.519		4.475
LBC-87	4	17.231	17.276	0.731	1.681		1.619
LBC-88	5	17.276	17.324	1.278	2.940		2.878
LBC-89	4.5	17.324	17.369	0.912	2.099		2.036
LBC-90	4.5	17.369	17.416	1.123	2.583		2.521
LBC-91	5	17.416	17.466	0.151	0.348		0.286
LBC-92	5	17.466	17.516	0.128	0.295		0.233
LBC-93	5	17.516	17.566	0.334	0.769		0.706
LBC-94	5	17.566	17.616	0.646	1.486		1.424
LBC-95	5	17.616	17.666	0.657	1.512		1.450
LBC-96	5	17.666	17.711	3.572	8.216		8.154
LBC-97	4	17.711	17.751	3.405	7.833		7.770
LBC-98	4	17.751	17.790	1.573	3.618		3.555
LBC-99	5	17.810	17.823	0.814	1.872		1.809
LBC-100	5.5	17.863	17.878	0.647	1.489		1.426
LBC-101	5.5	17.918	17.930	1.222	2.810		2.748
LBC-102	5	17.970	17.980	0.570	1.311		1.249
LBC-103	5	18.020	18.030	1.114	2.563		2.501
LBC-104	5	18.070	18.135	2.779	6.392		6.330
LBC-105	4	18.115	18.175	1.341	3.086		3.024
LBC-106	4	18.155	18.220	3.401	7.823		7.761
LBC-107	5	18.200	18.270	0.974	2.241		2.179
LBC-108	5	18.250	18.313	0.636	1.462		1.400
LBC-109	3.5	18.293	18.348	0.289	0.665		0.602
LBC-110	3.5	18.328	18.328	0.532	1.224		1.162

LBC-111	5	18.883	18.883	0.805	1.853		1.790
LBC-112	4	18.928	18.928	1.602	3.685		3.623
LBC-113	4	18.968	18.968	1.292	2.972		2.909
LBC-114	4	19.008	19.008	0.655	1.506		1.444
LBC-115	5	19.053	19.053	0.348	0.800		0.738
LBC-116	5	19.103	19.103	0.346	0.795		0.733
LBC-117	5	19.153	19.153	0.447	1.028		0.966
LBC-118	5	19.203	19.223	0.524	1.205		1.143
LBC-119	5	19.253	19.313	0.453	1.041		0.979
LBC-120	5	19.303	19.363	1.610	3.704		3.641
LBC-121	5	19.353	19.413	2.810	6.463		6.401
LBC-122	5	19.403	19.463	0.201	0.462		0.400
LBC-123	5	19.453	19.513	0.358	0.823		0.761
LBC-124	4	19.498	19.558	0.607	1.397		1.334
LBC-125	5	19.543	19.603	0.384	0.883		0.821
LBC-126	5	19.593	19.653	0.121	0.278		0.216
LBC-127	5	19.643	19.703	0.228	0.525		0.463
LBC-128	4	19.688	19.748	0.279	0.641		0.579
LBC-129	4	19.728	19.788	0.222	0.512		0.449
LBC-130	5	19.807	19.807	0.355	0.816		0.753
LBC-131	5	19.857	19.817	0.616	1.418		1.356
LBC-132	3	19.897	19.857	0.761	1.750		1.688
LBC-133	3	19.927	19.887	0.818	1.882		1.819
LBC-134	5	19.967	19.927	8.846	20.348		20.286
LBC-135	4.5	20.015	19.975	1.405	3.231		3.169
LBC-136	4.5	20.060	20.020	0.593	1.364		1.302
LBC-137	5	20.107	20.067	0.357	0.821		0.759
LBC-138	5	20.157	20.157	0.224	0.516		0.454
LBC-139	5	20.207	20.207	0.211	0.486		0.424
LBC-140	5	20.257	20.257	0.297	0.682		0.620
LBC-141	5	20.307	20.307	0.511	1.175		1.113
LBC-142	5	20.357	20.357	1.640	3.773		3.710
LBC-143	4	20.402	20.402	1.621	3.730		3.667
LBC-144	4	20.442	20.442	0.212	0.488		0.425
LBC-145	5	20.487	20.487	0.151	0.348		0.285
LBC-146	5	20.537	20.537	0.114	0.261		0.199
LBC-147	5	20.587	20.587	0.151	0.347		0.285
LBC-148	5	20.637	20.637	0.115	0.264		0.201
LBC-149	5	20.687	20.687	0.273	0.628		0.565

LBC-150	5	20.737	20.737	1.569	3.610		3.548